(Sample of Approval Sheet)

APPROVAL SHEET

Title of Dissertation: Development and Characterization of a Transgenic Mouse Model of Cytokine-Mediated Prostate Inflammation

Name of Candidate: Arya Ashok
Doctor of Philosophy, 2016

Dissertation and Abstract Approved: _____

Charles Bieberich
Professor
Biological Sciences

Date Approved: 28 JUL 16

ABSTRACT

Title of Document:	Development and Characterization of a Transgenic Mouse Model of Cytokine-Mediated Prostate Inflammation.
	Arya Ashok, Ph.D., and 2016
Directed By:	Charles J.Bieberich, Ph.D. Professor Department of Biological Sciences

A causal link between prostate inflammation and prostate diseases including prostatitis, benign prostatic hyperplasia (BPH) and prostate cancer is unclear. This can be attributed to the fact that prostate inflammation is an extremely common histological finding. However, epidemiological, histopathological and molecular evidence suggest that inflammation may play a causal role in prostatitis, BPH and prostate adenocarcinoma. Discerning molecular mechanisms of chronic inflammation is almost impossible to do in humans. However, a physiologically relevant mouse model that encompasses prostate inflammation and its sequela could be highly informative. In this study, an innovative mouse model was developed that allows inducible expression of Interleukin 1β. Interleukin 1β is a proinflammatory cytokine implicated in major diseases including solid tumors, autoimmune disorders and neurodegenerative disorders. This potent cytokine is implicated in chronic prostatitis and is suggested to be a key mediator of pain. The IL-1β-Mediated Inflammation Model (IMPI) characterized in this study, is based on the Tet-On

technology, and therefore, is doxycycline inducible. Here, we report the development and characterization of the IMPI model, including the inflammatory phenotype and induction kinetics. The basic approach used to establish this model can be extended to other cytokines/chemokines implicated in prostate disease. Furthermore, we established the role of IL-1β in mediating pelvic hypersensitivity that can be attenuated with IL-1β-blockade. Most importantly, we determined that the model recapitulates histopathological features of human inflammatory and pre-neoplastic lesions. This study provides evidence to support the notion that IL-1β-mediated chronic inflammation can induce pre-neoplastic lesions in the mouse prostate epithelium. Lastly, the genome-wide RNA expression changes mediated by IL-1β–induced prostate inflammation were identified. Pathways involved in inflammation, apoptosis, oxidative stress and chemokine signaling were determined. The IMPI model is a novel platform to test anti-inflammatory therapies and will aid in the development of novel inflammatory biomarkers.

Development and Characterization of a Transgenic Mouse Model of Cytokine-Mediated Prostate Inflammation

By

Arya Ashok

Dissertation submitted to the Faculty of the Graduate School of the
University of Maryland, Baltimore County, in partial fulfillment
of the requirements for the degree of
Ph.D. in Biological Sciences
2016

Dedication

Dedicated to my father, who has always believed in me.

Acknowledgements

I would like to express my gratitude to my mentor, Dr. Chuck Bieberich. Over the past six years, he has helped me develop by scientific intellect and deepened my passion for science. He is an amazing teacher, leader and motivator. His scientific and moral integrity is something I admire.

My thesis committee members, Dr. Steve Miller, Dr. Weihong Lin, Dr. Pratima Sinha, Dr. Cynthia Wagner, Dr. Richard Alexander and Dr. Angela De Marzo have always been extremely supportive and gave me valuable feedback.

To all my undergraduate students, Sagar Bajpai, Stephanie Stookey, Candice Craig and Emily Melluso who have supported this project.

A special thanks to our collaborators at Johns Hopkins, Dr. Srinivasan Yegnasubramanian, Dr. Charles Drake and Dr. Angelo De Marzo.

Being almost 8,000 miles away from my family was one of the hardest challenges for me. This thesis would not have been completed without the support of my parents and sister. Lastly, my dear husband who has been extremely encouraging and motivating.

Table of Contents

List of Tables

List of Figures

Chapter 1: Background

Chapter 2: A Novel Pre-Clinical Mouse Model of Prostate Inflammation Mediated by Interleukin-1β

Chapter 4: Interleukin-1β-Mediated Inflammation Model Develops Pathological Features Consistent with Human PIA and PIN

Chapter 5: Conclusions and Future Directions

Significance

The two clinically defined nonmalignant diseases of the prostate are benign prostatic hyperplasia (BPH) and prostatitis. BPH is a disorder that results in an enlarged prostate. Prostatitis, while technically meaning inflammation of the prostate gland, in clinical practice, it is defined by symptoms such as chronic pelvic pain. The incidence of symptomatic BPH is about 42% for the age group 51 to 60, and this incidence increases with age (Nickel, 2008). BPH symptoms include dysuria, urinary urgency, and nocturia. CP/CPPS is a class of prostatitis where patients complain of recurrent chronic pelvic pain even in the absence of any identifiable pathogen. Chronic prostatitis/chronic pelvic pain syndrome (CP/CPPS) accounts for more than two million annual office visits in the United States alone (Pontari, 2003). Treatments available for prostatitis and BPH patients can help manage the disease, however, patients often relapse with heightened pain, as the etiology of these diseases remains obscure. However, these treatments are accompanied by life-altering side effects including decreased libido, impotence, abnormal ejaculation, orthostatic hypotension, and dizziness (Bruskewitz, 2003). Prostatitis patients experience long-term pain and patients with BPH are left with few options before resorting to surgery. Hence, prostatitis and BPH are poorly characterized diseases of unknown etiology with painful symptoms affecting a large population of men in the U.S. Apart from BPH and prostatitis, another condition that affects the prostate is prostate cancer. Prostate cancer is the second leading cause of cancer-related death for males in the United States. There is emerging evidence that prostate inflammation could have a causal link to prostate cancer. The major association has been derived from histological examination of prostate tissues that have

proliferative inflammatory atrophy (PIA) lesions. These PIA lesions are observed in inflamed prostates and often merge with high-grade prostatic intraepithelial neoplasia (PIN), a major direct cancer precursor lesion (De Marzo et al., 1999; Wang et al., 2009).

Several studies link prostate inflammation to BPH, prostatitis, and prostate cancer (Alexander et al., 1998; De Marzo et al., 1999; De Marzo et al., 2007; Kramer et al., 2007; McLaren et al., 2011; Nickel, 2008). Cytokines are important mediators of inflammation, and overexpression of cytokines has been associated with prostate diseases (Alexander et al., 1998; Culig and Puhr, 2012). Interleukin 1β (IL-1β) is a proinflammatory cytokine that is implicated in prostate diseases (Alexander et al., 1998; Nadler et al., 2000). By developing a novel mouse model of inducible prostate inflammation, we are testing our hypothesis that IL-1β–mediated inflammation can transform the prostate microenvironment and initiate pre-malignant and malignant changes. Recent evidence suggests that localized inflammation could result in DNA damage leading to differential gene expression in epithelial cells (Hahn et al., 2008; Hmadcha et al., 1999; Hodge et al., 2005; Qian et al., 2008). Our hypothesis is warranted because several studies have supported the idea that inflammation results in the accumulation of reactive oxygen species (ROS) and reactive nitrogen species (RNS) that leads to tissue damage. The overall objective of this study is to test our hypothesis by complete characterization of the IL-1β-mediated inflammation model, and then assess the aberrant gene expression changes mediated by inflammation while also conducting pain evaluation studies. This contribution is significant because this model will help elucidate molecular mechanisms involved in major inflammatory

diseases of the prostate. This will help to identify novel therapeutic targets and inflammatory molecules that would be useful diagnostic markers. Thus, important advances in the treatment of prostate inflammatory diseases can be expected along with clues to understanding the etiology of these diseases. Additionally, this model, when fully characterized, would serve as a valuable preclinical model to test potential therapeutic drugs against prostatic inflammatory-related diseases. Furthermore, by breeding to extant prostate cancer models, the role of inflammation in prostate cancer development and progression can be investigated.

In order to better rationalize the research work presented here, I provide a literature review as well as essential background information in the next chapter.

Chapter 1:

Background

Abbreviations

AcP	Accessory Protein
APC	Antigen Presenting Cell
AR	Androgen Receptor
AARs	Alpha-Adrenergic Receptors
AUR	Acute Urinary Retention
BOO	Bladder Outlet Obstruction
BPH	Benign Prostatic Hyperplasia
CMV	Human Cytomegalovirus
CNS	Central Nervous System
COX-2	Cyclooxygenase-2
CP	Chronic Prostatitis
CPPS	Chronic Pelvic Pain Syndrome
CPSI	Chronic Prostatitis Symptom Index
CRP	C-Reactive Protein
CRPC	Castration-Resistant Prostate Cancer
DAMPS	Danger-Associated Molecular Patterns
DHT	Dihydrotestosterone
Dox	Doxycycline
EPS	Expressed Prostatic Secretions
ERG	ETS-Related Gene
FGF	Fibroblast Growth Factor
GFP	Green Fluorescent Protein

GSTP1	Gluthathione-S Transferase Promoter
HGPIN	High Grade Prostate Intraepithelial Neoplasia
IL-1	Interleukin 1
IL-1β	Interleukin 1β
IL-1R1	Interleukin 1 Receptor 1
LUTS	Lower Urinary Tract Symptoms
MDSCs	Myeloid-Derived Tumor Suppressor Cells
MTOPS	The Medical Therapy of Prostatic Symptoms
NGF	Nerve Growth Factor
NIH	National Institutes of Health
NIH-CPSI	National Institutes of Health Chronic Prostatitis Symptom Index
NLR	Nucleotide Binding Domain-Like Receptors
NLRP3	Nucleotide Binding Domain-Like Receptor Protein 3
NOD	Non-Obese Diabetic
NSAID	Non-Steroid Anti-Inflammatory Drug
PAMPS	Pathogen-Associated Molecular Patterns
PCPT	Prostate Cancer Prevention Trial
PIA	Proliferative Inflammatory Lesions
PIN	Prostate Intraepithelial Neoplasia
PSA	Prostate Specific Antigen
REDUCE	The Reduction by Dutasteride of Prostate Cancer Events
RtTA	Reverse Tetracycline Transactivator

Tet	Tetracycline
TetO	Tetracycline Operator
TetR	Tetracycline Repressor
TGF-β	Tumor Growth Factor
TNF-α	Tumor Necrosis Factor-α
TRE	Tetracycline Response Element
tTA	Tetracycline Transactivator
TURP	Transurethral Resection of Prostate
UGM	Urogenital Mesenchyme
UGS	Urogenital Sinus
UPOINT	Urinary, Psychosocial, Organ Specific, Neurologic, Tenderness
WBCs	White Blood Cells

1.1 Prostate Gland

1.1 Morphology

Approximately 30,000 men die of prostate cancer each year in the United States, making prostate cancer the second leading cause of death from cancer for men in the U.S. (Siegel et al., 2014). The human prostate gland is located between the pelvic diaphragm and peritoneal cavity. It is situated just below the bladder, encasing the proximal urethra as it extends from the bladder. It is traditionally described as 'walnut shaped' due to its conical structure and size. The human prostate anatomy described by McNeal consists of different zones: the central zone, peripheral zone and the transition zone (McNeal, 1981). The zones can be differentiated by histology, anatomical location, and their susceptibility to prostate pathologies (Lee et al., 2011). Most carcinomas develop from the peripheral zone, which constitutes 70% of the glandular prostate. The central zone comprises 25% of the glandular prostate and the transition zone makes up the remaining 5% (De Marzo et al., 2007). The transition zone is often associated with benign prostatic hyperplasia (BPH) or enlarged prostate, a common condition that arises with age. The transition zone and peripheral zone often harbor focal atrophy, acute, and chronic inflammation, while these features are seldom observed in the central zone (De Marzo et al., 2007) (Figure 1). While all the zones have a glandular and stromal compartment, the glandular-to-stromal ratio differs among the zones. The transition zone is primarily fibromuscular. This could explain the transition zone's high susceptibility to develop BPH, which is considered a disease of the fibromuscular stroma.

In contrast to human prostates, the murine prostate can be divided into four lobes: ventral, dorsal, lateral and anterior prostate. The anterior lobe is adjacent to the seminal vesicles while the other lobes surround the bladder and urethra. Although the lobes have similar white, opaque, and spongy appearances, they can be differentiated by histology and anatomical landmarks.

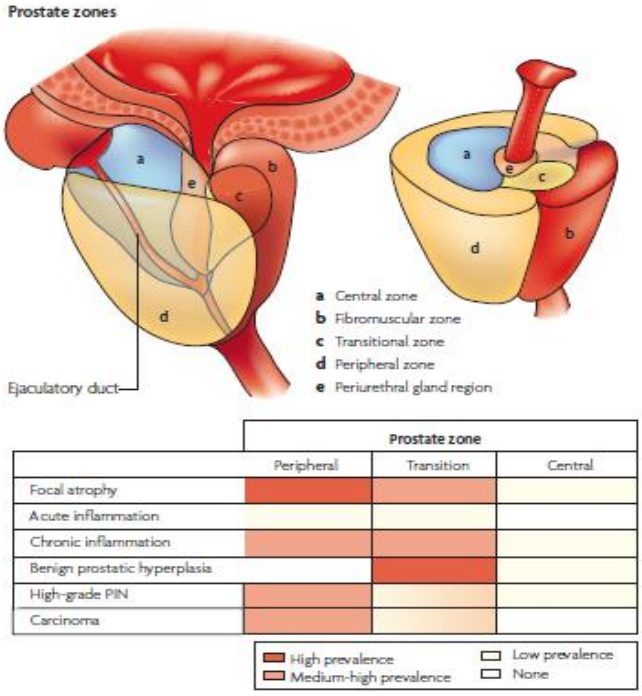

Figure 1: Incidence of inflammation in human prostate zones. Note high prevalence of inflammation in the peripheral zone (De Marzo et al., 2007)

The prostate gland's primary function is to contribute secretory proteins into the seminal fluid that coat and uncoat spermatozoa. These secretory proteins are also vital for interactions with the cervical mucus. One of the most well studied secretory proteins is the prostate specific antigen (PSA). PSA is a secretory prostate protein that can be measured in the serum and the results are reported as ng/ml. The PSA test is an FDA-approved test to aid in prostate cancer diagnosis and prognosis. .PSA is secreted by columnar epithelial cells and is usually present at very low levels. However, in prostate cancer patients, a higher PSA level is often linked to poor prognosis of prostate cancer (Hayward and Cunha, 2000).

Unlike the architecture of the human prostate gland, the mouse prostate is anatomically different. The most distinctive difference between human and mouse prostate anatomy is that the murine prostate is lobular, while the human prostate is zonal and enclosed in a pseudocapsule. Although the mouse and human prostates have structural differences, they have similarities in physiological function and are composed of the same cell types. Both the human and mouse prostatic ducts are lined by a single layer of columnar luminal epithelial cells, beneath which lie basal cells and scattered neuroendocrine cells.

1.1.2 Development

In all mammals, the prostate develops from the urogenital sinus (UGS) that is surrounded by the urogenital mesenchyme (UGM). The UGS is derived from the cloaca, the caudal terminus of the hindgut. The endodermal UGS is an embryonic constituent of both sexes. It develops into the prostate, prostatic urethra, and bulbourethral gland in males, while it develops into the urethra and vagina in females. It also develops into the bladder in both sexes. Fetal androgens play an important role in directing this differentiation, initiating the epithelial bud development from the UGS. A specific prostate ductal pattern exists that is well regulated in rodents. The prostatic ducts develop into the ventral, dorsal, anterior, and lateral glands. In rodents, cytodifferentiation of epithelial cells occur 12-20 days post-natally. The presence of prostate secretory proteins is also detected post-natally. While the epithelium undergoes differentiation, the mesenchyme differentiates into smooth muscle cells and fibroblasts (Cunha et al., 2004).

Epithelial-mesenchymal interactions play a vital role during prostate growth, development, and morphogenesis, and epithelial-stromal interactions are crucial in maintaining a functional homeostasis in the adult prostate. Disruption in these interactions has been postulated to play a role in benign and malignant prostate diseases (Cunha et al., 2004).

1.2 BPH and chronic prostatitis

1.2.1 Benign prostatic hyperplasia

BPH is a debilitating condition that results in enlargement of the prostate gland. It primarily affects men above the age of 50, with 80% of men in their 70s diagnosed with BPH (Yoo and Cho, 2012). BPH is a chronic disease that significantly lowers the quality of life in suffering men. Patients experience lower urinary tract symptoms (LUTS) such as painful micturition, dribbling, urinary incontinence, urinary retention, and nocturia. The etiology of BPH is currently unclear; however, several treatments have evolved over the years. The economic and financial implications associated with BPH are a concern for the health care system in the United States. Over four billion dollars are spent every year on BPH and these costs are increasing as treatments for the condition continue to emerge (Taub and Wei, 2006).

The prostate has two major spurts of growth. The first is during puberty when the prostate doubles in size, and the second, more slower growth occurs after the age of 25. From then on, it continues to grow gradually for the rest of a male's life. BPH occurs in the transition zone of the human prostate that encases the proximal urethra. As the prostate enlarges, it presses against the base of the bladder resulting in urinary

symptoms. Gradually, the bladder weakens, resulting in urinary incontinence and/or bladder obstruction due to the prostate tissue.

Diagnosis for this condition begins with a digital rectal examination that will allow the physician to assess the size of the prostate, as well as check for any nodules that could indicate the presence of a malignancy. This may be followed by urine analysis to rule out infectious agents, a urine flow test that will aid to develop treatment options based on the severity of the condition, or urodynamic studies to determine bladder outlet obstruction (BOO). Although BPH is not a precursor to prostate cancer, it may be present concomitantly with cancer.

Etiology

Age and androgens were the first suggested etiological factors of BPH. Today, inflammation, lifestyle, and metabolic syndrome are also being considered as risk factors. Studies have shown that the incidence of metabolic syndrome has increased to 39% in the United States. The link to BPH emerged from studies where patients diagnosed with Type II diabetes had a larger prostate. This may be attributed to insulin resistance, resulting in aberrant endocrine changes and the increase in insulin-like growth factor, allowing higher proliferation of prostatic cells. Data from the placebo arm of the Prostate Cancer Prevention Trial (PCPT) revealed an increased risk of BPH with lack of exercise as well as consumption of high-fat food and red meat (Kristal et al., 2008). Androgens are vital for prostate growth as they initiate several signaling pathways via the Androgen Receptor (AR). The use of 5α-reductase inhibitors that block the conversion of testosterone, a primary androgen, to dihydrotestosterone, has been effective for the majority of BPH patients. However, BPH being a multifactorial

disease, not all patient symptoms are relieved by this treatment. Testosterone is converted to the potent estrogen, estradiol-17-β, by aromatase, and since estrogen directly regulates prostate growth, studies are ongoing to understand how estrogens might be involved in prostate growth, and more importantly, to BPH (Nicholson and Ricke, 2011). Over the past few years, the role of inflammation in BPH progression has been gathering special interest, in part due to epidemiological data linking inflammation as a poor prognosis factor (Kramer and Marberger, 2006; Kramer et al., 2007; McLaren et al., 2011). The next paragraph will discuss this association in detail, as it highlights the importance of my research.

Inflammation and BPH

Inflammation is a frequent histological finding that is closely associated with BPH. Epidemiological studies have associated inflammation as a causal factor in this disease. Cytokine expressions in serum or expressed prostatic secretions have been proposed as potential biomarkers for BPH. The Reduction by Dutasteride of Prostate Cancer Events (REDUCE) study revealed that greater than 78% of biopsies had inflammation, and the severity of inflammation correlated with LUTS (Nickel et al., 2008). Kramer *et al.* identified T lymphocytes, B cells and macrophages as the major population of prostate infiltrates, and also observed increased cytokine expression of interferon gamma, tumor growth factor (TGF-β), and IL-2. They

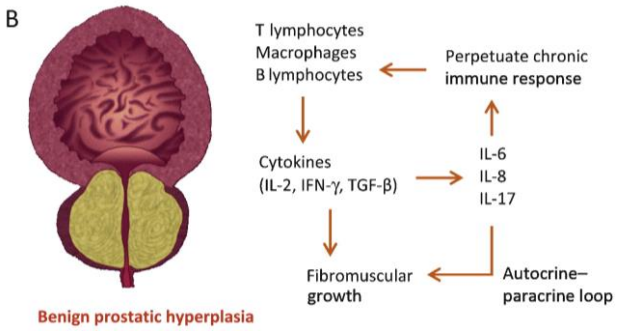

Figure 2: A model that depicts the link between inflammation and BPH (Kramer and Marberger, 2006)

speculated that the activation of lymphocytes and TGF-β induces fibromuscular growth that results in an enlarged prostate. IL-17 production by T helper17 cells could induce Cyclooxygenase-2 (COX-2) expression in prostate epithelial cells in BPH (Kramer and Marberger, 2006). Figure 2 represents a model that illustrates a causal link between inflammation and BPH. As shown in the figure, several cytokines like IL-6, IL-8, and IL-15 have been reported to be overexpressed in BPH patients (Giri and Ittmann, 2001; Handisurya et al., 2001).

Treatment Options

Depending on the severity of the disease, different surgical and medical therapy options are available for BPH patients. The majority of common treatments are described below:

NON- SURGICAL OPTIONS

1. Alpha-adrenergic blockers - The Alpha-Adrenergic Receptors (AARs) are present ubiquitously in the smooth muscle of the human body. There are several subtypes of AARs; however, the α1A-AR subtype is mainly expressed in the prostate and urethra, while the α1D-AR subtype is present on the detrusor muscle of the bladder. Treatment with alpha-1 blockers relaxes the muscles on the bladder, urethra, and prostate, relieving symptoms such as BOO, irregular urine flow, and painful urination. Some of the most commonly used alpha-1 blockers that are usually administered as the first line of treatment include alzusosin, doxazosin, tamsulosin, and terazosin (Kawabe et al., 2006; Yoo and Cho, 2012). Most of these drugs have different binding affinities; however, they exhibit only minor differences with respect to adverse effects. Side effects of

alpha-1 blockers include severe hypotension, retrograde ejaculation, reduced sexual function, dizziness, and fatigue. Moreover, the long term use of alpha-1 blockers has not demonstrated a reduced risk for acute urinary retention (AUR) or BPH-related surgery (Emberton et al., 2008).

2. 5-alpha reductase inhibitors - 5-alpha reductase is a vital enzyme required for the conversion of testosterone into its more potent form, dihydrotestosterone (DHT). 5-alpha reductase inhibitors block this conversion resulting in regression of epithelial cells as well as a decreased prostate volume. Finasteride and dutasteride are commonly used BPH treatment drugs. While finasteride inhibits 5-alpha reductase isoenzyme II and III, dutasteride blocks all three. The Medical Therapy of Prostatic Symptoms (MTOPS) trial examined the effects of monotherapy with doxazosin or finasteride, and dual therapy with doxazosin and finasteride. The trial revealed that 67% of patients administered dual therapy had a decrease in BPH progression whereas only about 34% exhibited a decrease in BPH severity for monotherapy with finasteride or doxazosin. This line of treatment is often advised for patients with LUTS symptoms associated with enlarged prostate (Yoo and Cho, 2012).

SURGICAL OPTIONS

1. Transurethral Resection of Prostate (TURP) - Surgical options are considered for BPH/LUTS patients when non-invasive treatment options are less effective. TURP is the most effective procedure to relieve patients that have BOO. This procedure involves inserting a catheter into the urethra and removing sections that are obstructing the bladder. However,

complications during surgery can arise such as post-operative bleeding, infections, or the need for follow-up surgery.

2. Open prostatectomy - This procedure can remove prostate tissue composing BPH without resulting in adverse effects such as TUR syndrome, a life-threatening condition that arises as a result of absorption of the electrolyte-free irrigation liquid used during operation. Laparoscopic simple prostatectomy is an alternatively less invasive procedure. Table 1 provides a comprehensive list of BPH treatments.

TABLE 1. Treatment options for benign prostatic hyperplasia

Watchful waiting		
Nonsurgical treatment	Medical treatment	Alpha-adrenergic blockers
		5-Alpha reductase inhibitor
		Phosphodiesterase 5 inhibitors
		Aromatase inhibitors
		Plant extracts (phytotherapy)
		Combination of these agents
Surgical treatment	Minimally invasive & endoscopic surgery	Transurethral resection of the prostate
		Transurethral needle ablation of the prostate
		Transurethral microwave therapy of the prostate
		Transurethral incision of the prostate
		Intraprostatic stents
	Laser surgery	Vaporization of the prostate
		Enucleation of the prostate
	Invasive surgery	Open simple prostatectomy
		Laparoscopic simple prostatectomy

Table 1: Treatment options for benign prostatic hyperplasia (Yoo and Cho, 2012)

1.2.2 Prostatitis

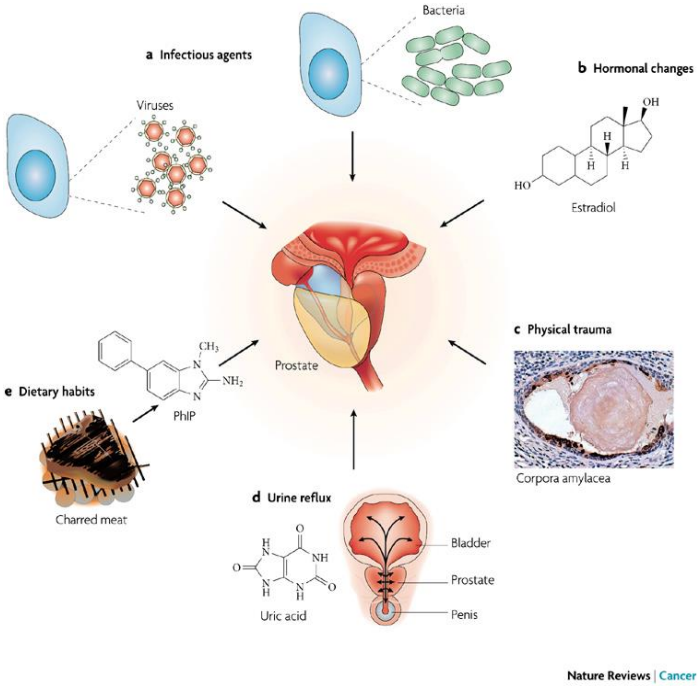

Figure 3: Agents that induce inflammation in the human prostate (De Marzo et al., 2007)

Prostatitis is a painful condition often associated with inflammation. The symptoms associated with prostatitis include chronic pelvic pain, urinary frequency, urinary retention, painful urination, painful ejaculation, and sexual dysfunction. Inflammation in the prostate is triggered by various factors such as bacteria, viral agents, hormonal changes, urine reflux, physical injury, and dietary habits (Figure 3). Prostatitis can affect men of any age. It accounts for two million office visits annually in the US alone and is the most common urinary tract condition among men under the age of 50. CP/CPPS is the least understood type of prostatitis that affects 10-15% of U.S. males (Murphy et al., 2009). To correctly diagnose and treat this condition, the National Institutes of Health (NIH) have devised the following categories for prostatitis:

Category I- Acute Bacterial Prostatitis: A bacterial infection of the prostate gland that can be treated with appropriate antibiotics. This condition is diagnosed by the presence of White Blood Cells (WBCs) in the urine or Expressed Prostatic Secretions (EPS), and a urine culture to determine the presence of a foreign pathogen.

Category II- Chronic Bacterial Prostatitis: An infection that lasts for more than three months is classified as 'chronic infection.' Diagnosis is similar to Category I.

Category III- Chronic prostatitis/chronic pelvic pain syndrome (CP/CPPS): 90-95% of prostatitis cases belong to Category III (Habermacher et al., 2006). This condition was formerly known as non-bacterial prostatitis and is further sub-divided into two types:

Type IIIa- Infammatory CP/CPPS

Type IIIb- Non-inflammatory CP/CPPS

Both Type IIIa and IIIb patients have chronic pelvic pain accompanied by the absence of any foreign pathogens. The factor distinguishing these two sub-types is the presence of WBCs in Type IIIa patient urine/EPS and the absence of WBCs in IIIb patients.

Category IV- Asymptomatic Prostatitis (CP/CPPS): This condition exhibits the presence of WBCs along with the absence of pain or presence of bacterial agents. This is often diagnosed while evaluating other conditions.

Apart from the above mentioned diagnosis strategies, a digital rectal exam and a complete history are also evaluated. NIH has also formulated a NIH-CPSI (Chronic Prostatitis Symptom Index) to quantify the pain experienced by patients.

Etiology

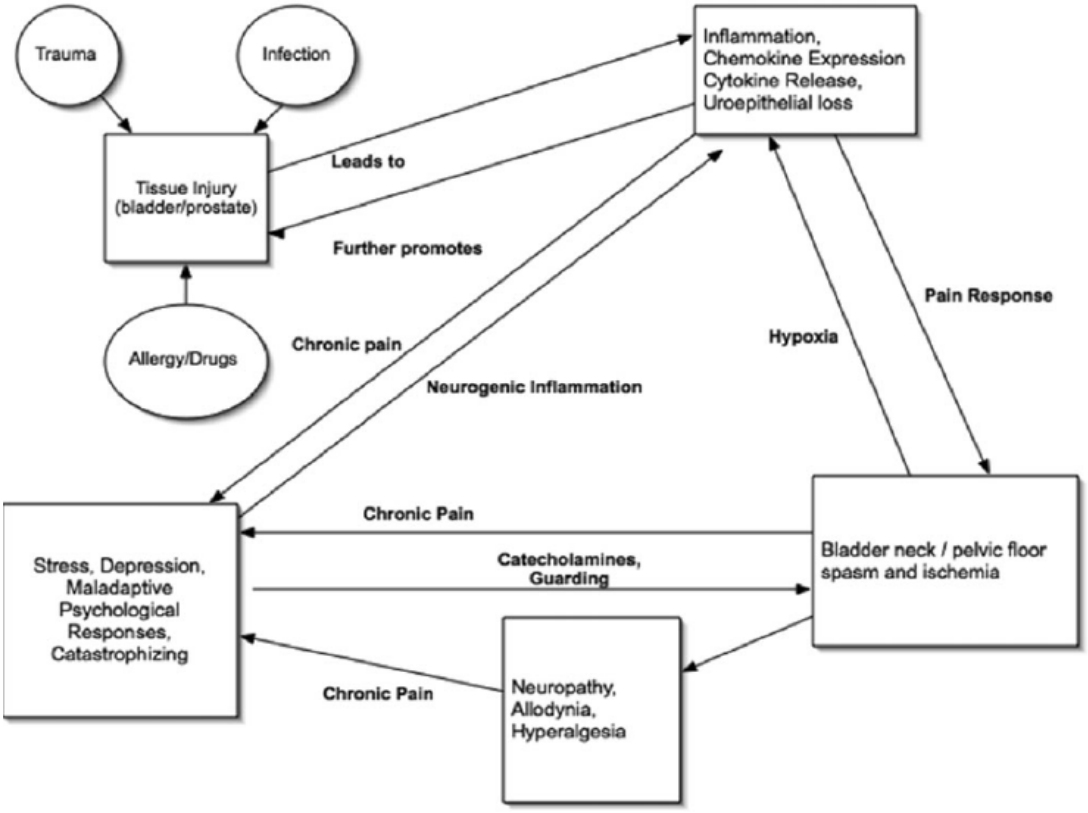

Figure 4: Multifactorial etiology of CP/CPPS (Shoskes and Nickel, 2013)

For bacterial prostatitis, several pathogens have been isolated from chronic prostatitis (CP) patients. These are listed below:

1. Gram-negative uropathogens (i.e. Escherichia coli, Klebsiella spp, Pseudomonas spp, etc.)
2. Gram-positive uropathogens, e.g. Enterococcus spp, and other organisms such as Chlamydia and Mycoplasma (Nickel, 2000)

Apart from these viruses, diphtheroids and anaerobes have also been proposed to be causal factors.

Unfortunately, for most cases of non-bacterial prostatitis or CP/CPPS, the cause is unknown. Inflammation triggered by diet, hormonal changes, or urine reflux has been proposed to be a major factor in CP/CPPS. But the exact evidence or mechanism is still unclear and this will be discussed in detail below. Moreover, chemicals, neurological factors, stress, depression, drugs, prostate injury, as well as chemokine and cytokine overexpression have been linked to the pain symptoms associated with CP/CPPS (See Figure 4 for more details)

Inflammation and Prostatitis

Several research groups have attempted to understand the link between inflammation and prostatitis. Cytokines are important immune modulators, however, their overexpression has been linked to prostate pathology. A study conducted to determine the levels of the cytokines tumor necrosis factor-α (TNF-α) and IL-1β in semen isolated from CP patients reported elevated levels in CP patients in comparison to controls (Alexander et al., 1998). A similar study with a larger cohort of 202 patients reported that 85% of cases have elevated levels of proinflammatory cytokines IL-6 and IL-8. They also observed a correlation between the level of cytokines and symptom score (NIH-CPSI score) (Paulis et al., 2003). Cytokines, in particular IL-1β, will be discussed in detail later in this section.

Treatment Options

Antibiotics are prescribed for treatment of the majority of acute bacterial prostatitis cases, and are generally efficacious. Unfortunately, most antibiotics have poor penetration into the prostate tissue; hence, fluoroquinols (eg: Ciprofloxacin and Levofloxacin) have been the preferred choice for treatment. However, the development of fluoroquinol resistance has resulted in additional treatments with a third-generation Cephalosporin (eg, Ceftazidime or Ceftriaxone).

Several monotherapies are available for CP/CPPS patients. These include anti-microbial therapy, hormonal therapy, phytotherapy, alpha-blockers, antibiotics, and non-pharmacological therapies. While some patients have benefitted by these treatments, a large majority of patients have recurrent or worsening symptoms. Treatment with alpha-blockers such as Alfusozin, Silodosin, and Terazosin has proven to be beneficial in randomized controlled trials (Cheah et

Domain	Diagnostic criteria	Potential treatments
Urinary	Bothersome irritative or obstructive urinary symptoms	Alpha-blockers Antimuscarinics
	High postvoid residual	
Psychosocial	Clinical depression	Psychologic or Psychiatric counseling
	Catastrophizing (verbalized helplessness and hopelessness)	Cognitive behavioral therapy
Organ specific (bladder or prostate)	Specific prostate tenderness	Quercetin (e.g., Prosta-Q)
	Hematospermia	
	Symptom relief with voiding	Pollen extract (e.g., Q-Urol)
		Pentosan polysulfate
Infection	Positive cultures of prostatic fluid in absence of UTI	Antibiotics
	Concomitant urethritis	
Neurologic/ systemic	Pain outside pelvis	Pregabalin
	Systemic pain syndrome	Amitriptyline
Tenderness	Pelvic floor spasm	Pelvic physical therapy
	Muscle trigger points	Myofascial Release

Table 2: UPOINT phenotyping criteria for CP/CPPS patients (Shoskes and Nickel, 2013)

al., 2003; Nickel et al., 2006; Nickel et al., 2011); however, two multi-center tests showed negative results (Alexander et al., 2004).

Antibiotics are a common mode of therapy even in the absence of bacterial outgrowth in cultured prostatic fluid specimens. However, several authors have speculated on the presence of cryptic, non-culturable microorganisms in the prostate reviewed in an article by Dr. Sfanos (Sfanos et al., 2013). A study conducted to discern the effects of Levofloxacin in CP/CPPS patients revealed improvement of symptoms in both the control and treated groups (Nickel et al., 2003). Although the results from this study strongly suggest that Levofloxacin is not an effective drug to treat prostatitis, it is still routinely prescribed by urologists (Shoskes and Nickel, 2013). This could be due to anecdotal reports of mild relief after prescribing Levofloxacin to prostatitis patients.

Several non-traditional therapies have been investigated for efficacy in treating CP patients. Phytotherapy, a treatment incorporating supplements containing extracts from bee pollen and plants/fruits improved the symptoms in certain CP/CPPS patients (Elist, 2006). Quercetin, a natural bioflavanoid commonly occurring in fruits, leaves, and vegetables, has been reported to be useful for chronic prostatitis patients due to its antioxidant and anti-inflammatory properties (Shoskes and Nickel, 2013; Shoskes et al., 1999).

Pharmacological agents targeting the Central Nervous System (CNS) have been tested on CP/CPPS patients. However, in a randomized controlled trial, Pregabalin, used to treat neuropathic pain, showed no significant improvement in CP/CPPS

patients. Moreover, 59% of the patients enrolled in the drug group presented with mild to moderate reactions (Pontari et al., 2010).

Development of UPOINT System

Most monotherapies discussed previously did not significantly improve the quality of life for CP/CPPS patients (Cheah et al., 2003; Nickel et al., 2006; Shoskes et al., 1999). To better direct the treatment approach, CP/CPPS symptoms were divided into several domains: Urinary, Psychosocial, Organ specific, Neurologic, or Tenderness (UPOINT). The rationale behind this approach is that CP/CPPS is a heterogeneous disease that often presents with multiple symptoms that require a multi-modal treatment approach. Doctors can now clinically parse the symptoms into one or more of these domains and treat for the positive domains. Multiple domain involvement often results in longer duration of treatment and is related to more severe symptoms. Table 2 outlines each domain and its specific treatment options.

1.3 Prostate Cancer

1.3.1 Prostate Cancer Etiology

Prostate adenocarcinoma refers to cancers originating from epithelial cells. If left untreated, these cancers can metastasize to liver, lung, lymph nodes, and bone. Prostate cancer is the most common non-cutaneous cancer in American men. It accounts for ~220,000 new cancer cases every year, and ~27,500 deaths are anticipated in 2016. The development of the PSA blood test three decades ago has resulted in over-diagnosis of prostate cancer and is a well recognized problem. This means that many patients with low grade cancer were treated that most likely did not need to be treated. PSA is serine protease that is a component of normal prostate secretions but can be

detected in the peripheral blood when normal prostate architecture is disrupted (Shen and Abate-Shen, 2010).

One of the major etiological factors associated with prostate cancer is age, as it mainly manifests in men above the age of 60 (American Cancer Society, 2009). Environmental factors and diet have also been studied as risk factors, since the incidence of prostate cancer is higher in the U.S. compared to Asian countries (Dunn, 1975; Haenszel and Kurihara, 1968). 10% of prostate cancer cases have been traced to hereditary factors with early onset disease (Schaid, 2004; Wiklund et al., 2004). As men age, the ratio of androgens to estrogens varies, and this could be a contributing factor to cancer initiation (De Marzo et al., 2007).

1.3.2 Prostate Cancer Development

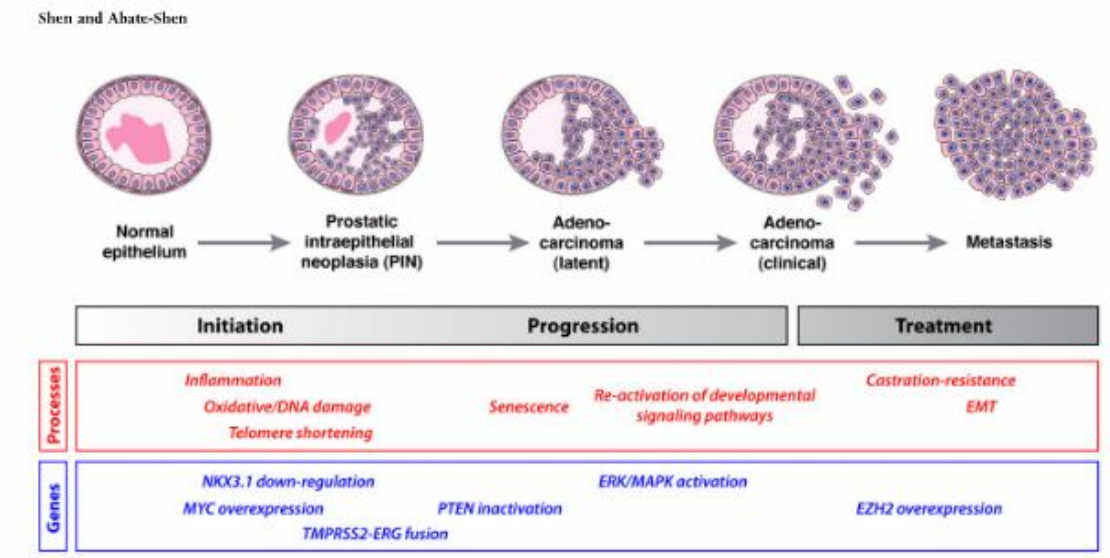

Figure 5: Stages of human prostate cancer are illustrated with key genes/pathways that are significant at different stages (Shen and Abate-Shen, 2010)

PIN, or prostate intraepithelial neoplasia, is a pre-neoplastic lesion that is histologically characterized by luminal cell crowding as well as nuclear and nucleolar

enlargement. PIN is widely accepted as a precursor to prostate cancer and it can be distinguished by immunostaining with p63 and CK5/18 antibodies that detect the basal cell population, while the cells are similar in appearance to invasive carcinoma. A loss in the basal cell population and the histological appearance of carcinoma can confirm carcinogenesis (Humphrey, 2007). Most prostate cancer cases are adenocarcinoma or of epithelial origin; however, less than 2% of these cases are mucinous carcinogenesis defined by extraluminal mucin or originating from neuroendocrine cells (Abate-Shen and Shen, 2000). PIN lesions often develop into adenocarcinoma where the cells invade the extracellular matrix and the basal lamina, and, if left untreated, they could metastasize. The most common sites of metastasis are lung, liver, pleura, and the bone, resulting in osteoblastic lesions (Bubendorf et al., 2000). There are several molecular changes that are associated with the progression from PIN to metastasis. NKX3.1 downregulation and Myc overexpression have been reported in a majority of prostate cancer cases (Bethel et al., 2006; Gurel et al., 2008). These molecular changes occur early in prostate cancer. Gene fusions in which an ETS transcription factor is fused to an androgen regulated gene occur in upto 50-60% of prostate cancers. The most common one is TMPRSS2-ERG fusion (Tomlins et al., 2005). Greater than 90% of cases overexpressing ERG have this genetic fusion (Tomlins et al., 2008). Recently, ETS gene fusion status has been used to molecularly classify prostate cancer cases. Additionally, other genetic changes have been identified as a result of genomic instability. In the case of NKX3.1, deletion of one allele of chromosome 8p is frequently observed in a majority of prostate cancer cases. Some of these changes have been highlighted in figure 5. In advanced prostate cancer cases, after multiple waves of

effective androgen deprivation therapy, the cancer can progress into androgen independence or castration resistant prostate cancer. The AR pathways compensate for the loss of androgens either by gene amplification or other mechanisms such as activating point mutations (Shen and Abate-Shen, 2010)

The treatment options for prostate cancer depend on the stage of cancer, age of the individual, and if the cancer is organ confined. Active surveillance or watchful waiting is an option available to patients presenting with low PSA levels and long life expectancy. Studies comparing prostatectomy vs. watchful waiting reported a decrease in overall mortality in the prostatectomy group (Bill-Axelson et al., 2014). Radiation, prostatectomy, or cryosurgical ablation are the common treatment options for organ-confined prostate cancer (Wasson et al., 1993). More than five decades ago, Charles Huggins demonstrated that removal of the testes resulted in significant regression of the prostate tumor as a result of the ensuing androgen deprivation. Currently, chemotherapeutic androgen ablation therapy is used to suppress the androgen signaling axis, which is effective in 60-80% of patients who present with androgen-dependent cancer. Unfortunately, the majority of these cases transition to androgen-independent cancer that progresses and eventually metastasizes (Feldman and Feldman, 2001). Docetaxel, a chemotherapeutic agent that interferes with cell division, has shown promising results for metastatic castration-resistant prostate cancer since 2004. It has been tested in clinical trials to study its effects as a monotherapeutic drug and as a combination drug (Petrylak et al., 2015). To date, no drug administered in combination with Docetaxel has improved survival compared to Docetaxel alone in a phase III trial (Petrylak et al., 2015). Enzalutamide is an androgen-signaling molecule that inhibits

nuclear translocation of AR, DNA binding, and cofactor recruitment. It extends survival in patients with metastatic castration-resistant cancer that have undergone chemotherapy (Scher et al., 2012).

Sipuleucel-T, an Antigen-Presenting Cell (APC) cell-based immunotherapy was developed that resulted in a 41% reduction in risk of patient death in comparison to placebo (Kantoff et al., 2010). Other immunotherapies based on immune checkpoint inhibitors have been gaining significant interest. Anti-CTLA-4 is a monoclonal antibody that blocks the inhibitory signal generated by the interaction between CTLA-4 and PD-1 found on T cells. This antibody has already been approved for treatment in late stage melanoma and is currently in phase III clinical trials to treat metastatic Castration-Resistant Prostate Cancer (CRPC) (Schweizer and Drake, 2014).

1.3.3 The Link Between Inflammation and Prostate Cancer

Data from several independent studies have revealed that inflammation is a frequent histological finding in the prostate. The baseline group of the REDUCE study reported that 80% of the examined biopsies had some level of inflammation (Nickel et al., 2008). Furthermore, NIH category I, II, and III prostatitis affect 16% of U.S. men at some point in their lives (Brede and Shoskes, 2011; Collins et al., 2002). However, the incidence of asymptomatic prostatitis is confounding and hence there is an urgent need to evaluate the inflammatory phenotype associated with prostate pathology.

Chronic inflammation is thought to be an etiological factor in 20% of all adult cancers (De Marzo et al., 2007). The role of inflammation in prostate cancer initiation and progression is still unclear. However, more evidence has emerged that causally links inflammation to prostate cancer. For example, the use of aspirin, a Non-Steroid

Anti-Inflammatory Drug (NSAID), has demonstrated the ability to reduce the overall risk of prostate cancer development in a population, but other NSAIDs did not produce a similar effect (Veitonmäki et al., 2013). C-Reactive Protein (CRP), an acute-phase reactant produced by the liver, can be detected in the blood plasma during inflammation. A study conducted to evaluate the link between CRP and CRPC reported that higher levels of CRP were linked to poor prognosis in CRPC patients. Since CRP is a marker of inflammation, this study provides evidence that it may play a role in late stage prostate cancer development (Prins et al., 2012).

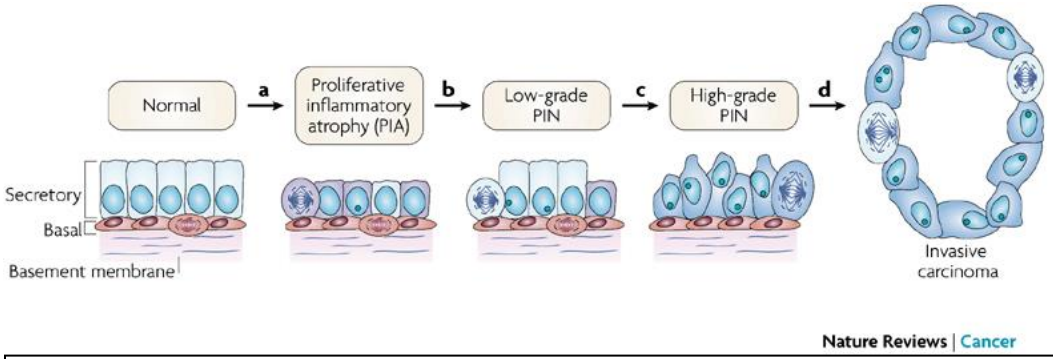

Figure 6: A model illustrating how inflammatory lesions can give rise to PIN and eventually cancer (De Marzo et al., 2007)

There is mounting evidence indicating that prostate inflammation plays a causative role in prostate cancer. Epidemiology data link the incidence of prostatitis and sexually transmitted infections with a small to moderate risk of prostate cancer (Dennis et al., 2002; Nelson et al., 2004). Additionally, the use of anti-inflammatory drugs and antioxidants have a significant effect on reducing prostate cancer risk (Nelson et al., 2004). Hypermethylation and gene silencing of Glutathione-S Transferase Promoter (GSTP1), a gene required to assist the cell during oxidative damage, is detected in a majority of prostate cancer cases (Gonzalgo et al., 2003;

Nakayama et al., 2003). Gene expression changes in NKX3.1, MYC and AR detected in high-grade pin (HGPIN) and prostate cancer were also detected in proliferative inflammatory atrophy (PIA) (Celma et al., 2014). PIA lesions are epithelial cells with a high proliferative index among the presence of activated lymphocytes and other inflammatory cells. Molecular pathology data revealed PIA at times as a direct precursor to PIN and subsequently to prostate cancer (Figure 6) (Gurel et al., 2014). This study provides the most convincing data for prostate inflammation playing a causative role in prostate cancer initiation/progression. Further studies will be required to corroborate these data and dissect the mechanisms that will aid in better diagnostics and therapeutics for inflammation-associated pathology. One potentially fruitful area of exploration is the development of engineered animal models in which prostate inflammation develops. An inducible mouse model where the effects of sustained inflammation and episodic inflammatory events can be studied will be highly valuable.

Studying the effect of prostate inflammation in prostate diseases is almost impossible to do in humans. However, a mouse model that closely resembles features of prostate diseases can be highly beneficial. Moreover, if the mouse model is inducible, wherein the gene of interest can be ‘turned-on’ and ‘turned-off’ at will, this will further extend the utility of the model.

1.4 Tetracycline-Controlled Tissue Specific Gene Expression

1.4.1 Tet-On Systems

Conditional expression of a transgene is important to generate a useful

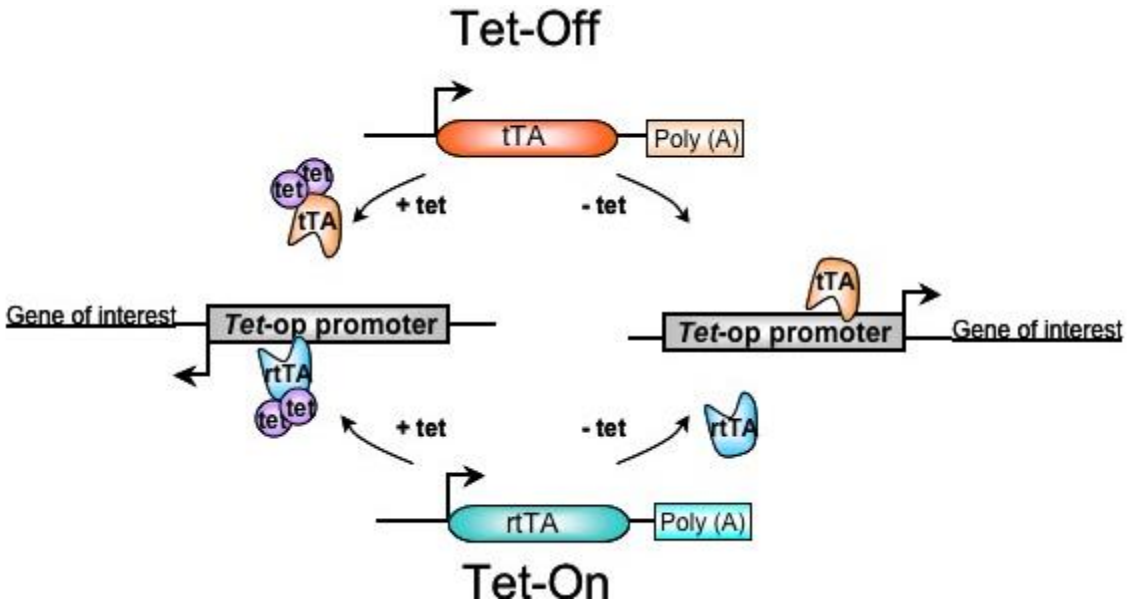

Figure 7: The Tet-On and Tet-Off system https://www.genoway.com/technologies/tet-system.htm

transgenic mouse where the function of a particular transgene relevant in human pathologies can be evaluated accurately. The Tet-On and Tet-Off systems allow inducible expression of the transgene that is tightly regulated by a Tetracycline (Tet) derivative called doxycycline (Dox) (Sprengel and Hasan, 2007). The Tet-inducible expression systems have been extensively used *in vitro* and *in vivo* for a wide variety of applications. These systems allow the investigator to control gene expression in a spatial and temporal manner (Sun et al., 2007).

The components of this system have been borrowed from the bacterial Tet-resistance operon. In gram-negative bacteria, the TetA resistance protein helps to protect the organism from the potent antibiotic, Tet. Under normal circumstances, TetA is not expressed in the bacteria as the Tetracycline Repressor (TetR) dimers bind to Tet

Operator (TetO) sequences and physically hinder transcriptional activation at TetR and TetA promoter regions. When the intracellular concentrations of Tet rise, they bind to TetR, resulting in a change in conformation that releases it from TetO sequences and allows transcriptional activation of TetA resistance protein. The TetR-Tet complex changes when Tet levels decrease intracellularly (Sprengel and Hasan, 2007).

The pioneering work by Gossen and Bujard has allowed this system to be translated into all eukaryotes (Gossen et al., 1995). The Tetracycline Transactivator (tTa) protein was developed by fusing the herpes simplex virus transcription activator (VP16) to the C-terminus of TetR. The tTa was then able to bind to TetO sequences through the TetR domain. In this way, the TetR protein was converted to a transcriptional activator. Then, a Tet Response Element (TRE) was synthesized by combining seven TetO sequences with the Pol II transcriptional start site isolated from the human Cytomegalovirus (CMV). In the presence of Tet or Dox, tTA is unable to bind to the TRE and hence the gene of interest is not expressed. In the absence of Tet, the tTA is free to bind and activate transcription. This is the Tet-Off system (Figure 7).

By adding four point mutations to the tTA protein, the rtTA protein was generated (Urlinger et al., 2000). Reverse tetracycline Transactivator, rtTA, works as the inverse of tTA protein. Hence, in the Tet-On system (Figure 7), in the presence of Dox, rtTA forms a complex with Dox and initiates transcription for the gene of interest. Upon Dox withdrawal, the gene of interest is not transcribed, as the rtTA-Dox complex cannot form.

Doxycycline inducible transgenic mice can be generated by developing two different strains of genetically engineered mice, one carrying the activator cassette and

a second carrying the responder cassette. These two mice strains can be interbred to generate double transgenic animals. Tetracycline-regulated systems allow temporal and spatial control of the gene of interest. Ubiquitous promoters are used to drive tTA or rtTA when transgene expression is examined in the whole organism. Tissue-specific promoters are used to isolate the function of the transgene in an organ-specific manner. There are several promoters available to drive prostate-specific transgene expression, the most commonly used one being Probasin, an androgen-dependent promoter. Our lab has developed Hoxb13, a transcription factor that belongs to the Homebox gene family. Hoxb13 regulatory elements have been extensively studied in our laboratory to drive prostate-specific gene expression. Hoxb13 is described in detail in a later section.

The decision to use either the Tet-On or Tet-Off system depends on the type of experiment. If the gene of interest needs to be rapidly turned on at a specific developmental stage, then the Tet-On system is useful. In contrast, the Tet-Off system is useful when the gene of interest needs to be on for a considerably longer period of time. One of the major limitations with Tet-based systems is the leakiness of the Tet promoter, which is the result of the rtTA protein having weak affinity for the TetO, in the absence of doxycycline. The leakage is also promoter dependent and depends on the integration site. This limitation can be overcome by having multiple founder lines and screening for the transgenic line with minimum leakiness.

1.4.2 Hoxb13 Driven Reverse Tetracycline Transactivator System for Conditional Expression in the Prostate

Hox genes, first identified in Drosophila as an important player in anterior/posterior patterning, are conserved across species from nematodes to vertebrates (McMullin et al., 2009). During evolution, the Hox clusters expanded and resulted in 13 paralogous groups. Most Hox genes are expressed exclusively during embryonic development (see Figure 8), but some Hox genes are expressed throughout organogenesis and in adult tissue (McMullin et al., 2010). During development, Hoxb13 is expressed in the central nervous system, paraxial mesoderm, urogenital sinus and hindgut (Rao et al., 2012). Adult Hoxb13 expression is restricted to prostate, distal colon, and rectum. Hoxb13 expression is highest in the ventral prostate lobe compared to the anterior and dorso-lateral lobes (McMullin et al., 2009). Several prostate-restricted promoter elements are available, but Hoxb13 regulatory elements are largely androgen independent. An androgen independent promoter like Hoxb13 will allow robust transgene expression even in the absence of testicular androgens (see Figure 9). The androgen-independent feature will be useful when breeding inducible

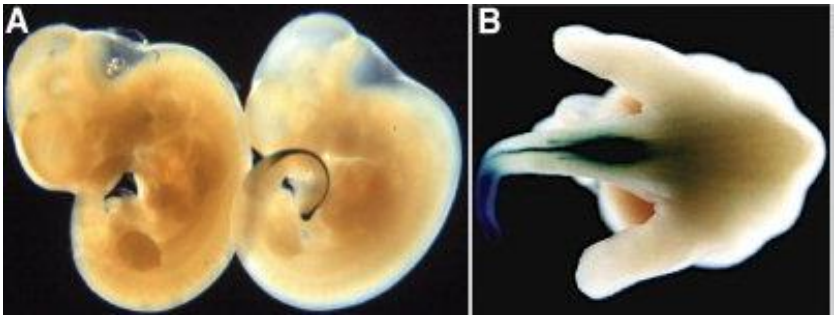

Figure 8: Hoxb13-lacZ expression in the caudal regions of embryos. A- right-Whole mount X-gal stained embryo and left-negative control .B-dorsal-posterior view of positive stained embryo (McMullin et al., 2009)

inflammation models to extant models of prostate cancer, where androgen-independent prostate cancer needs to be examined in detail.

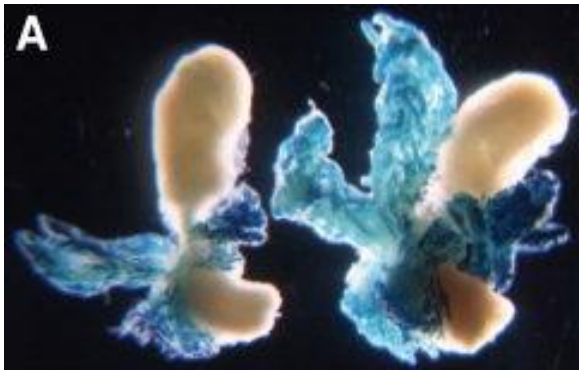

Figure 9: Hoxb13-lac Z expression in adult prostates (blue). Left –castrated mouse, right-normal prostate. Note robust Hoxb13 expression in the presence or absence of testicular androgens **(**McMullin et al., 2009**)**

Mouse models allowing inducible gene expression vastly increase the utility of a model as the consequences of dynamic gene expression changes can be studied. To create a prostate-specific inducible mouse model, rtTA expression was driven by *Hoxb13 cis*-regulatory elements (Rao et al., 2012).

Hoxb13-rtTA animals were crossed with TetO-GFP mice to generate Hoxb13-rtTA|TetO-GFP animals. A cohort of double transgenic mice were either treated with Dox (+Dox) or left untreated (-Dox). Their whole prostates were examined under white light and UV light (see Figure 10)

After Dox treatment, Green Fluorescent Protein (GFP) mRNA expression was detected at six hours post-treatment and it then peaked by 24 hours. After Dox-withdrawal, GFP mRNA expression significantly decreased at 24 hours and was

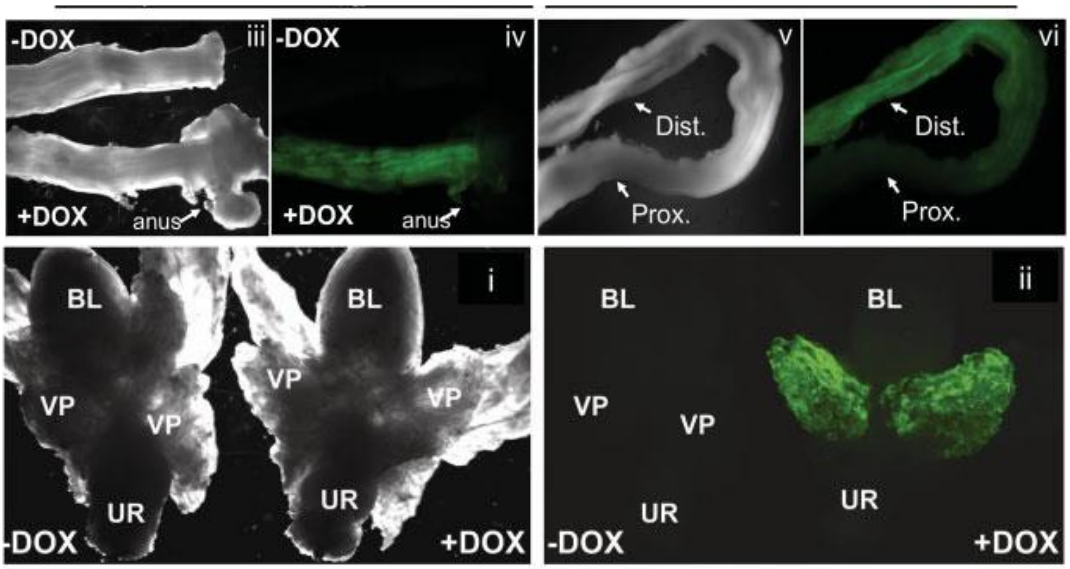

Figure 10: GFP expression only observed in Dox-treated TetO-GFP|Hoxb13-rtTA mice (+Dox) but not controls (-Dox). Images clicked under white and UV light. Note GFP expression only observed in distal colon. BL-Bladder, VP- Ventral Prostate, UR-Urethra, Dist/Prox- Distal or Proximal colon (Rao et al., 2012)

completely depleted at 48 hours. These data demonstrate the rapid induction and withdrawal kinetics of this system (Rao et al., 2012).

Apart from inducible transgene expression, an ideal mouse model should be physiologically relevant to human prostate diseases. Interleukins are major players in mediating chronic inflammation. The characteristics of interleukins and their role in prostate malignancies are discussed below.

1.5 Interleukins

Cytokines are small secretory proteins that are important regulators of the immune system. Interleukins are a subset of cytokines that are released by a wide-range of immune cells to regulate cell differentiation, proliferation, cell activation, maturation,

and migration. The exact function of each interleukin is difficult to determine, but it depends on the secretory cell, the phase of inflammation, and the receptor cell. These immunomodulatory proteins can bind to high-affinity cell surface receptors and elicit either a proinflammatory or anti-inflammatory response. Interleukins have been classified into major families based on genetic and structural similarities (Brocker et al., 2010). The Interleukin 1 (IL-1) super family consists of 11 cytokines with structural similarities, such as the presence of packed β-sheets (Dinarello, 2011). Members of the Interleukin 1 family include IL-1α, IL-1β and IL-RA. These three molecules have each been extensively studied for their unique biological function, however they share some structural similarities and bind to the same receptor, Interleukin 1 Receptor 1 (IL-1R1). They also have a shared conformation known as the β-trefoil: a structure comprised of 12-packed β-sheets.

1.5.1 Interleukin 1β

Interleukin 1β (IL-1β) is one of the best-characterized members of the IL-1 family. IL-1β is an important member of the innate immune system that elicits a proinflammatory response at the site of secretion. IL-1β is synthesized as a precursor, pro-IL-1β, that is cleaved into the mature 17kDa version, by proteolytic cleavage by Caspase 1. IL-1β is secreted by keratinocytes, fibroblasts, endothelial, neuronal, and immune cells (Ren and Torres, 2009).

Upon binding of IL-1β to its receptor IL-1R1, it dimerizes with Accessory Protein (AcP) and initiates an intracellular signaling cascade (Pillarisetti, 2011). It plays an important role in maintaining homeostatic functions in the organism such as

regulating sleep, temperature, and feeding (Dinarello, 1996). However, overexpression of IL-1β is implicated in inflammatory bowel disease, rheumatoid arthritis, and multiple sclerosis (Ren and Torres, 2009).

1.5.2 Role of Interleukin 1β During Pain and Inflammation

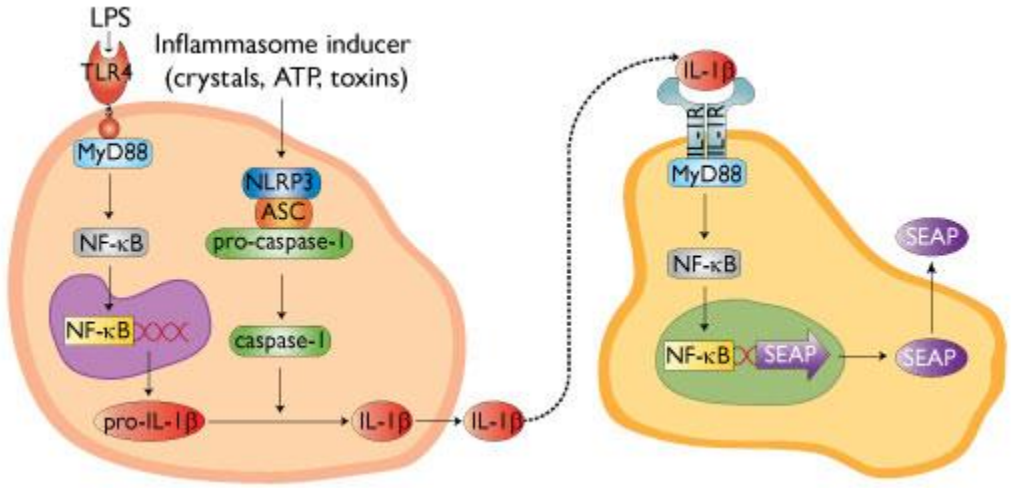

Figure 11: An illustration depicting the interaction between an immune cell and nerve cell. Note IL-1β can directly bind to receptors on neurons. Source: http://www.invivogen.com/hek-blue-il1b

Interleukin-1 was discovered in the 1970s and was referred to as lymphocyte-activating factor (Krause et al., 2012). IL-1β protects the host from a range of pathogens including viruses, fungi, and bacteria (Gross et al., 2009; Hsu et al., 2008). Unlike other cytokines that have a signal sequence to aid in cell secretion, IL-1β is secreted in a two-step process. First, NF-κB-mediated transcriptional upregulation of pro-IL-1β is required. This is then followed by Caspase-1 cleavage (Martinon et al., 2002). Caspase-1 is activated by the inflammasome, a complex consisting of Nucleotide-binding domain Like Receptors (NLR) and other adaptor proteins. NLR protein 3 (NLRP3) is the most studied protein in this family. A range of signals via

Pathogen-Associated Molecular Patterns (PAMPS) and Danger-Associated Molecular Patterns (DAMPS) activates the inflammasome. PAMPS that activate the NLRP3 inflammasome include viral DNA, viral RNA, and bacterial toxins. DAMPS include nanoparticles, skin irritants, extracellular ATP, etc. IL-1β can mediate an inflammatory response by promoting T cell survival, B cell antibody production, increased expression of IL-2 receptor on lymphocytes, and supporting Th17 differentiation (Krause et al., 2012). Although this cytokine is important for host defense, overexpression of IL-1β has been implicated in gout, type II diabetes, arthritis, and cancer (Maedler et al., 2002; Okamoto et al., 2010; Schumacher et al., 2012). Overexpression of IL-1β in mouse epithelium resulted in infiltration of neutrophils and macrophages. This led to enhanced mucin production, airway fibrosis, and airspace enlargement (Lappalainen et al., 2005).

Apart from immune cells, IL-1β is also expressed in neurons in the central nervous system (CNS) and is associated with nerve injury (Parnet et al., 1994). Expression of IL-1β by neurons, microglia, and astrocytes can result in the influx of neutrophils that could result in neuroinflammation. Studies on animal pain models and human data indicate that IL-1β expression is often associated with neuroinflammation and neuropathic pain (Milligan et al., 2003; Watkins and Maier, 2002; Watkins et al., 1995). IL-1β levels were elevated in animal models after spinal injury, sciatic nerve transection, and other constriction injury models. In a murine model of bone cancer, elevated pain levels were measured by thermal hyperalgesia and then treated with a therapeutic anti-IL-1β antibody, Anakinra (Baamonde et al., 2007).

The question that arises next is how does IL-1β induce pain? IL-1β-mediated inflammation can induce cyclooxygenase 2 (COX-2) to produce prostaglandins (Ahn

et al., 2005; Samad et al., 2001). Prostaglandins can sensitize peripheral nociceptive receptors resulting in pain. IL-1β production also results in the production of Nerve Growth Factor (NGF) that can increase neuronal survival, differentiation, and axonal development. Blocking COX-2 has shown significant relief in pain hypersensitivity initiated centrally. NGF levels are upregulated in acute and chronic inflammatory conditions. Plantar injection of IL-1β led to increased hypersensitivity and elevated NGF levels that were blocked by IL-1β inhibition. The thermal hyperalgesia was prevented by treatment with anti-NGF antibody but the NGF levels remained the same. Furthermore, IL-1β expression can result in increased synthesis of nociceptors and can directly activate nociceptive channels inducing pain hypersensitivity. The p38 mitogen-activated protein kinase pathways appear to play an important role in this process (Pillarisetti, 2011).

1.5.3 Interleukin 1β in Cancer

Evidence from clinical studies suggests that polymorphisms in pro-inflammatory cytokines, for example, IL-1β, TNF-a, and IL-6, are associated with various diseases including cancer (Bidwell et al., 1999; Howell et al., 2002). About 20% of all human cancers arise as a result of chronic inflammation (De Marzo et al., 2007). The role of inflammation in gastric cancer has been well studied. One study examined IL-1β overexpression in the stomach epithelium to induce gastric cancer and mobilize myeloid-derived suppressor cells in mice (Tu et al., 2008). The rationale behind this study was that often polymorphisms associated with IL-1β were linked to increased expression of this cytokine. In the prostate, polymorphisms of IL-1β have

been linked to higher risk of prostate cancer, however direct evidence linking IL-1β and prostate cancer is lacking (Michaud et al., 2006).

Several models of prostate inflammation have been developed and characterized. Each model has its own unique features. Key findings and details of extant prostate inflammation models are described below.

1.6 Rodent Models of Prostate Inflammation: Key Findings

Animal models are an effective platform to understand the molecular mechanisms of human diseases. For decades, rodents have been the primary choice to develop animal models relevant to human diseases. Since 1974, when Rudolf Jaenisch created the first genetic mouse model, there has been an expansion in transgenic mouse genetics with significant discoveries about new biomarkers and therapies for human malignancies (Buschard, 2011; Yang and Santamaria, 2006). Key findings from rodent models related to prostatitis, BPH, and prostate inflammation-mediated cancer are discussed below.

1.6.1 Prostate inflammation models

Several animal models have been developed and characterized to decipher this multi-etiological disorder. They are classified into the following groups: spontaneous, infections, autoimmune, and others.

Spontaneous models- Certain strains of rats, for example, male Lewis rats, develop prostate inflammation in the lateral lobe at around 12 weeks of age. This occurs in ~70% of the animals in this strain. This number increases to around 77% in male Wistar rats. However, in a different strain, Sprague-Dawley, the percentage decreases to 16%

in male rats. The prostate inflammation is specific to the ventral lobe in Sprague-Dawley, while in the Wistar rats they appear in the dorso-lateral lobe. The inflammation in these rats is nonbacterial and the incidence increases with age in most of the above-mentioned strains, with the exception of Sprague-Dawley. In the case of mice, Non-Obese Diabetic (NOD) mice have been reported to develop prostate inflammation that is apparent at approximately 20 weeks of age. In summary, the rats provide a good model for prostate inflammation; however, the unpredictable incidence of inflammation is a drawback that limits further characterization (Lundgren et al., 1984; Sharma et al., 1992; Vykhovanets et al., 2007) .

Infectious models- Several mice and rat models of bacterial prostatic inflammation have been developed and characterized. Bushman *et al.* reported that mice infected with *E.coli* for five days developed chronic inflammation that persisted for 12 weeks post-inoculation (Boehm et al., 2012). Oxidative damage and increase in cell proliferation was observed in epithelial cells compared to controls (Elkahwaji et al., 2007). Another independent study revealed upregulation of various cytokines such as TNF-α, IL-1β, IL-6, IL-10, and IL-18 in *E.coli*-infected mice (Boehm et al., 2012). A human bacterial isolate was used to initiate prostate inflammation in a mouse model which resulted in decreased AR expression in the prostate epithelium and an increase in macrophages and lymphocytes, especially Th17 cells (Simons et al., 2015). Although these models are useful to study acute and chronic bacterial prostatitis, they do not model nonbacterial cases of CP/CPPS that account for 90% of all prostatitis cases.

Autoimmune models- One experimental autoimmune model was developed by injecting rat prostatic antigen mixed with an adjuvant into NOD mice. The mice developed an

autoimmune response mediated by T cells. Another model was developed by adoptive transfer of ovalbumin specific $CD8^+$ T cells to induce an inflammatory response in an ovalbumin-expressing mouse prostate (POET model). The POET model displayed both acute and chronic inflammatory infiltrates. These included $CD4^+$ cells, $CD8^+$ cells, Myeloid-Derived Tumor Suppressor Cells (MDSCs), and T-regulatory cells (Haverkamp et al., 2011).

Hormone induced- Wistar and Lewis rats were studied to develop hormone-induced prostatitis. 17 β-estradiol injections to adult males increased the incidence and severity of spontaneous prostatitis. Neonatal estrogen treatments followed by testosterone injections in adult rats resulted in lateral and ventral lobe-specific prostatitis (Vykhovanets et al., 2007).

1.6.2 Rodent Models of Prostate Cancer and Inflammation

Morphological transitions between PIA and high-grade PIN have been observed frequently (Putzi and De Marzo, 2000; Wang et al., 2009). Several models have been developed to study prostate inflammation and prostate cancer independently (Haverkamp et al., 2008). However, models to discern the mechanisms of inflammation-mediated prostate carcinogenesis are limited. Prostate cancer animal models are being investigated to understand the effects of inflammation. T cells, macrophages, and mast cells are likely to alter the tumor microenvironment and promote carcinogenesis. The POET model described earlier was crossed with HiMYC mice, a model that overexpresses Myc transcriptional factor in the prostate. In this model, prostate inflammation and prostate cancer could be studied in the same system. Inflammation increased the incidence of mPIN in the HiMyc/POET model compared

to HiMyc mice alone (Mimeault and Batra, 2013). Other models have demonstrated the DNA damage evoked by reactive oxygen and nitrogen species, which are byproducts of inflammation (Haverkamp et al., 2008). Developing improved model systems will help to understand the role of chemokines, cytokines, and lymphocytes in cancer initiation and/or progression.

There is an urgent need to develop an inducible mouse model of prostate inflammation that is physiologically relevant to human prostate inflammation. The model will help to discern the link between chronic inflammation and CP/CPPS and BPH. Furthermore, this model will help determine the role of inflammation in prostate carcinogenesis that can aid in the development of novel inflammatory biomarkers and therapies.

1.7 References

Abate-Shen, C., and M. M. Shen, 2000, Molecular genetics of prostate cancer: Genes Dev, v. 14, p. 2410-34.

Ahn, D. K., J. M. Chae, H. S. Choi, H. M. Kyung, O. W. Kwon, H. S. Park, D. H. Youn, and Y. C. Bae, 2005, Central cyclooxygenase inhibitors reduced IL-1beta-induced hyperalgesia in temporomandibular joint of freely moving rats: Pain, v. 117, p. 204-13.

Alexander, R. B., S. Ponniah, J. Hasday, and J. R. Hebel, 1998, Elevated levels of proinflammatory cytokines in the semen of patients with chronic prostatitis/chronic pelvic pain syndrome: Urology, v. 52, p. 744-9.

Alexander, R. B., K. J. Propert, A. J. Schaeffer, J. R. Landis, J. C. Nickel, M. P. O'Leary, M. A. Pontari, M. McNaughton-Collins, D. A. Shoskes, C. V. Comiter, N. S. Datta, J. E. Fowler, R. B. Nadler, S. I. Zeitlin, J. S. Knauss, Y. Wang, J. W. Kusek, L. M. Nyberg, M. S. Litwin, and C. P. C. R. Network, 2004, Ciprofloxacin or tamsulosin in men with chronic prostatitis/chronic pelvic pain syndrome: a randomized, double-blind trial: Ann Intern Med, v. 141, p. 581-9.

Baamonde, A., V. Curto-Reyes, L. Juárez, A. Meana, A. Hidalgo, and L. Menéndez, 2007, Antihyperalgesic effects induced by the IL-1 receptor antagonist anakinra and increased IL-1beta levels in inflamed and osteosarcoma-bearing mice: Life Sci, v. 81, p. 673-82.

Bethel, C. R., D. Faith, X. Li, B. Guan, J. L. Hicks, F. Lan, R. B. Jenkins, C. J. Bieberich, and A. M. De Marzo, 2006, Decreased NKX3.1 protein expression

in focal prostatic atrophy, prostatic intraepithelial neoplasia, and adenocarcinoma: association with gleason score and chromosome 8p deletion: Cancer Res, v. 66, p. 10683-90.

Bidwell, J., L. Keen, G. Gallagher, R. Kimberly, T. Huizinga, M. F. McDermott, J. Oksenberg, J. McNicholl, F. Pociot, C. Hardt, and S. D'Alfonso, 1999, Cytokine gene polymorphism in human disease: on-line databases: Genes Immun, v. 1, p. 3-19.

Bill-Axelson, A., L. Holmberg, H. Garmo, J. R. Rider, K. Taari, C. Busch, S. Nordling, M. Häggman, S. O. Andersson, A. Spångberg, O. Andrén, J. Palmgren, G. Steineck, H. O. Adami, and J. E. Johansson, 2014, Radical prostatectomy or watchful waiting in early prostate cancer: N Engl J Med, v. 370, p. 932-42.

Boehm, B. J., S. A. Colopy, T. J. Jerde, C. J. Loftus, and W. Bushman, 2012, Acute bacterial inflammation of the mouse prostate: Prostate, v. 72, p. 307-17.

Brede, C. M., and D. A. Shoskes, 2011, The etiology and management of acute prostatitis: Nat Rev Urol, v. 8, p. 207-12.

Brocker, C., D. Thompson, A. Matsumoto, D. W. Nebert, and V. Vasiliou, 2010, Evolutionary divergence and functions of the human interleukin (IL) gene family: Hum Genomics, v. 5, p. 30-55.

Bruskewitz, R. C., 2003, Quality of life and sexual function in patients with benign prostatic hyperplasia: Rev Urol, v. 5, p. 72-80.

Bubendorf, L., A. Schöpfer, U. Wagner, G. Sauter, H. Moch, N. Willi, T. C. Gasser, and M. J. Mihatsch, 2000, Metastatic patterns of prostate cancer: an autopsy study of 1,589 patients: Hum Pathol, v. 31, p. 578-83.

Buschard, K., 2011, What causes type 1 diabetes? Lessons from animal models: APMIS Suppl, p. 1-19.

Celma, A., P. Servián, J. Planas, J. Placer, M. T. Quilez, M. A. Arbós, I. de Torres, and J. Morote, 2014, Clinical significance of proliferative inflammatory atrophy in prostate biopsy: Actas Urol Esp, v. 38, p. 122-6.

Cheah, P. Y., M. L. Liong, K. H. Yuen, C. L. Teh, T. Khor, J. R. Yang, H. W. Yap, and J. N. Krieger, 2003, Terazosin therapy for chronic prostatitis/chronic pelvic pain syndrome: a randomized, placebo controlled trial: J Urol, v. 169, p. 592-6.

Collins, M. M., J. B. Meigs, M. J. Barry, E. Walker Corkery, E. Giovannucci, and I. Kawachi, 2002, Prevalence and correlates of prostatitis in the health professionals follow-up study cohort: J Urol, v. 167, p. 1363-6.

Culig, Z., and M. Puhr, 2012, Interleukin-6: a multifunctional targetable cytokine in human prostate cancer: Mol Cell Endocrinol, v. 360, p. 52-8.

Cunha, G. R., W. Ricke, A. Thomson, P. C. Marker, G. Risbridger, S. W. Hayward, Y. Z. Wang, A. A. Donjacour, and T. Kurita, 2004, Hormonal, cellular, and molecular regulation of normal and neoplastic prostatic development: J Steroid Biochem Mol Biol, v. 92, p. 221-36.

De Marzo, A. M., V. L. Marchi, J. I. Epstein, and W. G. Nelson, 1999, Proliferative inflammatory atrophy of the prostate: implications for prostatic carcinogenesis: Am J Pathol, v. 155, p. 1985-92.

De Marzo, A. M., E. A. Platz, S. Sutcliffe, J. Xu, H. Grönberg, C. G. Drake, Y. Nakai, W. B. Isaacs, and W. G. Nelson, 2007, Inflammation in prostate carcinogenesis: Nat Rev Cancer, v. 7, p. 256-69.

Dennis, L. K., C. F. Lynch, and J. C. Torner, 2002, Epidemiologic association between prostatitis and prostate cancer: Urology, v. 60, p. 78-83.

Dinarello, C. A., 1996, Biologic basis for interleukin-1 in disease: Blood, v. 87, p. 2095-147.

Dinarello, C. A., 2011, Interleukin-1 in the pathogenesis and treatment of inflammatory diseases: Blood, v. 117, p. 3720-32.

Dunn, J. E., 1975, Cancer epidemiology in populations of the United States--with emphasis on Hawaii and California--and Japan: Cancer Res, v. 35, p. 3240-5.

Elist, J., 2006, Effects of pollen extract preparation Prostat/Poltit on lower urinary tract symptoms in patients with chronic nonbacterial prostatitis/chronic pelvic pain syndrome: a randomized, double-blind, placebo-controlled study: Urology, v. 67, p. 60-3.

Elkahwaji, J. E., W. Zhong, W. J. Hopkins, and W. Bushman, 2007, Chronic bacterial infection and inflammation incite reactive hyperplasia in a mouse model of chronic prostatitis: Prostate, v. 67, p. 14-21.

Emberton, M., E. B. Cornel, P. F. Bassi, R. O. Fourcade, J. M. Gómez, and R. Castro, 2008, Benign prostatic hyperplasia as a progressive disease: a guide to the risk factors and options for medical management: Int J Clin Pract, v. 62, p. 1076-86.

Feldman, B. J., and D. Feldman, 2001, The development of androgen-independent prostate cancer: Nat Rev Cancer, v. 1, p. 34-45.

Giri, D., and M. Ittmann, 2001, Interleukin-8 is a paracrine inducer of fibroblast growth factor 2, a stromal and epithelial growth factor in benign prostatic hyperplasia: Am J Pathol, v. 159, p. 139-47.

Gonzalgo, M. L., C. P. Pavlovich, S. M. Lee, and W. G. Nelson, 2003, Prostate cancer detection by GSTP1 methylation analysis of postbiopsy urine specimens: Clin Cancer Res, v. 9, p. 2673-7.

Gossen, M., S. Freundlieb, G. Bender, G. Müller, W. Hillen, and H. Bujard, 1995, Transcriptional activation by tetracyclines in mammalian cells: Science, v. 268, p. 1766-9.

Gross, O., H. Poeck, M. Bscheider, C. Dostert, N. Hannesschläger, S. Endres, G. Hartmann, A. Tardivel, E. Schweighoffer, V. Tybulewicz, A. Mocsai, J. Tschopp, and J. Ruland, 2009, Syk kinase signalling couples to the Nlrp3 inflammasome for anti-fungal host defence: Nature, v. 459, p. 433-6.

Gurel, B., T. Iwata, C. M. Koh, R. B. Jenkins, F. Lan, C. Van Dang, J. L. Hicks, J. Morgan, T. C. Cornish, S. Sutcliffe, W. B. Isaacs, J. Luo, and A. M. De Marzo, 2008, Nuclear MYC protein overexpression is an early alteration in human prostate carcinogenesis: Mod Pathol, v. 21, p. 1156-67.

Gurel, B., M. S. Lucia, I. M. Thompson, P. J. Goodman, C. M. Tangen, A. R. Kristal, H. L. Parnes, A. Hoque, S. M. Lippman, S. Sutcliffe, S. B. Peskoe, C. G. Drake, W. G. Nelson, A. M. De Marzo, and E. A. Platz, 2014, Chronic inflammation in benign prostate tissue is associated with high-grade prostate cancer in the placebo arm of the prostate cancer prevention trial: Cancer Epidemiol Biomarkers Prev, v. 23, p. 847-56.

Habermacher, G. M., J. T. Chason, and A. J. Schaeffer, 2006, Prostatitis/chronic pelvic pain syndrome: Annu Rev Med, v. 57, p. 195-206.

Haenszel, W., and M. Kurihara, 1968, Studies of Japanese migrants. I. Mortality from cancer and other diseases among Japanese in the United States: J Natl Cancer Inst, v. 40, p. 43-68.

Hahn, M. A., T. Hahn, D. H. Lee, R. S. Esworthy, B. W. Kim, A. D. Riggs, F. F. Chu, and G. P. Pfeifer, 2008, Methylation of polycomb target genes in intestinal cancer is mediated by inflammation: Cancer Res, v. 68, p. 10280-9.

Handisurya, A., G. E. Steiner, U. Stix, R. C. Ecker, S. Pfaffeneder-Mantai, D. Langer, G. Kramer, N. Memaran-Dadgar, and M. Marberger, 2001, Differential expression of interleukin-15, a pro-inflammatory cytokine and T-cell growth factor, and its receptor in human prostate: Prostate, v. 49, p. 251-62.

Haverkamp, J., B. Charbonneau, and T. L. Ratliff, 2008, Prostate inflammation and its potential impact on prostate cancer: a current review: J Cell Biochem, v. 103, p. 1344-53.

Haverkamp, J. M., B. Charbonneau, S. A. Crist, D. K. Meyerholz, M. B. Cohen, P. W. Snyder, R. U. Svensson, M. D. Henry, H. H. Wang, and T. L. Ratliff, 2011, An inducible model of abacterial prostatitis induces antigen specific inflammatory and proliferative changes in the murine prostate: Prostate, v. 71, p. 1139-50.

Hayward, S. W., and G. R. Cunha, 2000, The prostate: development and physiology: Radiol Clin North Am, v. 38, p. 1-14.

Hmadcha, A., F. J. Bedoya, F. Sobrino, and E. Pintado, 1999, Methylation-dependent gene silencing induced by interleukin 1beta via nitric oxide production: J Exp Med, v. 190, p. 1595-604.

Hodge, D. R., B. Peng, J. C. Cherry, E. M. Hurt, S. D. Fox, J. A. Kelley, D. J. Munroe, and W. L. Farrar, 2005, Interleukin 6 supports the maintenance of p53 tumor suppressor gene promoter methylation: Cancer Res, v. 65, p. 4673-82.

Howell, W. M., P. C. Calder, and R. F. Grimble, 2002, Gene polymorphisms, inflammatory diseases and cancer: Proc Nutr Soc, v. 61, p. 447-56.

Hsu, L. C., S. R. Ali, S. McGillivray, P. H. Tseng, S. Mariathasan, E. W. Humke, L. Eckmann, J. J. Powell, V. Nizet, V. M. Dixit, and M. Karin, 2008, A NOD2-NALP1 complex mediates caspase-1-dependent IL-1beta secretion in response to Bacillus anthracis infection and muramyl dipeptide: Proc Natl Acad Sci U S A, v. 105, p. 7803-8.

Humphrey, P. A., 2007, Diagnosis of adenocarcinoma in prostate needle biopsy tissue: J Clin Pathol, v. 60, p. 35-42.

Kantoff, P. W., C. S. Higano, N. D. Shore, E. R. Berger, E. J. Small, D. F. Penson, C. H. Redfern, A. C. Ferrari, R. Dreicer, R. B. Sims, Y. Xu, M. W. Frohlich, P. F. Schellhammer, and I. S. Investigators, 2010, Sipuleucel-T immunotherapy for castration-resistant prostate cancer: N Engl J Med, v. 363, p. 411-22.

Kawabe, K., M. Yoshida, Y. Homma, and S. C. S. Group, 2006, Silodosin, a new alpha1A-adrenoceptor-selective antagonist for treating benign prostatic hyperplasia: results of a phase III randomized, placebo-controlled, double-blind study in Japanese men: BJU Int, v. 98, p. 1019-24.

Kramer, G., and M. Marberger, 2006, Could inflammation be a key component in the progression of benign prostatic hyperplasia?: Curr Opin Urol, v. 16, p. 25-9.

Kramer, G., D. Mitteregger, and M. Marberger, 2007, Is benign prostatic hyperplasia (BPH) an immune inflammatory disease?: Eur Urol, v. 51, p. 1202-16.

Krause, K., M. Metz, M. Makris, T. Zuberbier, and M. Maurer, 2012, The role of interleukin-1 in allergy-related disorders: Curr Opin Allergy Clin Immunol, v. 12, p. 477-84.

Kristal, A. R., K. B. Arnold, J. M. Schenk, M. L. Neuhouser, P. Goodman, D. F. Penson, and I. M. Thompson, 2008, Dietary patterns, supplement use, and the risk of symptomatic benign prostatic hyperplasia: results from the prostate cancer prevention trial: Am J Epidemiol, v. 167, p. 925-34.

Lappalainen, U., J. A. Whitsett, S. E. Wert, J. W. Tichelaar, and K. Bry, 2005, Interleukin-1beta causes pulmonary inflammation, emphysema, and airway remodeling in the adult murine lung: Am J Respir Cell Mol Biol, v. 32, p. 311-8.

Lee, C. H., O. Akin-Olugbade, and A. Kirschenbaum, 2011, Overview of prostate anatomy, histology, and pathology: Endocrinol Metab Clin North Am, v. 40, p. 565-75, viii-ix.

Lundgren, R., B. Holmquist, M. Hesselvik, and J. Müntzing, 1984, Treatment of prostatitis in the rat: Prostate, v. 5, p. 277-84.

Maedler, K., P. Sergeev, F. Ris, J. Oberholzer, H. I. Joller-Jemelka, G. A. Spinas, N. Kaiser, P. A. Halban, and M. Y. Donath, 2002, Glucose-induced beta cell

production of IL-1beta contributes to glucotoxicity in human pancreatic islets: J Clin Invest, v. 110, p. 851-60.

Martinon, F., K. Burns, and J. Tschopp, 2002, The inflammasome: a molecular platform triggering activation of inflammatory caspases and processing of proIL-beta: Mol Cell, v. 10, p. 417-26.

McLaren, I. D., T. J. Jerde, and W. Bushman, 2011, Role of interleukins, IGF and stem cells in BPH: Differentiation, v. 82, p. 237-43.

McMenamin, M. E., P. Soung, S. Perera, I. Kaplan, M. Loda, and W. R. Sellers, 1999, Loss of PTEN expression in paraffin-embedded primary prostate cancer correlates with high Gleason score and advanced stage: Cancer Res, v. 59, p. 4291-6.

McMullin, R. P., A. Dobi, L. N. Mutton, A. Orosz, S. Maheshwari, C. S. Shashikant, and C. J. Bieberich, 2010, A FOXA1-binding enhancer regulates Hoxb13 expression in the prostate gland: Proc Natl Acad Sci U S A, v. 107, p. 98-103.

McMullin, R. P., L. N. Mutton, and C. J. Bieberich, 2009, Hoxb13 regulatory elements mediate transgene expression during prostate organogenesis and carcinogenesis: Dev Dyn, v. 238, p. 664-72.

McNeal, J. E., 1981, The zonal anatomy of the prostate: Prostate, v. 2, p. 35-49.

Michaud, D. S., S. E. Daugherty, S. I. Berndt, E. A. Platz, M. Yeager, E. D. Crawford, A. Hsing, W. Y. Huang, and R. B. Hayes, 2006, Genetic polymorphisms of interleukin-1B (IL-1B), IL-6, IL-8, and IL-10 and risk of prostate cancer: Cancer Res, v. 66, p. 4525-30.

Milligan, E. D., C. Twining, M. Chacur, J. Biedenkapp, K. O'Connor, S. Poole, K. Tracey, D. Martin, S. F. Maier, and L. R. Watkins, 2003, Spinal glia and proinflammatory cytokines mediate mirror-image neuropathic pain in rats: J Neurosci, v. 23, p. 1026-40.

Mimeault, M., and S. K. Batra, 2013, Development of animal models underlining mechanistic connections between prostate inflammation and cancer: World J Clin Oncol, v. 4, p. 4-13.

Murphy, A. B., A. Macejko, A. Taylor, and R. B. Nadler, 2009, Chronic prostatitis: management strategies: Drugs, v. 69, p. 71-84.

Nadler, R. B., A. E. Koch, E. A. Calhoun, P. L. Campbell, D. L. Pruden, C. L. Bennett, P. R. Yarnold, and A. J. Schaeffer, 2000, IL-1beta and TNF-alpha in prostatic secretions are indicators in the evaluation of men with chronic prostatitis: J Urol, v. 164, p. 214-8.

Nakayama, M., C. J. Bennett, J. L. Hicks, J. I. Epstein, E. A. Platz, W. G. Nelson, and A. M. De Marzo, 2003, Hypermethylation of the human glutathione S-transferase-pi gene (GSTP1) CpG island is present in a subset of proliferative inflammatory atrophy lesions but not in normal or hyperplastic epithelium of the prostate: a detailed study using laser-capture microdissection: Am J Pathol, v. 163, p. 923-33.

Nelson, W. G., A. M. De Marzo, T. L. DeWeese, and W. B. Isaacs, 2004, The role of inflammation in the pathogenesis of prostate cancer: J Urol, v. 172, p. S6-11; discussion S11-2.

Nicholson, T. M., and W. A. Ricke, 2011, Androgens and estrogens in benign prostatic hyperplasia: past, present and future: Differentiation, v. 82, p. 184-99.

Nickel, J. C., 2000, Prostatitis: lessons from the 20th century: BJU Int, v. 85, p. 179-85.

Nickel, J. C., 2008, Inflammation and benign prostatic hyperplasia: Urol Clin North Am, v. 35, p. 109-15; vii.

Nickel, J. C., J. Downey, J. Clark, R. W. Casey, P. J. Pommerville, J. Barkin, G. Steinhoff, G. Brock, A. B. Patrick, S. Flax, B. Goldfarb, B. W. Palmer, and J. Zadra, 2003, Levofloxacin for chronic prostatitis/chronic pelvic pain syndrome in men: a randomized placebo-controlled multicenter trial: Urology, v. 62, p. 614-7.

Nickel, J. C., M. Elhilali, M. Emberton, G. Vallancien, and A.-O. S. Group, 2006, The beneficial effect of alfuzosin 10 mg once daily in 'real-life' practice on lower urinary tract symptoms (LUTS), quality of life and sexual dysfunction in men with LUTS and painful ejaculation: BJU Int, v. 97, p. 1242-6.

Nickel, J. C., M. P. O'Leary, H. Lepor, K. E. Caramelli, H. Thomas, L. A. Hill, and G. E. Hoel, 2011, Silodosin for men with chronic prostatitis/chronic pelvic pain syndrome: results of a phase II multicenter, double-blind, placebo controlled study: J Urol, v. 186, p. 125-31.

Nickel, J. C., C. G. Roehrborn, M. P. O'Leary, D. G. Bostwick, M. C. Somerville, and R. S. Rittmaster, 2008, The relationship between prostate inflammation and lower urinary tract symptoms: examination of baseline data from the REDUCE trial: Eur Urol, v. 54, p. 1379-84.

Okamoto, M., W. Liu, Y. Luo, A. Tanaka, X. Cai, D. A. Norris, C. A. Dinarello, and M. Fujita, 2010, Constitutively active inflammasome in human melanoma cells mediating autoinflammation via caspase-1 processing and secretion of interleukin-1beta: J Biol Chem, v. 285, p. 6477-88.

Parnet, P., S. Amindari, C. Wu, D. Brunke-Reese, E. Goujon, J. A. Weyhenmeyer, R. Dantzer, and K. W. Kelley, 1994, Expression of type I and type II interleukin-1 receptors in mouse brain: Brain Res Mol Brain Res, v. 27, p. 63-70.

Partin, A. W., J. Yoo, H. B. Carter, J. D. Pearson, D. W. Chan, J. I. Epstein, and P. C. Walsh, 1993, The use of prostate specific antigen, clinical stage and Gleason score to predict pathological stage in men with localized prostate cancer: J Urol, v. 150, p. 110-4.

Paulis, G., E. Conti, S. Voliani, M. A. Bertozzi, M. L. Sarteschi, and F. Menchini Fabris, 2003, Evaluation of the cytokines in genital secretions of patients with chronic prostatitis: Arch Ital Urol Androl, v. 75, p. 179-86.

Petrylak, D. P., N. J. Vogelzang, N. Budnik, P. J. Wiechno, C. N. Sternberg, K. Doner, J. Bellmunt, J. M. Burke, M. O. de Olza, A. Choudhury, J. E. Gschwend, E. Kopyltsov, A. Flechon, N. Van As, N. Houede, D. Barton, A. Fandi, U. Jungnelius, S. Li, R. de Wit, and K. Fizazi, 2015, Docetaxel and prednisone with or without lenalidomide in chemotherapy-naive patients with metastatic castration-resistant prostate cancer (MAINSAIL): a randomised, double-blind, placebo-controlled phase 3 trial: Lancet Oncol, v. 16, p. 417-25.

Pillarisetti, S., 2011, Targeting interleukin-1β for pain: CNS Neurol Disord Drug Targets, v. 10, p. 571-5.

Pontari, M. A., 2003, Chronic prostatitis/chronic pelvic pain syndrome in elderly men: toward better understanding and treatment: Drugs Aging, v. 20, p. 1111-25.

Pontari, M. A., J. N. Krieger, M. S. Litwin, P. C. White, R. U. Anderson, M. McNaughton-Collins, J. C. Nickel, D. A. Shoskes, R. B. Alexander, M. O'Leary, S. Zeitlin, S. Chuai, J. R. Landis, L. Cen, K. J. Propert, J. W. Kusek, L. M. Nyberg, A. J. Schaeffer, and C. P. C. R. Network-2, 2010, Pregabalin for the treatment of men with chronic prostatitis/chronic pelvic pain syndrome: a randomized controlled trial: Arch Intern Med, v. 170, p. 1586-93.

Prins, R. C., B. L. Rademacher, S. Mongoue-Tchokote, J. J. Alumkal, J. N. Graff, K. M. Eilers, and T. M. Beer, 2012, C-reactive protein as an adverse prognostic marker for men with castration-resistant prostate cancer (CRPC): confirmatory results: Urol Oncol, v. 30, p. 33-7.

Putzi, M. J., and A. M. De Marzo, 2000, Morphologic transitions between proliferative inflammatory atrophy and high-grade prostatic intraepithelial neoplasia: Urology, v. 56, p. 828-32.

Qian, X., C. Huang, C. H. Cho, W. M. Hui, A. Rashid, and A. O. Chan, 2008, E-cadherin promoter hypermethylation induced by interleukin-1beta treatment or H. pylori infection in human gastric cancer cell lines: Cancer Lett, v. 263, p. 107-13.

Rao, V., J. C. Heard, H. Ghaffari, A. Wali, L. N. Mutton, and C. J. Bieberich, 2012, A Hoxb13-driven reverse tetracycline transactivator system for conditional gene expression in the prostate: Prostate, v. 72, p. 1045-51.

Ren, K., and R. Torres, 2009, Role of interleukin-1beta during pain and inflammation: Brain Res Rev, v. 60, p. 57-64.

Samad, T. A., K. A. Moore, A. Sapirstein, S. Billet, A. Allchorne, S. Poole, J. V. Bonventre, and C. J. Woolf, 2001, Interleukin-1beta-mediated induction of Cox-2 in the CNS contributes to inflammatory pain hypersensitivity: Nature, v. 410, p. 471-5.

Schaid, D. J., 2004, The complex genetic epidemiology of prostate cancer: Hum Mol Genet, v. 13 Spec No 1, p. R103-21.

Scher, H. I., K. Fizazi, F. Saad, M. E. Taplin, C. N. Sternberg, K. Miller, R. de Wit, P. Mulders, K. N. Chi, N. D. Shore, A. J. Armstrong, T. W. Flaig, A. Fléchon, P. Mainwaring, M. Fleming, J. D. Hainsworth, M. Hirmand, B. Selby, L. Seely, J. S. de Bono, and A. Investigators, 2012, Increased survival with enzalutamide in prostate cancer after chemotherapy: N Engl J Med, v. 367, p. 1187-97.

Schumacher, H. R., J. S. Sundy, R. Terkeltaub, H. R. Knapp, S. J. Mellis, N. Stahl, G. D. Yancopoulos, Y. Soo, S. King-Davis, S. P. Weinstein, A. R. Radin, and S. Group, 2012, Rilonacept (interleukin-1 trap) in the prevention of acute gout flares during initiation of urate-lowering therapy: results of a phase II randomized, double-blind, placebo-controlled trial: Arthritis Rheum, v. 64, p. 876-84.

Schweizer, M. T., and C. G. Drake, 2014, Immunotherapy for prostate cancer: recent developments and future challenges: Cancer Metastasis Rev, v. 33, p. 641-55.

Sfanos, K. S., W. B. Isaacs, and A. M. De Marzo, 2013, Infections and inflammation in prostate cancer: Am J Clin Exp Urol, v. 1, p. 3-11.

Sharma, O. P., H. Adlercreutz, J. D. Strandberg, B. R. Zirkin, D. S. Coffey, and L. L. Ewing, 1992, Soy of dietary source plays a preventive role against the pathogenesis of prostatitis in rats: J Steroid Biochem Mol Biol, v. 43, p. 557-64.

Shen, M. M., and C. Abate-Shen, 2010, Molecular genetics of prostate cancer: new prospects for old challenges: Genes Dev, v. 24, p. 1967-2000.

Shoskes, D. A., and J. C. Nickel, 2013, Classification and treatment of men with chronic prostatitis/chronic pelvic pain syndrome using the UPOINT system: World J Urol, v. 31, p. 755-60.

Shoskes, D. A., S. I. Zeitlin, A. Shahed, and J. Rajfer, 1999, Quercetin in men with category III chronic prostatitis: a preliminary prospective, double-blind, placebo-controlled trial: Urology, v. 54, p. 960-3.

Siegel, R., J. Ma, Z. Zou, and A. Jemal, 2014, Cancer statistics, 2014: CA Cancer J Clin, v. 64, p. 9-29.

Simons, B. W., N. M. Durham, T. C. Bruno, J. F. Grosso, A. J. Schaeffer, A. E. Ross, P. J. Hurley, D. M. Berman, C. G. Drake, P. Thumbikat, and E. M. Schaeffer, 2015, A human prostatic bacterial isolate alters the prostatic microenvironment and accelerates prostate cancer progression: J Pathol, v. 235, p. 478-89.

Sprengel, R., and M. T. Hasan, 2007, Tetracycline-controlled genetic switches: Handb Exp Pharmacol, p. 49-72.

Sun, Y., X. Chen, and D. Xiao, 2007, Tetracycline-inducible expression systems: new strategies and practices in the transgenic mouse modeling: Acta Biochim Biophys Sin (Shanghai), v. 39, p. 235-46.

Taub, D. A., and J. T. Wei, 2006, The economics of benign prostatic hyperplasia and lower urinary tract symptoms in the United States: Curr Urol Rep, v. 7, p. 272-81.

Tomlins, S. A., B. Laxman, S. Varambally, X. Cao, J. Yu, B. E. Helgeson, Q. Cao, J. R. Prensner, M. A. Rubin, R. B. Shah, R. Mehra, and A. M. Chinnaiyan, 2008, Role of the TMPRSS2-ERG gene fusion in prostate cancer: Neoplasia, v. 10, p. 177-88.

Tomlins, S. A., D. R. Rhodes, S. Perner, S. M. Dhanasekaran, R. Mehra, X. W. Sun, S. Varambally, X. Cao, J. Tchinda, R. Kuefer, C. Lee, J. E. Montie, R. B. Shah, K. J. Pienta, M. A. Rubin, and A. M. Chinnaiyan, 2005, Recurrent fusion of TMPRSS2 and ETS transcription factor genes in prostate cancer: Science, v. 310, p. 644-8.

Tu, S., G. Bhagat, G. Cui, S. Takaishi, E. A. Kurt-Jones, B. Rickman, K. S. Betz, M. Penz-Oesterreicher, O. Bjorkdahl, J. G. Fox, and T. C. Wang, 2008, Overexpression of interleukin-1beta induces gastric inflammation and cancer and mobilizes myeloid-derived suppressor cells in mice: Cancer Cell, v. 14, p. 408-19.

Urlinger, S., U. Baron, M. Thellmann, M. T. Hasan, H. Bujard, and W. Hillen, 2000, Exploring the sequence space for tetracycline-dependent transcriptional activators: novel mutations yield expanded range and sensitivity: Proc Natl Acad Sci U S A, v. 97, p. 7963-8.

Veitonmäki, T., T. L. Tammela, A. Auvinen, and T. J. Murtola, 2013, Use of aspirin, but not other non-steroidal anti-inflammatory drugs is associated with

decreased prostate cancer risk at the population level: Eur J Cancer, v. 49, p. 938-45.

Vykhovanets, E. V., M. I. Resnick, G. T. MacLennan, and S. Gupta, 2007, Experimental rodent models of prostatitis: limitations and potential: Prostate Cancer Prostatic Dis, v. 10, p. 15-29.

Wang, W., A. Bergh, and J. E. Damber, 2009, Morphological transition of proliferative inflammatory atrophy to high-grade intraepithelial neoplasia and cancer in human prostate: Prostate, v. 69, p. 1378-86.

Wasson, J. H., C. C. Cushman, R. C. Bruskewitz, B. Littenberg, A. G. Mulley, and J. E. Wennberg, 1993, A structured literature review of treatment for localized prostate cancer. Prostate Disease Patient Outcome Research Team: Arch Fam Med, v. 2, p. 487-93.

Watkins, L. R., and S. F. Maier, 2002, Beyond neurons: evidence that immune and glial cells contribute to pathological pain states: Physiol Rev, v. 82, p. 981-1011.

Watkins, L. R., S. F. Maier, and L. E. Goehler, 1995, Immune activation: the role of pro-inflammatory cytokines in inflammation, illness responses and pathological pain states: Pain, v. 63, p. 289-302.

Wiklund, F., B. A. Jonsson, A. J. Brookes, L. Strömqvist, J. Adolfsson, M. Emanuelsson, H. O. Adami, K. Augustsson-Bälter, and H. Grönberg, 2004, Genetic analysis of the RNASEL gene in hereditary, familial, and sporadic prostate cancer: Clin Cancer Res, v. 10, p. 7150-6.

Yang, Y., and P. Santamaria, 2006, Lessons on autoimmune diabetes from animal models: Clin Sci (Lond), v. 110, p. 627-39.

Yoo, T. K., and H. J. Cho, 2012, Benign prostatic hyperplasia: from bench to clinic: Korean J Urol, v. 53, p. 139-48.

Zhang, R., S. Sutcliffe, E. Giovannucci, W. C. Willett, E. A. Platz, B. A. Rosner, J. D. Dimitrakoff, and K. Wu, 2015, Lifestyle and Risk of Chronic Prostatitis/Chronic Pelvic Pain Syndrome in a Cohort of United States Male Health Professionals: J Urol, v. 194, p. 1295-300.

Chapter 2: A Novel Pre-Clinical Mouse Model of Prostate Inflammation Mediated by Interleukin-1β

Disclaimer: This chapter is a manuscript in preparation that has been modified to adhere to dissertation format

Abbreviations

BPH	Benign Prostatic Hyperplasia
CK18	Cytokeratin 18
COX-2	Cyclooxygenase-2
CP	Chronic Prostatitis
CPPS	Chronic Pelvic Pain Syndrome
DAB	3,3'-Diaminobenzidine
Dox	Doxycycline
FACS	Fluorescent Activating Cell Sorting
FBS	Fetal Bovine Serum
FMF	Familial Mediterranean Fever
GABA	Gamma-Aminobutyric Acid
GAPDH	Glyceraldehyde 3-Phosphate Dehydrogenase
GFP	Green Fluorescent Protein
HRP	Horseradish Peroxidase
HTTR	High Temp Target Retrieval
IACUC	Institutional Animal Care and Use Committee
IHC	Immunohistochemistry
IL-1β	Interleukin 1β
IL-1R	Interleukin 1 Receptor
IL-1ra	Interleukin 1 Receptor Antagonist
IMPI	IL-1β-Mediated Prostate Inflammation
JNK	Jun N-Terminal Kinases

LPS	Lipopolysaccharide
MDSCs	Myeloid Derived Suppressor Cells
MTOPS	The Medical Therapy of Prostatic Symptoms
NGF	Nerve Growth Factor
NIH	National Institutes of Health
PBS	Phosphate-Buffered Saline
PC	Prostate Cancer
PIA	Proliferative Inflammatory Atrophy
PIN	Prostatic Intraepithelial Neoplasia
TBST	Tris-Buffered Saline and Tween
TET-O	Tetracycline Operator
TLS	Tertiary Lymphoid Structures
TNF-α	Tumor Necrosis Factor-α
TRE	Tet-Responsive Elements

Abstract

Discerning the roles of inflammation in the initiation and progression of prostate pathologies has been difficult, due in part to the lack of physiologically relevant pre-clinical models. Overexpression of cytokines that function as critical mediators of the inflammatory response has been linked to prostate pathology. Elevated levels of the proinflammatory cytokine, Interleukin 1ß (IL-1ß), have been observed in expressed prostatic secretions of patients with chronic prostatitis/chronic pelvic pain syndrome (CP/CPPS), and genetic polymorphisms associated with IL-1ß are linked to increased risk for aggressive prostate cancer. Here, we report a transgenic mouse model where prostate inflammation is driven by a Tetracycline-regulated IL-1ß transgene. IL-1ß expression in prostate epithelial cells resulted in profound acute inflammation in all prostate lobes, with high penetrance and variable expressivity. A detailed characterization of the model revealed atypical hyperplasia, reactive epithelia, and increased expression of cytokines including IL-6, TNF-α, and IL-17 after doxycycline (Dox) treatment to induce prostatic inflammation. Immunohistochemical analyses revealed a higher proliferative index, and decreased Nkx3.1 expression in the inflamed prostatic epithelial compartment compared to non-inflamed tissue. This model is a versatile platform to interrogate mechanisms of inflammation-associated benign and malignant prostate pathologies.

Introduction

Chronic inflammation has been shown to drive pathogenesis in cardiovascular diseases, diabetes, rheumatoid arthritis, and cancer (De Marzo et al., 2007; Firestein, 2003; Ridker et al., 1997). In the adult prostate gland, chronic inflammation is a frequent histological finding. While ~16% of U.S. men experience symptomatic prostatitis at some point in their lifetime, only 5-10% of these cases can be directly attributed to bacterial infection (Sfanos and De Marzo, 2012). Similarly, benign prostatic hyperplasia (BPH) biopsies frequently harbor inflammatory infiltrates without evidence of infection (Kramer et al., 2007). The Medical Therapy of Prostatic Symptoms (MTOPS) study, which was conducted to test the efficacy of Finasteride and Doxazosin in BPH, revealed that the presence of inflammatory markers, including CD45, CD4, and CD68 correlated with increased risk of BPH progression. However, a causal relationship could not be determined due in part to the confounding effect of anti-inflammatory drugs (Torkko et al., 2015). Inflammatory infiltrates adjacent to the prostate epithelium often coincide with focal atrophic lesions named Proliferative Inflammatory Atrophy (PIA), in which epithelial cells exhibit a higher proliferation index compared to normal epithelium. Histopathological and immunohistochemical studies revealed the juxtaposition of PIA lesions with both Prostatic Intraepithelial Neoplasia (PIN) lesions and adenocarcinoma (De Marzo et al., 2007). While these correlative observations are suggestive of a causative role for inflammation in the initiation or progression of prostate pathology, our understanding of potential

underlying mechanisms remains elusive. This lack of knowledge can be partially attributed to the lack of animal models that permit characterization of the pathological events involved in abacterial prostatic inflammatory events.

Cytokines are vital immunomodulatory secretory proteins that play an important role in directing the course of inflammation, however overexpression of cytokines can result in an over-activated immune response and is implicated in various autoinflammatory disorders including Familial Mediterranean Fever (FMF) and pyogenic arthritis (Dinarello, 2011). Although cytokines have been reported to be overexpressed in multiple prostate pathologies (Alcover et al., 2010; Alexander et al., 1998; McLaren et al., 2011; Michalaki et al., 2004), the role of cytokines in modulating prostatic diseases has not been well characterized. Elevated levels of IL-1β are observed in chronic prostatitis, rheumatoid arthritis, asthma, HIV infection, Alzheimer's disease, solid tumors, leukemia, transplant rejection and pancreatitis (Dinarello, 1996). Additionally, there is mounting evidence on the role of IL-1β in inflammation-associated disorders (Dinarello, 2011). Treatment with Interleukin 1 Receptor Antagonist (IL-1ra), inhibits the IL-1β cascade by competitively binding to its receptor (IL-1R) and has been effectively used in animal models and humans (Dinarello, 2011). IL-1β expression can be induced by a range of factors, lipopolysaccharide (LPS), other cytokines (TNF-α,IL-2, IL-3), cell matrix proteins, clotting factors, lipids, inflammatory by-products (c-reactive protein, neuroactive substances), lipids, and stress factors (Dinarello, 1996). IL-1β is highly inflammatory, lies at the top of the inflammatory cascade, resulting in the activation of NF-κB signaling, the JNK (Jun N-terminal Kinases) and the p38 mitogen-activated protein

kinase pathways which collectively induce the expression of a wide-range of cytokines and chemokines, including Interleukin-6 (IL-6), Interleukin-8 (IL-8), and Cyclooxygenase-2 (COX-2) (Weber et al., 2010). Genetic polymorphisms associated with IL-1β are associated with increased risk for aggressive prostate cancer (Zabaleta et al., 2009), and increased levels of IL-1β were detected in semen isolated from chronic prostatitis patients (Alexander et al., 1998). Overexpression of IL-1β induces gastric inflammation, gastric cancer and recruits Myeloid Derived Suppressor Cells (MDSCs) in mice (Tu et al., 2008). Direct evidence for the role of IL-1β in prostate pathology is lacking, therefore a mouse model where the effects of IL-1β-mediated inflammation can be dissected, is highly valuable.

Several animal models have been developed to understand the molecular pathways, genetic factors, and environmental agents that trigger prostate inflammation (Vykhovanets et al., 2007). A majority of these rodent prostate inflammation models are based on intra-urethral instillation of bacteria (Boehm et al., 2012; Elkahwaji et al., 2007; Khalili et al., 2010). The morphological changes in the prostatic epithelium in response to bacterial inflammation include atypical hyperplasia, dysplasia, and fibrosis (Boehm et al., 2012; Elkahwaji et al., 2007). However, 90-95% of human prostatitis cases have no link to known bacteria or other infectious agents (Habermacher et al., 2006). Therefore, these models are of limited utility in understanding mechanisms of abacterial prostatitis. Several abacterial models of prostatitis have been established that involve hormone-manipulation or immune activation by foreign stimulants (Haverkamp et al., 2011; Naslund et al., 1988). These stimulants can include rat prostate extracts, spermine-binding protein peptide and irritants including transurethral

ethanol/dinitrobenzenesulfonic acid (Altuntas et al., 2013; Lang et al., 2000). Although these models have provided some insight into the relation between inflammation and prostate pathology, an overarching concern with extant models is that they are unlikely to reflect the etiology of most human prostate inflammation cases.

Here, we present the characterization of a novel transgenic mouse system with inducible prostatic inflammation. This model is based on the Tet-On system, wherein the Tetracycline operator (Tet-O) drives expression of IL-1β. Administration of Dox to mice that are doubly transgenic for the *Hoxb13-rtTA* transgene and a newly developed *TetO-IL-1ß* responder allele resulted in an influx of inflammatory cells that infiltrated the stroma, interstitial space, and intra-epithelial region. Inflammation was sustained with continuous Dox administration and upon Dox-withdrawal, the inflammation resolved. This transgenic system represents a robust platform in which the effects of transient and sustained prostatic inflammation can be modeled to determine the pathologic sequelae of inflammatory insult. For convenience, we shall refer to the doubly heterozygous *Hoxb13-rtTA*$^{+/+}$ |*TetO-IL-1ß*$^{+/+}$ mice as IMPI $^{+/-}$ (**I**L-1β-**M**ediated **P**rostate **I**nflammation) and the doubly homozygous mice as IMPI$^{+/+}$ respectively. A subset of these mice also carry the TetO-GFP transgene to test the functionality of the system, and they will be referred to as IMPI$^{+/+}$|GFP.

Materials and Methods

Animal Husbandry and Genotyping

Animal care was provided in accordance with National Institute of Health's *Guide for the care and use of laboratory animals.* All experimental procedures were approved by

the UMBC Institutional Animal Care and Use Committee (IACUC). Animals were housed in an animal facility with controlled temperature at 22±2°C, relative humidity at 55±15% and maintained on a 12h light/12h dark cycle. Water and food were made available to the mice *ad libitum.* Genotyping of IL-β founders was performed by Southern blot analysis of tail DNA. Genomic DNA was isolated using Puregene tissue kit (Qiagen). Ten micrograms of Genomic DNA was digested using EcoRI and EcoRV fast digest enzymes (Fermentas). DNA fragments were separated using gel electrophoresis and transferred to Nytran membrane (VWR cat-28151-400). A single stranded ^{32}P alpha-dATP labelled probe designed against the coding region of IL-1β was added to the hybridization buffer. The 123bp probe was prepared in a PCR reaction containing primer 5'-GAGCTCGTTTAGTGAACC-3', HindIII linearized TetO-IL-1β cassette, buffer, dNTPs, ^{32}P alpha-dATP, and Taq. A positive signal for transgene IL-1β was identified with a band size of 2.1kbp. Once the founder line was established, offsprings were genotyped by PCR. DNA was extracted using AccuStart Mouse genotyping kit (Quanta Biosciences). PCR genotyping primers for IL-1β: Forward- 5'-GAGCTCGTTTAGTGAACC-3'Reverse-ATGCTCTAGATTAGGAACACACAAATTG. Expected product size is 700bp. Doxycycline was obtained from Dr. Phuoc Tran lab at Johns Hopkins University. All Dox administration was performed at a concentration of 2mg/mL unless mentioned otherwise.

Transgene and Responder Cassette Construction

The coding sequence for human IL-1β was cloned downstream of the Tet Operator into pUGH10.3 vector, a gift received from Bujard. To ensure that IL-1β was secreted, the

coding sequence of interleukin 1 receptor antagonist was fused with the coding sequence of human IL-1β (Wingren et al., 1996). The fragment was inserted at the Xba1 restriction site. Colony PCR using the primers listed above followed by sequencing analysis confirmed the insertion of the fragment. The 2100 bp injection fragment was obtained by digesting the plasmid with AseI, DrdI, and XhoI, followed by sucrose gradient and dialysis. Digesting with these three enzymes would ensure efficient isolation of the injection fragment from the remaining plasmid for pro-nuclear injection.

Tissue Harvesting and Processing

Mice were euthanized after administration of Dox at pre-determined intervals: one week, three weeks, three week on/three weeks off and four weeks (n=3). The different lobes of the mouse prostate, bladder, urethra, distal, and proximal colon were fixed in 10% formalin for 48 hours and then switched to 1X Phosphate-Buffered Solution (PBS). The tissue was then processed for standard paraffin embedded sectioning and stained with hematoxylin and eosin.

IL-1β In Situ Hybridization

In-situ hybridization protocol to detect IL-1β mRNA was performed essentially as described (Guedes et al., 2016).

Immunohistochemistry

All tissue sections were deparaffinized at 60 degrees Celsius for 10 minutes followed by tissue rehydration with xylene and alcohol gradient. For Nkx3.1 antigen retrieval, slides were steamed with citrate buffer for 25 minutes and endogeneous peroxidase activity was quenched by incubating with peroxidase blocking solution for five

minutes. Immunohistochemical procedures were performed as described previously (Hubbard et al., 2016). Nkx3.1 primary antibody from UMBC (Chen et al., 2005) was diluted 1:6000, added to the tissue sample and left overnight at four degrees. Poly HRP (Horseradish Peroxidase) anti-rabbit IgG secondary antibody was added for 30 mins. Signal was detected upon addition of chromogen, DAB (3,3'-Diaminobenzidine). Slides were rinsed with Tris-Buffered Saline and Tween (TBST), counter stained with Hematoxylin, dehydrated and mounted. For Ki67 staining, antigen retrieval was performed by steaming with High Temp Target Retrieval (HTTR) (from Leica Biosystems) for 50 minutes. Ki67 antibody was diluted at 1:3000 and incubated with the tissue samples for 45 minutes at room temperature. Subsequent steps were similar to Nkx3.1 staining protocol.

qPCR

RNA was extracted from ventral prostates using the RNeasy RNA miniprep kit (Qiagen). The RNA extraction protocol was performed as per Qiagen guidelines. The ventral prostate tissues were homogenized in 2mL lysis buffer and eluted in 50 microliter volume. Dnase treatment was performed by using Dnase1 kit (Fermentas). Five hundred nanograms of RNA were utilized to make cDNA (Fermentas Maxima cDNA synthesis). The quantitative PCR was performed on the Biorad icycler iQ using the sybr Green master mix (Biorad). The PCR condition used was as follows, step one, 95°C for 1 minute and 30 seconds. Step two, 95°C for 10 seconds. Step three, 57°C for 20 seconds and step four, 72°C for ten seconds. Step two, three and four were repeated for 40 cycles. Data collection and real-time analysis was enabled including melt-curve data collection. Primers were designed using Primer3 software. Primer sequences are

as follows. Mouse IL-1β forward primer- CTG CTT CCA AAC CTT TGA CC , reverse primer- AGC TTC TCC ACA GCC ACA AT. IL-6 forward primer- AGT TGC CTT CTT GGG ACT GA, reverse primer- GAC AGG TCT GTT GGG AGT GG. IL-10 forward primer- CAT GGG TCT TGG GAA GAG AA, reverse primer- AAC TGG CCA CAG TTT TCA GG. IL-18 forward primer- ACA ACT TTG GCC GAC TTC AC, reverse primer- GGG TTC ACT GGC ACT TTG AT. TNF-α forward primer- AGC CCC CAG TCT GTA TCC TT, reverse primer- GAG GCA ACC TGA CCA CTC TC. The qPCR amplifications were performed in triplicates and data was analyzed using the Leevac method. Primers for quantitative PCR were optimized to 90-100% efficiency to quantify cytokine transcript levels that were upregulated in the prostate during inflammation. For the cytokine PCRs, normalization was performed using the housekeeping gene, GAPDH. For the dox-titration experiments, qPCR to quantify hIL-1β transcript levels was normalized with the luminal cell marker, Cytokeratin 18 (CK18). GAPDH forward primer sequence- GAAGGTGAAGGTCGGAGT, reverse primer- GAAGAT- GGTGATGGGATTTC. RtTA forward primer sequence- CTCTCACATCGCGACGGGGC and reverse primer- CCACGGCGGACAGAG-CGTAC. Statistical significance was determined using a student t-test in Prism Graphpad.

Flow Cytometry

IMPI$^{+/+}$|GFP mice at one week post-treatment (n=4), seven weeks post-treatment (n=4), and untreated controls (n=4) were anesthetized and perfused with 1x PBS, making certain to completely perfuse the organ(s) of interest. Prostate and other organs (spleen and lymph nodes) were harvested and suspended in RPMI media (harvest media).

Prostates were trimmed and minced with razor blades. The prostate tissue was incubated with Collagenase I (1 mg/mL, Life Technologies, 17100-017) and 5ml of harvest media for a minimum of 30 minutes at 37 degrees Celsius in shaker. After incubation, the tissue was pushed through a filter, and centrifuged at 913g for 10 minutes at room temperature with the brake on. The supernatant was aspirated and resuspended in 44% Percoll (GE Healthcare, 17-0891-01). Sixty-seven percent Percoll was carefully underlayed and centrifuged at 913g for 20 minutes at room temperature with the brake on. Lymphocytes concentrated at the interface between the two Percoll layers. The interface layer was carefully collected and centrifuged at 1200 RPM for 5-7 minutes at four degrees Celsius with brake on. After the supernatant was aspirated, it was resuspended in media for counting and plating.

For flow cytometry staining, cells were first incubated with Live/Dead Fixable Aqua (Invitrogen) diluted 1:5000 in 1x PBS for 30 minutes at room temperature in the dark, then washed with 1x PBS or FACS (Fluorescent Activated Cell Sorting) buffer (1x PBS and 5% Fetal Bovine Serum (FBS)). Flow antibodies (purchased from BD Pharmingen, eBiosciences, Biolegend or Invitrogen) were diluted in PBS or FACS buffer. Cells were incubated in the diluted antibody cocktails for 20-30 minutes at room temperature in the dark, then washed with 1x PBS or FACS buffer. Samples were either re-suspended in PBS or FACS buffer for immediate analysis or subjected to a gentle 30 min fixation in 2% paraformaldehyde at 4^{o}C for later analysis. Samples were analyzed using LSR II (BD) and flow cytometric data were exported and analyzed using FlowJo software (Tree Star, Inc.). Graphing and statistical analyses (unpaired,

two-tailed Student's t-test) were performed using Prism software (GraphPad Software, Inc.)

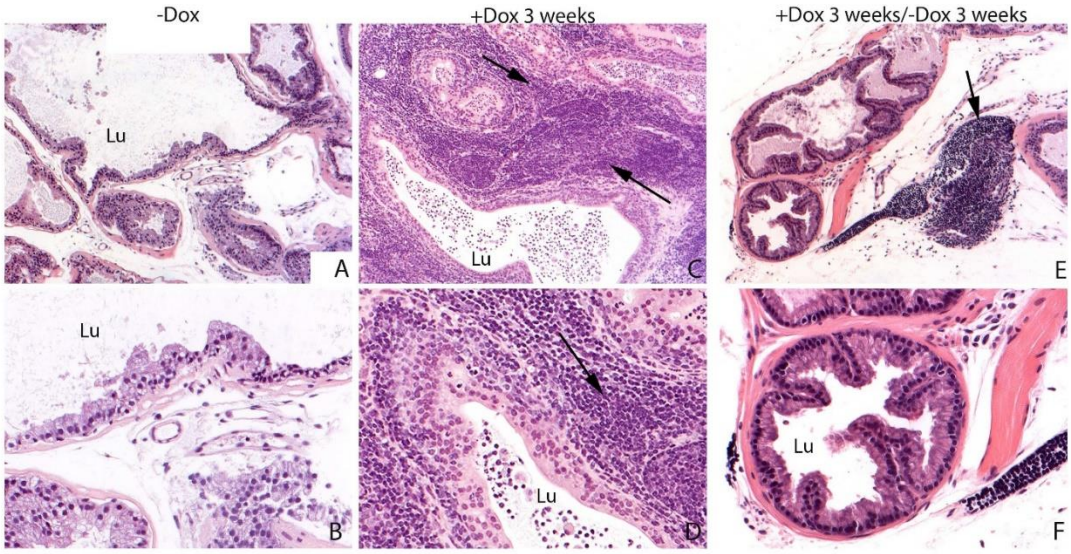

Figure 1: Representative Hematoxylin & Eosin (H&E) ventral prostate sections from control (-Dox), Dox-treated (+Dox 3 weeks), and +Dox 3 weeks/-Dox 3 weeks mice : A-B control ventral prostate. Note, single layer of columnar epithelial cells that produce secretions into the lumen (Lu). **C-D** 3 weeks treated prostate. Note intra-ductal and intra-epithelial immune infiltrates, **E-F** mice treated for 3 weeks then allowed 3 weeks recovery. Over all gland morphology similar to control prostate. However, nodular structures (see arrow in E) with immune infiltrates (see arrow in D) were observed. First row 25X, second 100X. Lu-Lumen. Arrows indicate inflammatory infiltrates

Results

Histological Characterization of IL-1β Expression in the Mouse Prostate

To generate a model with inducible expression of IL-1β, we employed a previously characterized Tet-On driver strain (Rao et al., 2012) that permits conditional gene expression in the prostate gland. The TetO-IL-1β cassette was developed by cloning the coding sequence of human IL-1β downstream of the Tet-Responsive Elements (TRE) in the pUHG16.3 vector (a gift from Dr. Bujard). To ensure that IL-

1β was secreted, a modified version of hIL-1β, wherein the signal sequence from the IL-1 receptor antagonist was fused to the 17 kDa mature form of IL-1β (Wingren et al., 1996) was employed. The resulting *TetO-IL-1β* fragment was excised from the pUHG plasmid and microinjected into single-cell *FVB/N* embryos. Using Southern blot analysis of tail DNA, we identified two independent *TetO-IL-1β* founder mice. To determine whether conditional expression of IL-1β could be achieved in the prostate gland, both *TetO-IL-1β* founders were bred to the extant *Hoxb13-rtTA* strain (Rao et al., 2012), and double transgenic *Hoxb13-rtTA*$^{+/-}$|*TetO-IL-1ß*$^{+/-}$ (IMPI$^{+/-}$) offspring were identified by Southern blot analysis. One *TetO-IL-1ß* founder failed to transmit the transgene in a Mendelian fashion and was not analyzed further. The remaining *TetO-IL-1ß* hemizygous founder transmitted the transgene in the expected ratios and was used in all subsequent experiments.

To determine if the induction of IL-1β expression would mediate an inflammatory response in the prostate, a cohort of IMPI$^{+/-}$ animals at six weeks of age were maintained on Dox-supplemented drinking water and their prostates were dissected at pre-determined intervals. Histological examination revealed intra-prostatic inflammatory infiltrates as early as three days post-Dox exposure (data not shown). After one week post Dox-treatment, an acute inflammatory infiltrate was observed in the ventral prostate where neutrophils were the predominant inflammatory feature. Neutrophilic accumulation was largely stromal; however, a mild intraductal infiltration was also evident. By three weeks (Figure 1), the inflammation had worsened considerably, and transitioned to a mixed/chronic event involving profound intra-epithelial, and stromal lymphocytic and neutrophilic infiltrates. Inflammation was most

extensive in the ventral prostate lobe; however, the anterior, dorsal, and lateral lobes also harbored infiltrating cells. These studies established that the induction of human IL-1β expression in the *IMPI*$^{+/-}$|*GFP* prostate initiated a profound inflammatory response that could be sustained by continuous Dox administration. A histological survey of other major tissues in Dox-treated *IMPI*$^{+/-}$|*GFP* mice, including bladder, urethra, liver, distal colon and proximal colon was also performed. Among these, only the distal colon showed evidence of inflammation (data not shown), as expected, given the prostate and colon specificity of the *Hoxb13-rtTA* transgene (Rao et al., 2012). Characterization of the colonic inflammation will be reported elsewhere. To determine the consequences of Dox withdrawal on the prostate inflammatory phenotype, IMPI$^{+/-}$ males were administered Dox at 2mg/mL in drinking water for three weeks, reverted to regular drinking water for three weeks, and analyzed histologically.

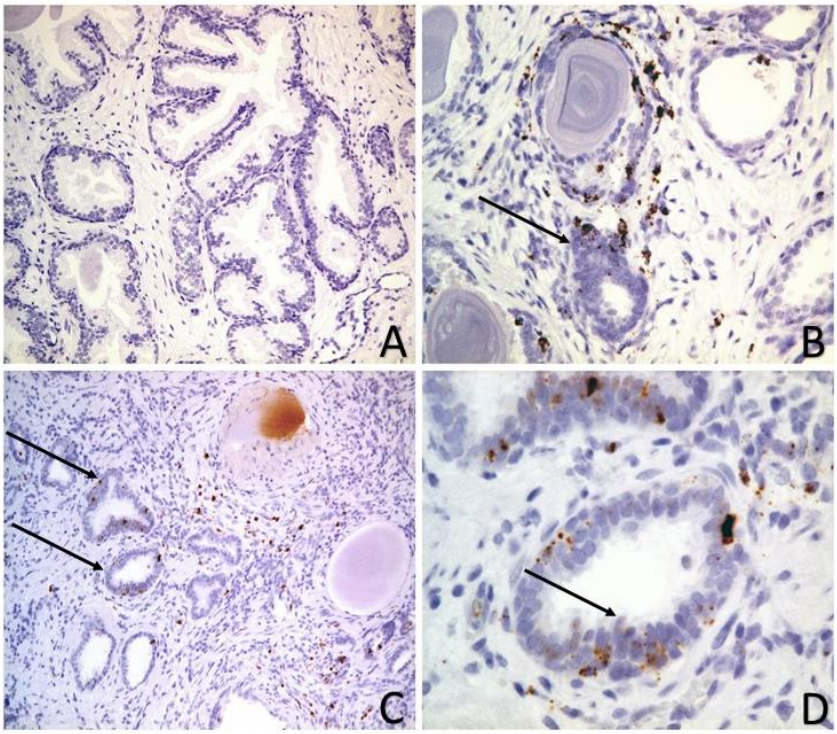

Figure 2: In-situ hybridization for IL-1β RNA on human PIA prostate tissue- A, Prostate tissue with normal appearance have no positive signal for IL-1β, however, PIA lesions from same patient **(B)** have positive signals. Similarly **C** (low mag), **D** (high mag) are prostate tissue derived from the same patient. Note, IL-1β positive signaling (brown staining) indicated by arrow.

Pathological analysis of '+Dox 3weeks/-Dox 3weeks' mice revealed essentially normal morphology with few inflammatory cells in the prostatic interstitial space. These data demonstrate that, in the absence of IL-1β expression, inflammation largely resolves. However, focal follicular structures consisting of densely packed lymphocytes perdured (Figure 1).

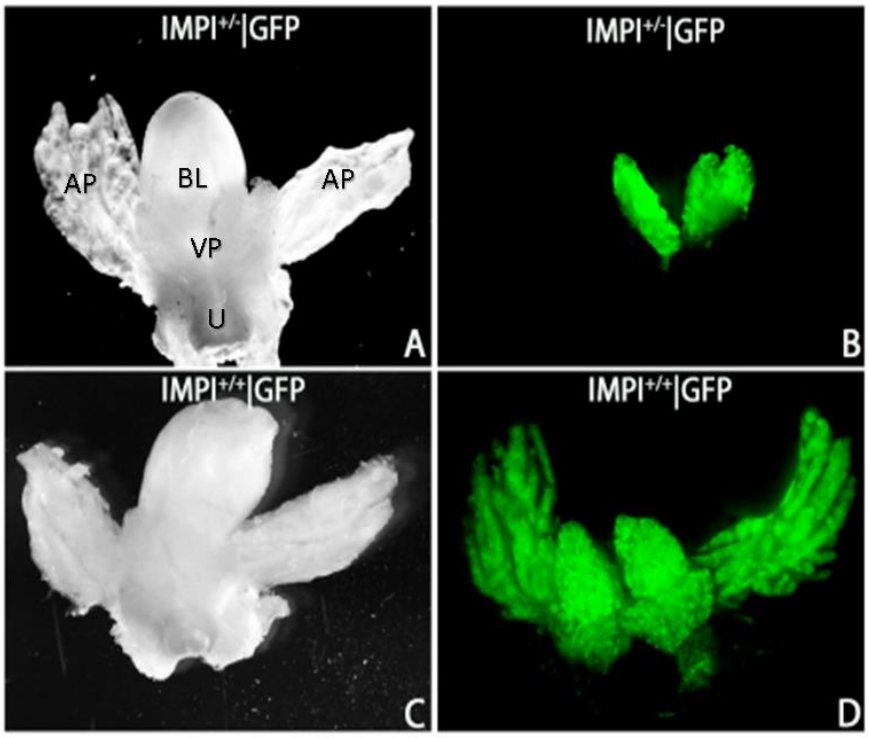

Figure 3: Homozygous *IMPI|GFP* mice have robust GFP expression in all prostate lobes - A,B Whole mount images of heterozygous *IMPI|GFP* and **C,D** homozygous *IMPI|GFP* mice under white light and UV light respectively. Note in heterozygous *IMPI|GFP* mice, GFP expression is observed in the ventral prostate alone. However, in homozygous mice GFP is expressed in all prostate lobes.. AP- Anterior prostate, VP-ventral prostate, BL-Bladder, U-Urethra

Follicular nodules were also observed in chronic inflammatory cases (N=5). To determine if the inflammatory response could be re-initiated after three weeks induction/three weeks recovery, we added a second episode of Dox exposure. Analysis of prostates from mice treated with the three weeks induction/three weeks recovery/three week induction regimen revealed a robust re-initiated inflammatory

response (data not shown). These data establish the utility of the model for examining the consequences of repeated episodes of inflammation in the prostate gland.

As discussed previously, IL-1β levels were upregulated in seminal plasma and expressed prostatic secretions of chronic prostatitis patients. However, it was important to determine whether IL-1β was expressed by human prostate epithelial cells. To determine the presence of IL-1β RNA in human prostate epithelial cells, tissue isolated during prostatectomy was studied. In-situ hybridization probe designed and validated by De Marzo *et al.* was tested in five prostate tissue samples with prostate inflammation. In figure 2, arrows indicate positive signal (brown staining) for IL-1β in human inflamed tissue. Figure 2A and 2B are tissue derived from the same patient, however IL-1β positive signal (brown color) was only observed in inflamed tissue (Figure 2B), and was absent in normal tissue (2B).

Leakiness in the Tet-O system has been reported previously (Shaikh and Nicholson, 2006). However, the second generation rtTA(S)-M2 gene employed here has demonstrated tighter regulation and higher sensitivity to Dox compared to the original iteration of rtTA (Urlinger et al., 2000). To ensure that IL-1β was secreted only in response to Dox administration, untreated $IMPI^{+/-}$ were examined histologically, and

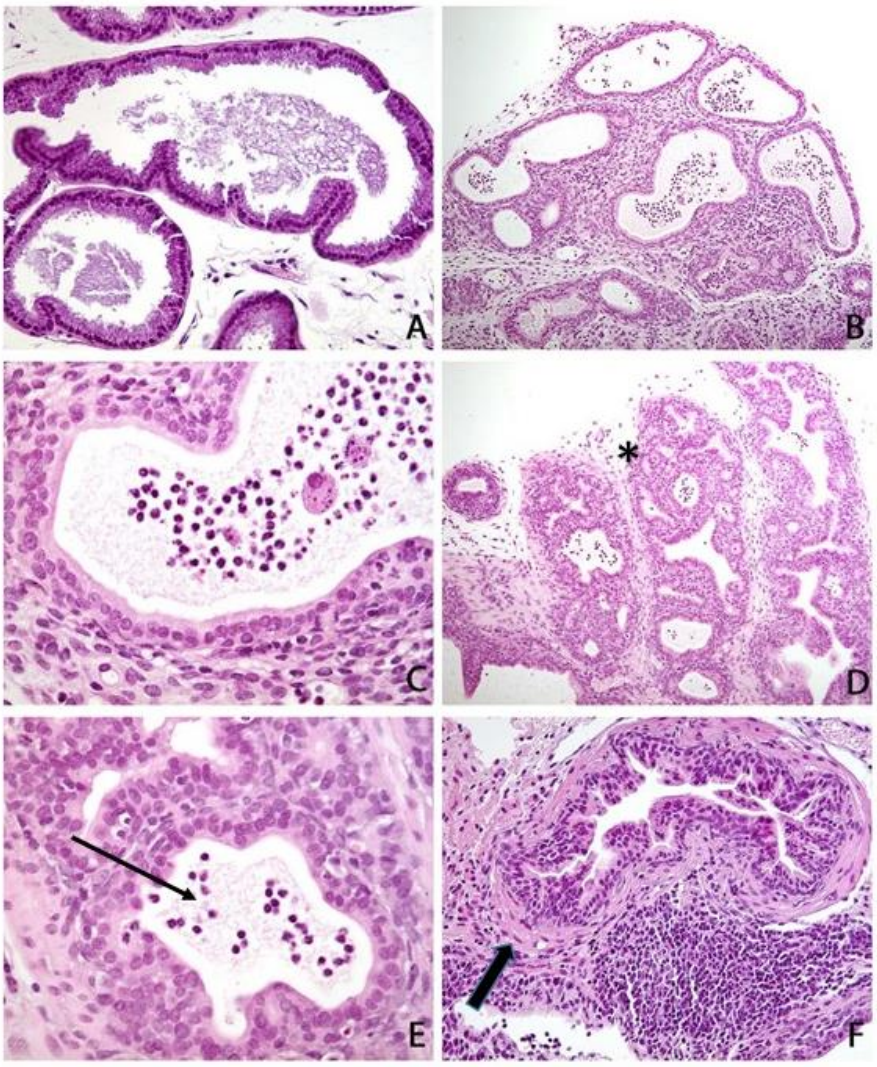

Figure 4: Histological examination of prostate lobes isolated from Dox-treated IMPI mice- A, untreated age-matched ventral prostate (VP) (magnification 200X). Note, single layer of columnar epithelial cells without an inflammatory presence in the control tissue. **B,** 4 weeks Dox-treated VP at magnification 100X and **C,** image captured at 400X. Note, intraductal inflammation **D,** Anterior prostate from 4 week Dox-treated mice captured at 100X magnification **E,** and image captured at 400X. * in D indicates extensive remodeling. Arrow in E indicates neutrophils. **F,** 4 weeks Dox-treated VP. Note, mixed lymphocytic population close to prostate gland. Block arrow indicates significant stromal thickening (magnification 200X)

transgenic IL-1β mRNA extracted from ventral prostates was quantified by RT-qPCR. *IMPI*$^{+/-}$ male prostate histology was indistinguishable from that of age-matched *FVB/N* (wild type) animals and Dox-treated *FVB/N* mice. As expected, quantification of human IL-1β expression by RT-qPCR revealed no differences between uninduced controls and Dox-treated *FVB/N* mice (data not shown). These data demonstrate that the IMPI system is tightly regulated, with no detectable IL-1β expression in the absence of Dox. Additionally, histological examination of Dox-

treated wildtype or *FVB/N* mice revealed no significant differences from untreated IMPI controls.

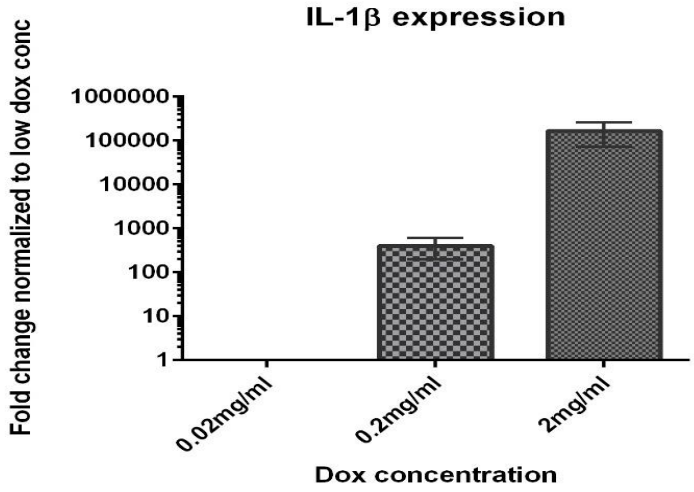

Figure 5: RT-qPCR evaluation of transgenic IL-1β transcripts with varying Dox concentrations: Graph represents fold change in IL-1β expression over control from VP of treated mice. IL-1β expression was normalized with luminal cell marker CK18. Treated mice were categorized into three cohorts, 0.02mg/ml, 0.2mg/ml and 2mg/ml Dox-treated mice (n=3 in each group). Note significant fold change differences among the group with variable Dox concentration. Error bars represent mean±SEM. Due to high variability within each cohort statistical significance could not be determined. However, a clear trend is evident.

To streamline development of IMPI cohorts for further analyses, we sought to develop doubly homozygous animals by interbreeding IMPI$^{+/-}$ hemizygotes. Offsprings were genotyped by PCR for rtTA and IL-1β transgenes. Double transgenic animals were then selected for southern blot analysis to determine animals homozygous for one or both transgenes. Homozygosity was confirmed by backcrossing to *FVB/N* mice and genotyping offsprings for rtTA and IL-1β. A subset of these animals also carried the *TetO-GFP* transgene to permit functional analysis of the Tet-On system. Suspected double homozygotes were bred to *FVB/N* mates to ensure homozygosity of both transgene loci. Remarkably, Dox administration to homozygous IMPI$^{+/+}$|GFP animals resulted in robust inflammation in all lobes of the mouse prostate when histologically examined. Similarly, GFP expression was observed in all lobes of the mouse prostate (Figure 3D). In contrast, the doubly hemizygous mice presented with inflammation predominantly

in the ventral lobe. GFP expression in doubly hemizygous mice were observed in ventral prostate alone as shown in the figure 3B.

These data extend the utility of the IMPI system by permitted analysis of IL-1β-induced effects in the dorsal, ventral, lateral, and anterior prostate lobes.

Changes in Prostate Gland Architecture Mediated by IL-1β Expression

We observed significant differences in the prostate size of Dox-treated IMPI$^{+/+}$|GFP mice versus non-treated controls. The Dox-treated prostates were larger with the anterior prostate being almost twice the size compared to controls. The prostate tissue appreared to be tougher and had a slight off-white coloration compared to controls. Histologically we observed architectural changes in the anterior prostate (Figure 4D) with some ducts enlosed by pockets of inflammatory cells, losing the classical papillary foldings. Reactive changes were observed in the ventral and dorsal-lateral lobes (Figure 4), including enlarged nuclei and dense cytoplasm. The ventral prostate had tranformed from an organized single layer of epithelial cells as seen in controls (Figure 4A), to a multi-layer of epithelial cells with histological evidence of apoptotic cells. Moreover, rapid cycling of cells was observed with accumulation of cell debris in the lumen. Stromal fibrosis, an increase in dense connective tissue was clearly evident in the H&E sections from the anterior and ventral prostate, and to a lesser extent in the dorsal-lateral lobes with inflammation (Figure 4F). Small pockets of densely populated lymphocytes were observed in the ventral prosatate and anterior prostate. Ducts closer to these pockets appeared more disorganized and damaged (Figure 4F).

Decreasing Dox Concentration can Reduce the Degree of Inflammation and IL-1β Expression

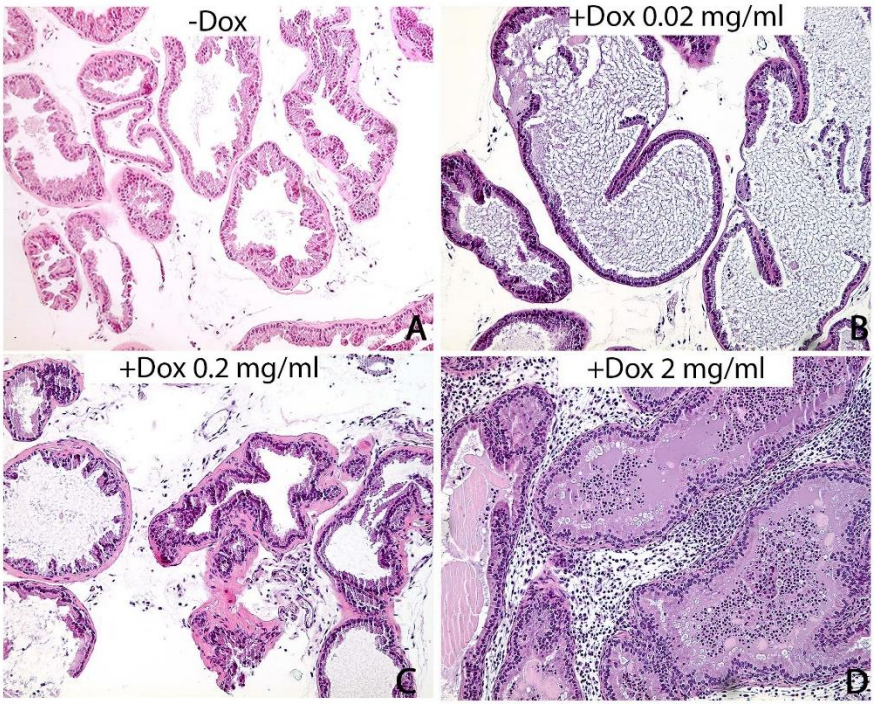

Figure 6: Dox titration allows variable degree of inflammation. A H&E stained VP section from untreated mice. **B** VP of mouse treated at 0.02mg/ml Dox concentration. Note histological resemblance to untreated mouse. **C** VP of mouse treated with 0.2mg/ml Dox. Note immune infiltrates and stromal thickening. **D** 2mg/ml Dox treated mice have higher immune infiltrates. Magnification 200X. Arrows indicate inflammation

To determine if the degree of inflammation could be modulated by varying Dox concentration, we administered cohorts of IMPI$^{+/+}$|GFP mice with 2mg/ml (high), 0.2mg/ml (medium) and 0.02mg/ml (low) Dox in drinking water (n=3 in each group). After one week of Dox administration, mice were euthanized for histology, and RNA was extracted from the ventral prostates to quantify transgenic IL-1β expression using RT-qPCR. To differentiate endogenous mouse IL-1β transcripts from transgenic IL-1β transcripts, primers were designed against the rabbit β-globin poly A tail that is specific to the transgenic IL-1β transcript. Cytokeratin 18 (CK18), a marker for luminal epithelial cells, was used to normalize gene expression. IL-1β expression followed a

linear trend among the three cohorts (Figure 5), with the high Dox-treated mice expressing the highest level of IL-1β expression, as expected. The high Dox group exhibited greater than 100,000 fold increase in IL-1β expression compared to the low Dox group (Figure 5). Mice in the low Dox cohort had about a 3-fold increase in IL-1β expression compared to controls, while the medium Dox cohort demonstrated a 400-fold increase in IL-1β expression compared to the low Dox group (Figure 5). H&E stained sections of ventral prostates from these animals displayed a similar trend, with the high Dox group exhibiting the highest degree of inflammation (Figure 6D) compared to the medium (Figure 6C) and low Dox groups (Figure 6B). This experiment validates the utility of this model to study the effects

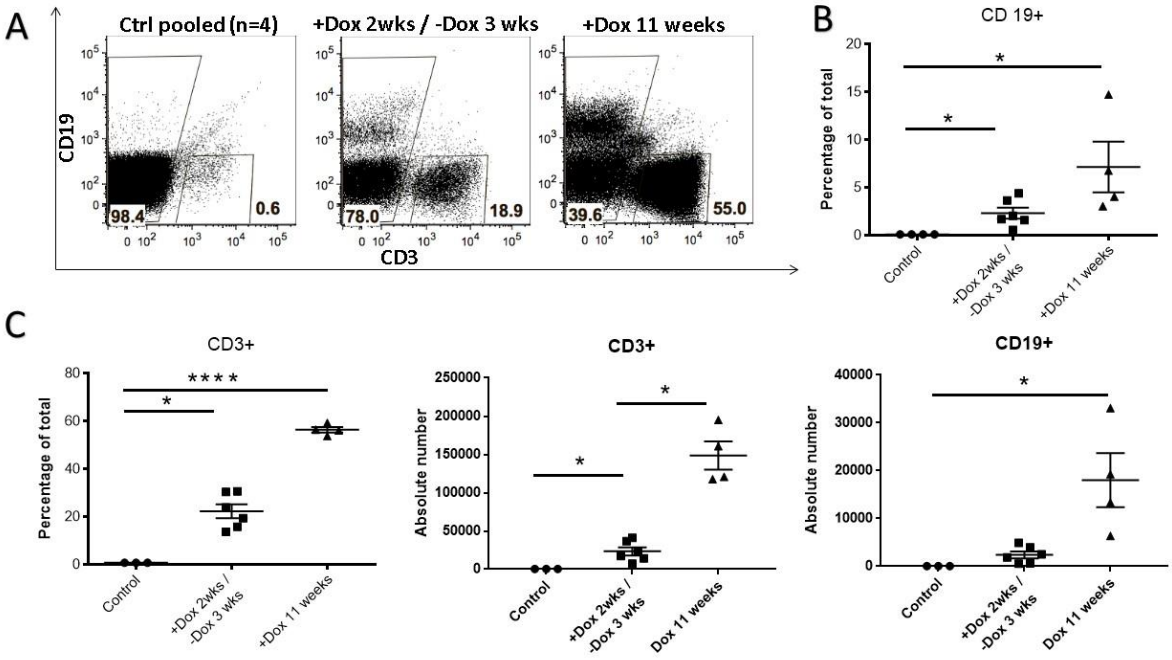

Figure 7: Flow cytometry analyses to determine CD3+ and CD19+ cell populations in control, +Dox/-Dox and 11 week Dox-treated mice: A, Representative dot plots from untreated controls, +Dox 2wks/-Dox 3wks and from mice Dox-treated for 11 weeks. Note, each group had four mice in total. The control group (n=4) was pooled for analyses; however, remaining samples (n=8) were analyzed individually. **B,** Graph illustrating CD19+ cells, represented as percentage of total prostate immune cells, and graph below, represents absolute number of CD19+ cells. **C,** Graph illustrating CD3+ cells represented as percentage of total prostate immune cells, and graph representing absolute number of CD3+ cells. P<0.5 considered significant.* indicates p<0.05 **** indicates p<0.0001

of varying degrees of inflammation in the prostate and determined 0.02mg/ml - 0.2mg/ml as the threshold to induce a robust IL-1β–mediated prostate inflammatory response.

Characterizing the Inflammatory Cell Population in the IMPI Model

Studies to determine the inflammatory cell phenotype that predict clinical outcome in BPH, prostatitis and prostate cancer patients is crucial, mostly for the development of useful inflammatory biomarkers. With an increase in clinical trials on immunotherapeutic drugs to treat prostate cancer, a greater understanding on the role of immune cells in mediating prostate pathogenesis is essential. Commonly

investigated immune cells in clinical settings include T cells (CD3), sub-populations of T cells (CD4, CD8), B cells (CD19) and innate cells including CD11b and CD11c. The experiments described below provide a detailed characterization of the immune cell population in the IMPI model to draw comparisons to clinical observations. To determine the nature of inflammatory cells that infiltrate the prostate post-IL-1β expression, flow cytometry was performed on whole IMPI$^{+/+}$|GFP mouse prostates. Mouse prostate inflammatory infiltrates were isolated at separate time points to quantify populations of innate and adaptive immune cells. In our first study, our objective was to compare the infiltrates at one week vs seven weeks of Dox treatment. From this study (data not shown) we validated our findings from histological analyses, wherein the inflammation was largely acute at one week that later transitioned into a chronic event with a significant increase in lymphocyte population.

To investigate the inflammatory infiltrates harbored in the follicular structure (described in Figure 1) upon Dox-withdrawal, flow cytometry was performed on +Dox 2 weeks/-Dox 3 weeks IMPI+/+|GFP mice. Four untreated IMPI+/+|GFP mice served as controls. Representative dot plots of one mouse from each cohort is represented in figure 7, with the exception of the control dot plot, which represents four untreated IMPI+/+|GFP prostates pooled. Additionally, a cohort of mice Dox treated for 11 weeks was also added to the flow analyses, to determine the long-term consequence of IL-1□ expression on immune cell population. CD3+ cells made up 23% of the total immune cells in the +Dox 2 weeks / -Dox 3 weeks cohort whereas this percentage significantly increased to 56 % in the 11 week Dox-treated group (Figure 7). Absolute number of CD3+ cells also revealed significant differences across cohorts with the

mean number of CD3+ cells being 400, 23,000 and 150,000 in controls, +Dox 2 weeks / -Dox 3 weeks and 11 week cohort respectively (Figure 7). Examining CD19+ cells or B cells revealed significant differences in the percentage of CD19+ cells in the +Dox 2 weeks / -Dox 3 weeks and 11 week cohort compared to controls. However, when absolute number of B cells were analyzed, significant differences were observed in the 11 week cohort alone. The mean absolute number of CD19+ cells in control, +Dox

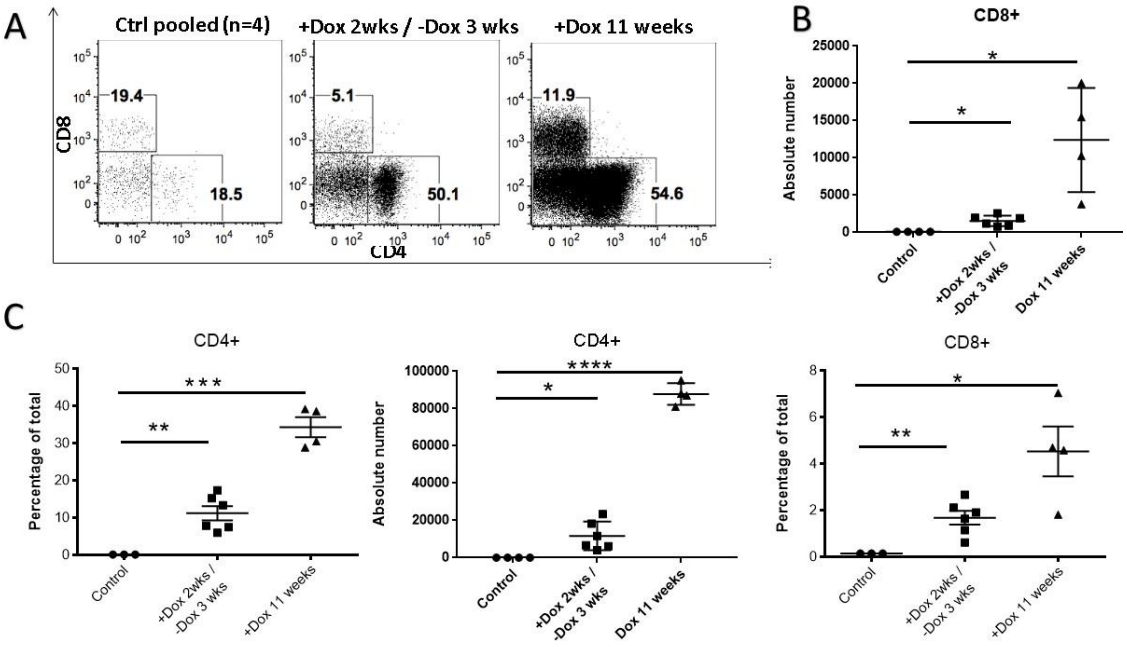

Figure 8: Flow cytometry analyses to determine CD4+ and CD8+ cell populations in control, +Dox/-Dox and 11 week Dox-treated mice: A, Representative dot plots from untreated controls, +Dox 2wks/-Dox 3wks and from mice Dox-treated for 11 weeks. Note, each group had four mice in total. The control group (n=4) was pooled for analyses; however, remaining samples (n=8) were analyzed individually. **B,** Graph illustrating CD8+ cells, represented as percentage of total prostate immune cells, and graph below, represents absolute number of CD8+ cells. **C,** Graph illustrating CD4+ cells represented as percentage of total prostate immune cells, and graph representing absolute number of CD4+ cells. P<0.5 considered significant.* indicates p<0.05.** indicated p<0.01. **** indicates p<0.0001

2wks / -Dox 3 wks

and 11 week cohort were 50, 2400 and 18,000 respectively (Figure 7).

Next, we wanted to examine the CD4+ and CD8+ populations (Figure 8) that represent T helper and T cytotoxic cells respectively. Percentages of CD4+ and CD8+

populations changed significantly in the +Dox 2 weeks / -Dox 3 weeks cohort and 11 week cohort compared to controls (Figure 8). The mean absolute number of CD4+ cells in the control, +Dox 2wks / -Dox 3 wks and 11 week cohort were 74, 12,000 and 88,000 respectively, which comprises for 0.1, 11 and 34 percent of total prostate immune cells.

Representative dot plots from all three cohorts illustrating CD11b+GR1+ population is depicted in figure 9. Significant differences in the percentage of

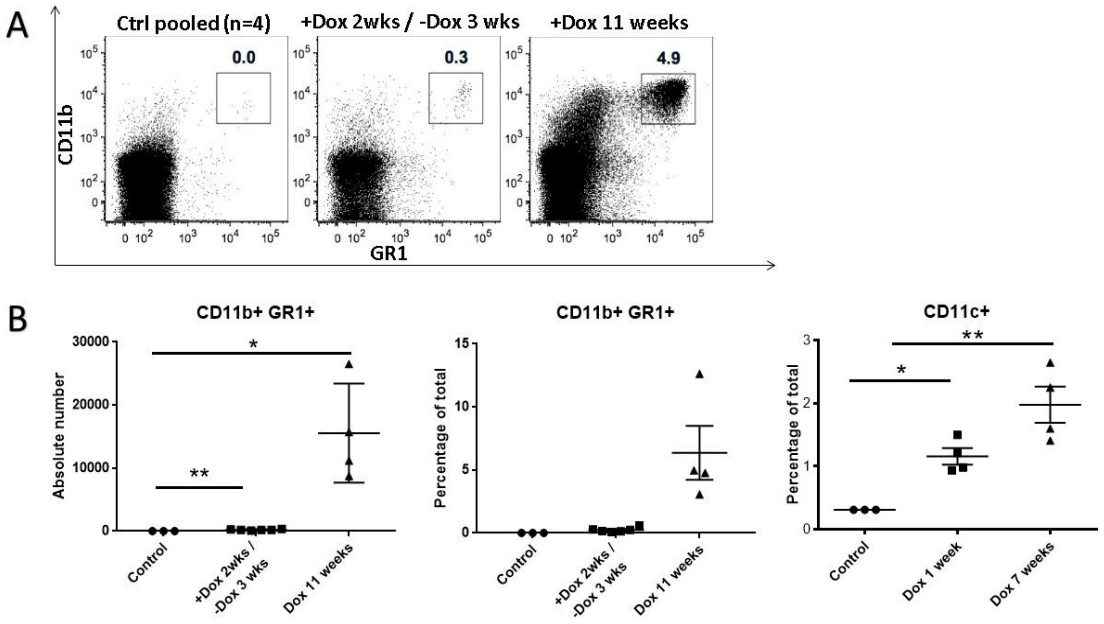

Figure 9: Flow cytometry analyses to determine GR1+ and CD11b+ cell populations in control, +Dox/-Dox and 11 week Dox-treated mice: A, Representative dot plots from untreated controls, +Dox 2wks/-Dox 3wks and from mice Dox-treated for 11 weeks. Note, each group had four mice in total. The control group (n=4) was pooled for analyses; however, remaining samples (n=8) were analyzed individually. **B,** First Graph from left is illustrating absolute number of CD11b+GR1+ cells, second graph represents CD11b+GR1+ cells, as percentage of total prostate immune cells, and third graph represents %CD11c+ cells P<0.5 considered significant.* indicates p<0.05.** indicated p<0.01.

CD11b+GR1+ was not observed across cohorts, however, the absolute numbers were significantly different (Figure 9). Interestingly, an average of 200 CD11b+GR1+ cells

were present in the +Dox 2 weeks / -Dox 3 weeks cohort whereas an average of seven cells were detected in the pooled control prostates. Prostate dendritic cells identified as CD11c+CD11b- were significantly increased at one week post-Dox treatment and this percentage increased significantly after seven weeks of inflammation. To summarize, our flow cytometry analyses revealed quantitative measure of the absolute number and percentages of adaptive and immune cells while highlighting trends in CD4+ vs CD8+ populations. This study also revealed that with sustained IL-1β expression there is a rapid increase in CD3 population and a relatively gradual increase in CD19 population. Our Dox-withdrawal experiments revealed that a majority of infiltrates in follicles observed histologically are CD3+ with a predominating CD4+ population.

Characterizing Expression of Cytokines in the IMPI Model

To characterize cytokine expression in IL-1β-mediated chronic inflammation, $IMPI^{+/+}$|GFP animals were Dox-treated for one week. Expression of Tumor Necrosis Factor-α (TNF-α), IL-17A, IL-18, IL-1a, mouse IL-1β, IL-10 and IL-6 was quantified using real-time PCR (Figure 10). IL-17A mRNA expression showed a 400-fold increase in Dox-treated $IMPI^{+/+}$|GFP compared to untreated controls. Glyceraldehyde 3-Phosphate Dehydrogenase (GAPDH) primers were used to normalize expression. A 130-fold increase in IL-6 expression, 50-fold increase in TNF-α expression, and almost 20-fold increase in IL-10 expression was noted. IL-18 expression decreased significantly compared to controls. As the IL-1 signaling cascade is expected to have a positive feedback loop we measured endogenous IL-1β and IL-1a expression. Both cytokines bind to the same receptor IL-1R1. Both endogenous mouse IL-1β expression

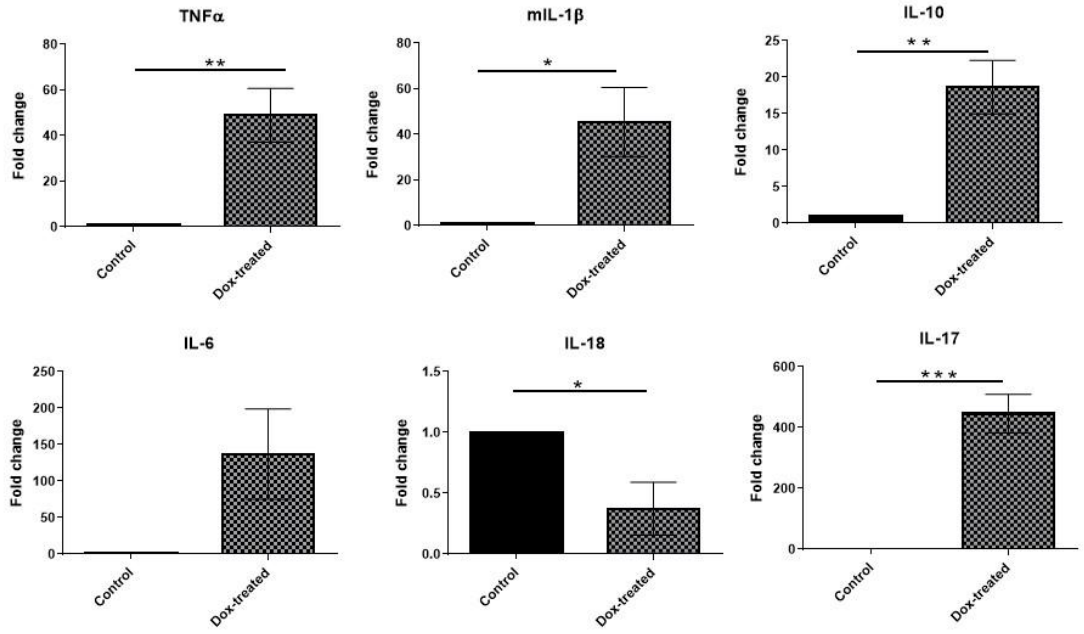

Figure 10: Evaluating cytokine expression by RT-qPCR in one week treated mouse VP (n=3). X-axis represents fold change over control after normalization with housekeeping gene. Note highest fold change observed in IL17A and IL-6 expression. Statistical significance was performed with a student t-test in Prism Graphpad. P<0.05 was considered significant. Error bars represent mean±SEM *P<0.05, ***P<0.001

and IL-1a expression (data not shown) increased by 45-fold and 5-fold respectively. Our cytokine analyses results were as expected and aligned with the literature supporting the role of IL-1 signaling in inducing the expression of various cytokines.

IHC Staining to Determine Proliferation and NKX3.1 Expression in Prostate Epithelial Cells

To determine the effects of acute and chronic inflammation on cell division in the prostate, Ki67 Immunohistochemistry (IHC) was performed at one week (data not shown) and four weeks post Dox-treatment (Figure 11). Non-inflamed control animals had few mitotic cells in the epithelium and stroma (Figure 11). In contrast, the epithelial

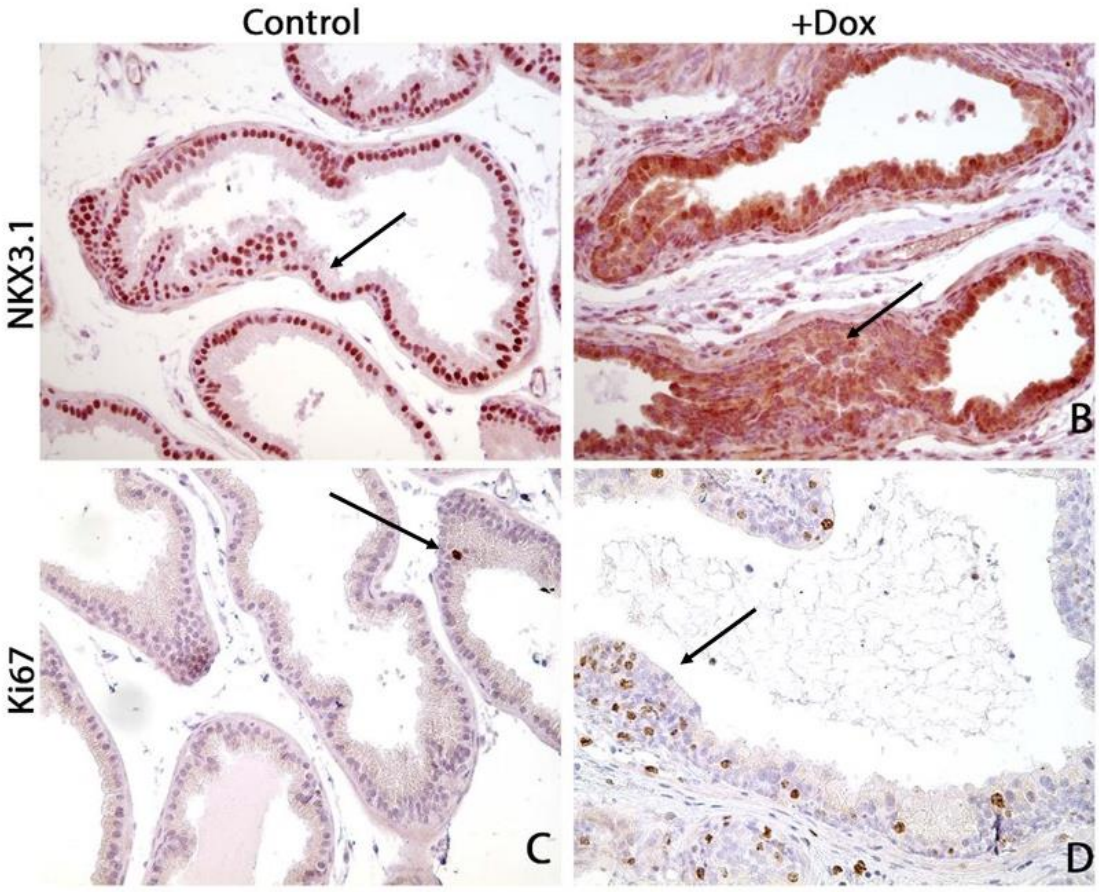

Figure 11: IHC staining for NKX3.1 and Ki67 comparing Dox-treated vs. untreated IMPI mice- A,B, NKX3.1 staining on control and 4 weeks-treated ventral prostate tissue. Note, robust nuclear NKX3.1 expression (brown staining) in control mice, however, in inflamed tissue, NKX3.1 expression is more diffused into the cytoplasm (see arrow). Few cells lost nuclear expression of NKX3.1.**C,D,** Ki67 staining on control and treated tissue respectively. Arrows indicate positive signal (brown color) for Ki67. Images captured at 200X.

compartment in inflamed prostates showed a dramatic increase in Ki67-positive cells. Ki67 was also observed to be upregulated in the inflamed stroma. In addition, the infiltrating lymphocytic cell population that appeared in clusters or ectopic follicular structures was also observed to have a high proliferation rate. These data demonstrate that acute and chronic

inflammation induced rapid cycling of prostate epithelial cells and stromal cells. To determine potential molecular mechanisms underlying the increase in proliferation,

levels of the prostate-specific Nkx3.1 tumor suppressor was measured by IHC. Consistent with previously reported studies from extant rodent models of inflammation (Khalili et al., 2010), Nkx3.1 expression was sporadically diminished in the context of chronic inflammation (Figure 11). Diminished Nkx3.1 expression correlated inversely with inflammation, with some cells showing no detectable Nkx3.1. Diffused cytoplasmic Nkx3.1 staining was also consistently observed in a subpopulation of epithelial cells in inflamed prostates.

Discussion

Chronic inflammation is a common feature of the human prostate, and has long been suspected to be an etiologic factor in both benign and malignant prostate diseases (De Marzo et al., 2007; Nickel, 2008). However, establishing causal links between the presence of inflammatory infiltrates and the onset or progression of disease has been difficult due, in large measure, to the lack of appropriate animal models. The IMPI system described here provides a versatile and robust model to discern the effects of short term, long term, or episodic cytokine-mediated prostate inflammation in the absence of an infectious agent. Although here, we describe the effects of inducing expression of the highly proinflammatory cytokine, IL-1β, the general approach can be extended to any cytokine or chemokine. Given the emergence of clinically useful therapeutic agents capable of modulating cytokine signaling (Efron and Moldawer, 2004; Gharaee-Kermani and Phan, 2001), it is critical to develop preclinical systems to investigate the sequelae of cytokine upregulation, and to test the efficacy of potential interventions. The model described here is the first genetic inducible model available

to study the effects of chronic inflammation on the mouse prostate, and to discern the effects of repeated inflammatory episodes.

IL-1-mediated signaling has been shown to play an important role in driving autoimmunity, inflammation and cancer (Dinarello, 1996, 2009). We described the appearance of ectopic follicles in our histological analyses. The presence of ectopic follicles is a histopathological feature that has been observed in human histology as well in our mouse model (Nickel et al., 1999). Ectopic follicles, or Tertiary Lymphoid Structures (TLS), have structural organization reminiscent to secondary lymphoid organs that have clusters of B and T cells. They have been reported to be important in influencing the course of action in infection, autoimmune diseases, cancer, and transplant rejections (Pitzalis et al., 2014). We further characterized the immune population in the ectopic follicles as predominantly CD4+ cells and few CD19+ cells. The presence of these follicular structures in our model could indicate antigen presentation in the follicles and the production of auto-antibodies against potential prostate antigens. Several research groups have proposed the theory that autoimmunity is an important factor in driving CP/CPPS. Interleukin 1β is an important mediator of inflammation and a physiologically relevant molecule that needs to be carefully studied, due to the following reasons. Firstly, increased expression of IL-1β was observed in prostatic secretions from CP/CPPS patients (Alexander et al., 1998). Secondly, pleiotropic effects of IL-1β including a strong role in mediating autoinflammatory diseases like rheumatoid arthritis has been established (Dinarello, 1996). Lastly, IL-1β polymorphisms are associated with increased risk of prostate cancer (Zabaleta et al., 2009). Our model can serve as a powerful tool to decipher

mechanisms underlying prostate autoimmunity, define potential prostate antigens, and serve as a pre-clinical model to test therapies.

Our flow cytometry results validated our histological characterization of the immune infiltrate. We observed an acute inflammatory phenotype after one week of Dox-treatment, characterized by neutrophils, which later transitioned into a chronic lymphocytic population. Bunt *et al.* reported that IL-1β-induced inflammation recruited Myeloid Derived Suppressor Cells (MDSCs, CD11b+ GR1+) to the site of expression and suppressed the activation of CD4 and CD8 positive cells (Bunt et al., 2006). Similar reports have validated this study in mouse models over expressing IL-1β and demonstrated the recruitment of MDSCs and its role in T-cell suppression (Song et al., 2005; Tu et al., 2008). We have observed the appearance of CD11b+Ly6G+ cells (granulocytic MDSC marker) after one week of inflammation and CD11b+GR1+ cells after 11 weeks of inflammation. MDSCs have gained immense interest as a potential target for therapy due its potential role in tumor growth (De Sanctis et al., 2016). The presence of CD11b+ GR1+ cells in our mouse model coupled with studies supporting the role of IL-1β in recruiting MDSCs makes us strongly suspect a sub-set of this population to contain MDSCs. However, it has to be noted that IL-1β also recruits neutrophils via IL-8 expression that are characterized by similar markers CD11b+GR1+. Studies to isolate CD11b+GR1+ cells from our IMPI model prostates and evaluate T-cell suppression are currently on-going. This study will support the role of cytokine-mediated prostate pathology, especially IL-1β as an important signaling molecule that can be targeted therapeutically.

Histological comparison of the *IMPI+/+|GFP* and *IMPI+/+* revealed that the presence of *TetO-GFP* significantly increased the inflammatory phenotype. While both strains display an inflammatory reaction, the mice with the *TetO-GFP* transgene have a more robust phenotype. The *TetO-GFP* allele may act like a modifier locus and increase IL-1β expression in our model. We have independently investigated *IMPI+/+* (without GFP) and *Hoxb13-rtTA*$^{+/-}$ |*TetO-GFP*$^{+/-}$ (GFP alone) mice, while the former strain had significant levels of inflammation, the latter strain had no signs of inflammation. Additionally, we can speculate that the rapid cycling observed in prostate epithelial cells results in Green Fluorescent Protein (GFP) presentation by antigen-presenting cells, and drives a more robust inflammatory reaction. GFP immunogenicity have been reported previously in mouse models and primates (Han et al., 2008). The immunogenicity of GFP is well known and has been exploited to trigger a more robust T-cell response in human therapies (Re et al., 2004). The overexpression of IL-1β may cause the tissue to lose tolerance to GFP (among other normal prostate antigens) and consider it as a foreign antigen. Further immunological characterization would be required to dissect the role of GFP in our model. Alexander *et al*. provided the first evidence for reactive T-cells to normal prostate antigen in CPPS patients (Alexander et al., 1997). Since then multiple research groups have added evidence in supporting the role of autoimmunity in chronic prostatitis (Batstone et al., 2002; Kouiavskaia et al., 2009). Here, we present a novel model to study these mechanisms and develop new strategies to treat inflammation. These studies would make the model more valuable in studying immune tolerance in the prostate, in addition to the role of IL-1β in prostate malignancies.

In summary, the downregulation of Nkx3.1 in inflamed prostate epithelial cells, remodeling of the prostate epithelium as a result of immune cell recruitment by IL-1β, and the rapid proliferation of prostate cells could all synergize to create a conducive atmosphere to trigger malignant prostate transformations. The long-term effects of chronic inflammation will be assessed in the mouse prostate. To date, the role of a cytokine has not been independently investigated in the mouse prostate. Here we present the effect of IL-1β, a cytokine differentially expressed in human prostate samples. IL-1β-associated therapies have been FDA approved for IL-1β-mediated disorders like rheumatoid arthritis and other autoimmune diseases. IL-1β neutralization has been effective in common diseases such as gout, type 2 diabetes, heart failure, recurrent pericarditis, rheumatoid arthritis, and smoldering myeloma (Dinarello, 2005; Lust et al., 2009; Nuki et al., 2002). IL-1β activation in cells is mediated by the inflammasome, a multi-protein complex and is integral to the innate immune system. The inflammasome activates caspase-1, which in turn cleaves pro-IL-1β into its mature form. Aberrations in inflammasome signaling results in overexpression of proinflammatory cytokines including IL-1β, and deregulated inflammasome signaling have been implicated in human pathologies including human prostate cancer and CP/CPPS (Chen et al., 2013; Guo et al., 2015; Veeranki, 2013).

The role of IL-1β in initiating and maintaining neuropathic pain in chronic human conditions has been established (Ren and Torres, 2009). IL-1β induces pain by upregulating nociceptors like Nerve Growth Factor (NGF), Prostaglandin, Substance-P, and directly engaging with nociceptive channels like the Transient Receptor Potential cation channel subfamily V member 1 (TRPV1), sodium channels and

Gamma-AminoButyric Acid (GABA) receptors (Schäfers and Sorkin, 2008). The development of chronic pelvic pain in our model will be tested by employing the von Frey assay to measure referred hyperalgesia. This study would be extremely beneficial in furthering our understanding of the etiology of pain in CP/CPPS. Pain, the hallmark of CP/CPPS have few effective treatments with most patients relapsing with severe pelvic pain. Upon further characterization of our model, we expect improved therapies and biomarkers of inflammation that would be valuable in diagnosis and treatment of IL-1β-mediated prostate pathologies. The unique feature of our IMPI system being genetic, allows the model to be bred with extant models of prostate cancer. Therefore, our model not only serves as a great pre-clinical tool but also allows the generation of similar models to dissect the roles of other inflammatory mediators that may play a role in prostate diseases.

References

Alcover, J., X. Filella, P. Luqué, R. Molina, L. Izquierdo, J. M. Augé, and A. Alcaraz, 2010, Prognostic value of IL-6 in localized prostatic cancer: Anticancer Res, v. 30, p. 4369-72.

Alexander, R. B., F. Brady, and S. Ponniah, 1997, Autoimmune prostatitis: evidence of T cell reactivity with normal prostatic proteins: Urology, v. 50, p. 893-9.

Alexander, R. B., S. Ponniah, J. Hasday, and J. R. Hebel, 1998, Elevated levels of proinflammatory cytokines in the semen of patients with chronic prostatitis/chronic pelvic pain syndrome: Urology, v. 52, p. 744-9.

Altuntas, C. Z., F. Daneshgari, E. Veizi, K. Izgi, F. Bicer, A. Ozer, K. O. Grimberg, B. Bakhautdin, C. Sakalar, C. Tasdemir, and V. K. Tuohy, 2013, A novel murine model of chronic prostatitis/chronic pelvic pain syndrome (CP/CPPS) induced by immunization with a spermine binding protein (p25) peptide: Am J Physiol Regul Integr Comp Physiol, v. 304, p. R415-22.

Batstone, G. R., A. Doble, and J. S. Gaston, 2002, Autoimmune T cell responses to seminal plasma in chronic pelvic pain syndrome (CPPS): Clin Exp Immunol, v. 128, p. 302-7.

Boehm, B. J., S. A. Colopy, T. J. Jerde, C. J. Loftus, and W. Bushman, 2012, Acute bacterial inflammation of the mouse prostate: Prostate, v. 72, p. 307-17.

Bunt, S. K., P. Sinha, V. K. Clements, J. Leips, and S. Ostrand-Rosenberg, 2006, Inflammation induces myeloid-derived suppressor cells that facilitate tumor progression: J Immunol, v. 176, p. 284-90.

Chen, C. S., P. J. Chang, W. Y. Lin, Y. C. Huang, and D. R. Ho, 2013, Evidences of the inflammasome pathway in chronic prostatitis and chronic pelvic pain syndrome in an animal model: Prostate, v. 73, p. 391-7.

Chen, H., L. N. Mutton, G. S. Prins, and C. J. Bieberich, 2005, Distinct regulatory elements mediate the dynamic expression pattern of Nkx3.1: Dev Dyn, v. 234, p. 961-73.

De Marzo, A. M., E. A. Platz, S. Sutcliffe, J. Xu, H. Grönberg, C. G. Drake, Y. Nakai, W. B. Isaacs, and W. G. Nelson, 2007, Inflammation in prostate carcinogenesis: Nat Rev Cancer, v. 7, p. 256-69.

De Sanctis, F., S. Solito, S. Ugel, B. Molon, V. Bronte, and I. Marigo, 2016, MDSCs in cancer: Conceiving new prognostic and therapeutic targets: Biochim Biophys Acta, v. 1865, p. 35-48.

Dinarello, C. A., 1996, Biologic basis for interleukin-1 in disease: Blood, v. 87, p. 2095-147.

Dinarello, C. A., 2005, Blocking IL-1 in systemic inflammation: J Exp Med, v. 201, p. 1355-9.

Dinarello, C. A., 2009, Immunological and inflammatory functions of the interleukin-1 family: Annu Rev Immunol, v. 27, p. 519-50.

Dinarello, C. A., 2011, Interleukin-1 in the pathogenesis and treatment of inflammatory diseases: Blood, v. 117, p. 3720-32.

Efron, P. A., and L. L. Moldawer, 2004, Cytokines and wound healing: the role of cytokine and anticytokine therapy in the repair response: J Burn Care Rehabil, v. 25, p. 149-60.

Elkahwaji, J. E., W. Zhong, W. J. Hopkins, and W. Bushman, 2007, Chronic bacterial infection and inflammation incite reactive hyperplasia in a mouse model of chronic prostatitis: Prostate, v. 67, p. 14-21.

Firestein, G. S., 2003, Evolving concepts of rheumatoid arthritis: Nature, v. 423, p. 356-61.

Gharaee-Kermani, M., and S. H. Phan, 2001, Role of cytokines and cytokine therapy in wound healing and fibrotic diseases: Curr Pharm Des, v. 7, p. 1083-103.

Guo, H., J. B. Callaway, and J. P. Ting, 2015, Inflammasomes: mechanism of action, role in disease, and therapeutics: Nat Med, v. 21, p. 677-87.

Habermacher, G. M., J. T. Chason, and A. J. Schaeffer, 2006, Prostatitis/chronic pelvic pain syndrome: Annu Rev Med, v. 57, p. 195-206.

Han, W. G., W. W. Unger, and M. H. Wauben, 2008, Identification of the immunodominant CTL epitope of EGFP in C57BL/6 mice: Gene Ther, v. 15, p. 700-1.

Haverkamp, J. M., B. Charbonneau, S. A. Crist, D. K. Meyerholz, M. B. Cohen, P. W. Snyder, R. U. Svensson, M. D. Henry, H. H. Wang, and T. L. Ratliff, 2011, An inducible model of abacterial prostatitis induces antigen specific inflammatory and proliferative changes in the murine prostate: Prostate, v. 71, p. 1139-50.

Khalili, M., L. N. Mutton, B. Gurel, J. L. Hicks, A. M. De Marzo, and C. J. Bieberich, 2010, Loss of Nkx3.1 expression in bacterial prostatitis: a potential link between inflammation and neoplasia: Am J Pathol, v. 176, p. 2259-68.

Kouiavskaia, D. V., S. Southwood, C. A. Berard, E. N. Klyushnenkova, and R. B. Alexander, 2009, T-cell recognition of prostatic peptides in men with chronic prostatitis/chronic pelvic pain syndrome: J Urol, v. 182, p. 2483-9.

Kramer, G., D. Mitteregger, and M. Marberger, 2007, Is benign prostatic hyperplasia (BPH) an immune inflammatory disease?: Eur Urol, v. 51, p. 1202-16.

Lang, M. D., J. C. Nickel, M. E. Olson, S. R. Howard, and H. Ceri, 2000, Rat model of experimentally induced abacterial prostatitis: Prostate, v. 45, p. 201-6.

Lust, J. A., M. Q. Lacy, S. R. Zeldenrust, A. Dispenzieri, M. A. Gertz, T. E. Witzig, S. Kumar, S. R. Hayman, S. J. Russell, F. K. Buadi, S. M. Geyer, M. E. Campbell, R. A. Kyle, S. V. Rajkumar, P. R. Greipp, M. P. Kline, Y. Xiong, L. L. Moon-Tasson, and K. A. Donovan, 2009, Induction of a chronic disease state in patients with smoldering or indolent multiple myeloma by targeting interleukin 1{beta}-induced interleukin 6 production and the myeloma proliferative component: Mayo Clin Proc, v. 84, p. 114-22.

McLaren, I. D., T. J. Jerde, and W. Bushman, 2011, Role of interleukins, IGF and stem cells in BPH: Differentiation, v. 82, p. 237-43.

Michalaki, V., K. Syrigos, P. Charles, and J. Waxman, 2004, Serum levels of IL-6 and TNF-alpha correlate with clinicopathological features and patient survival in patients with prostate cancer: Br J Cancer, v. 90, p. 2312-6.

Naslund, M. J., J. D. Strandberg, and D. S. Coffey, 1988, The role of androgens and estrogens in the pathogenesis of experimental nonbacterial prostatitis: J Urol, v. 140, p. 1049-53.

Nickel, J. C., 2008, Inflammation and benign prostatic hyperplasia: Urol Clin North Am, v. 35, p. 109-15; vii.

Nickel, J. C., J. Downey, I. Young, and S. Boag, 1999, Asymptomatic inflammation and/or infection in benign prostatic hyperplasia: BJU Int, v. 84, p. 976-81.

Nuki, G., B. Bresnihan, M. B. Bear, D. McCabe, and E. G. O. C. Investigators, 2002, Long-term safety and maintenance of clinical improvement following treatment with anakinra (recombinant human interleukin-1 receptor antagonist) in patients with rheumatoid arthritis: extension phase of a randomized, double-blind, placebo-controlled trial: Arthritis Rheum, v. 46, p. 2838-46.

Pitzalis, C., G. W. Jones, M. Bombardieri, and S. A. Jones, 2014, Ectopic lymphoid-like structures in infection, cancer and autoimmunity: Nat Rev Immunol, v. 14, p. 447-62.

Rao, V., J. C. Heard, H. Ghaffari, A. Wali, L. N. Mutton, and C. J. Bieberich, 2012, A Hoxb13-driven reverse tetracycline transactivator system for conditional gene expression in the prostate: Prostate, v. 72, p. 1045-51.

Re, F., R. Srinivasan, T. Igarashi, F. Marincola, and R. Childs, 2004, Green fluorescent protein expression in dendritic cells enhances their immunogenicity and elicits specific cytotoxic T-cell responses in humans: Exp Hematol, v. 32, p. 210-7.

Ren, K., and R. Torres, 2009, Role of interleukin-1beta during pain and inflammation: Brain Res Rev, v. 60, p. 57-64.

Ridker, P. M., M. Cushman, M. J. Stampfer, R. P. Tracy, and C. H. Hennekens, 1997, Inflammation, aspirin, and the risk of cardiovascular disease in apparently healthy men: N Engl J Med, v. 336, p. 973-9.

Schäfers, M., and L. Sorkin, 2008, Effect of cytokines on neuronal excitability: Neurosci Lett, v. 437, p. 188-93.

Sfanos, K. S., and A. M. De Marzo, 2012, Prostate cancer and inflammation: the evidence: Histopathology, v. 60, p. 199-215.

Shaikh, S., and L. F. Nicholson, 2006, Optimization of the Tet-On system for inducible expression of RAGE: J Biomol Tech, v. 17, p. 283-92.

Song, X., Y. Krelin, T. Dvorkin, O. Bjorkdahl, S. Segal, C. A. Dinarello, E. Voronov, and R. N. Apte, 2005, CD11b+/Gr-1+ immature myeloid cells mediate suppression of T cells in mice bearing tumors of IL-1beta-secreting cells: J Immunol, v. 175, p. 8200-8.

Torkko, K. C., R. S. Wilson, E. E. Smith, J. W. Kusek, A. van Bokhoven, and M. S. Lucia, 2015, Prostate Biopsy Markers of Inflammation are Associated with Risk of Clinical Progression of Benign Prostatic Hyperplasia: Findings from the MTOPS Study: J Urol.

Tu, S., G. Bhagat, G. Cui, S. Takaishi, E. A. Kurt-Jones, B. Rickman, K. S. Betz, M. Penz-Oesterreicher, O. Bjorkdahl, J. G. Fox, and T. C. Wang, 2008, Overexpression of interleukin-1beta induces gastric inflammation and cancer and mobilizes myeloid-derived suppressor cells in mice: Cancer Cell, v. 14, p. 408-19.

Urlinger, S., U. Baron, M. Thellmann, M. T. Hasan, H. Bujard, and W. Hillen, 2000, Exploring the sequence space for tetracycline-dependent transcriptional activators: novel mutations yield expanded range and sensitivity: Proc Natl Acad Sci U S A, v. 97, p. 7963-8.

Veeranki, S., 2013, Role of inflammasomes and their regulators in prostate cancer initiation, progression and metastasis: Cell Mol Biol Lett, v. 18, p. 355-67.

Vykhovanets, E. V., M. I. Resnick, G. T. MacLennan, and S. Gupta, 2007, Experimental rodent models of prostatitis: limitations and potential: Prostate Cancer Prostatic Dis, v. 10, p. 15-29.

Weber, A., P. Wasiliew, and M. Kracht, 2010, Interleukin-1 (IL-1) pathway: Sci Signal, v. 3, p. cm1.

Wingren, A. G., O. Björkdahl, T. Labuda, L. Björk, U. Andersson, U. Gullberg, G. Hedlund, H. O. Sjögren, T. Kalland, B. Widegren, and M. Dohlsten, 1996, Fusion of a signal sequence to the interleukin-1 beta gene directs the protein from cytoplasmic accumulation to extracellular release: Cell Immunol, v. 169, p. 226-37.

Zabaleta, J., L. J. Su, H. Y. Lin, R. A. Sierra, M. C. Hall, A. O. Sartor, P. E. Clark, J. J. Hu, and A. C. Ochoa, 2009, Cytokine genetic polymorphisms and prostate cancer aggressiveness: Carcinogenesis, v. 30, p. 1358-62.

Chapter 3: Interleukin 1β-Mediated Inflammation Induces Pelvic Hypersensitivity and Micturition Changes

Disclaimer: This chapter is a manuscript in preparation that has been modified to adhere to dissertation format

Abbreviations

CP	Chronic Prostatitis
CP/CPPS	Chronic Prostatitis/Chronic Pelvic Pain Syndrome
Dox	Doxycycline
IACUC	Institutional Animal Care and Use Committee
IL-1β	Interleukin 1β
IL-1R	Interleukin-1R
IL-1ra	Interleukin 1 Receptor Antagonist
IMPI	IL-1β-Mediated Prostate Inflammation
LPS	Lipopolysaccharide
NGF	Nerve Growth Factor
NIH	National Institutes of Health
PBS	Phosphate-Buffered Saline
RA	Rheumatoid Arthritis
TNF-α	Tumor Necrosis Factor
TRP	Transient Receptor Potential

Abstract

Chronic prostatitis/chronic pelvic pain syndrome (CP/CPPS) is a debilitating condition experienced by 16% of men in the United States. Poor comprehension of the natural history of this disease has made diagnosis and treatment extremely challenging. The majority of extant CP mouse models are based on bacterial infections; however, bacterial prostatitis only accounts for 10% of CP cases. We have developed and characterized a novel mouse model of prostate inflammation by overexpressing a proinflammatory cytokine, Interleukin-1β (IL-1β). IL-1β is overexpressed in the semen and expressed prostatic secretions of CP/CPPS patients. Incorporating the Tet-On technology, IL-1β expression is induced at will in the mouse prostate. In this study, we investigated IL-1β-mediated pelvic hypersensitivity, which was prevented by therapeutic intervention with an IL-1 receptor antagonist, Kineret. We also identified two key Transient Receptor Potential (TRP) channels, TRPV1 and TRPA1, that function as important nociceptors mediating pelvic hypersensitivity. Moreover, using a urine void assay, the effect of chronic inflammation on bladder function was quantified. Mice with inflamed prostates demonstrated decreased urine void area compared to their baseline void measurements and indicated urinary retention. The IMPI model closely recapitulates features of CP/CPPS including chronic pelvic pain and voiding dysfunction. The model can serve as a valuable platform to investigate pain mechanisms and bladder function influenced by IL-1β-driven prostate inflammation. Most importantly, the IMPI model will facilitate the identification of clinically relevant therapeutic targets to treat CP/CPPS.

Introduction

The National Institutes of Health (NIH) classifies CP into four categories: acute bacterial prostatitis, chronic bacterial prostatitis, CP/CPPS, and asymptomatic prostatitis. Ninety percent of CP cases belong to the CPPS category (Collins et al., 1998). After decades of research, the etiology of CPPS remains unclear. Lifestyle factors such as obesity, smoking, and hypertension were investigated; however, epidemiological studies revealed no association between these lifestyle factors and the risk of CPPS (Zhang et al., 2015). Without a clear understanding of CPPS etiology, the current therapeutic strategies merely treat the symptoms of the disease; consequently, patients often relapse with heightened pain (Nickel, 1998). Symptoms associated with CPPS include painful urination, muscle tenderness, sexual dysfunction, and pain originating from one or more urogenital organs (Rees et al., 2015). There is an urgent need to develop animal models that closely recapitulate the features in human CP/CPPS to decipher the molecular mechanisms of pain, identify novel therapeutic targets, and provide a platform for pre-clinical drug testing.

Several animal models have been developed to investigate the etiology of CP, and pain development associated with CPPS. Mouse models of prostate inflammation include spontaneous prostatitis models, models using infectious agents, immune-manipulated models, and hormone-induced prostatitis in rodents (Altuntas et al., 2013; Elkahwaji et al., 2007; Keith et al., 2001; Naslund et al., 1988; Rivero et al., 2002; Vykhovanets et al., 2007). Some of these models have been useful to model pain, the hallmark of CPPS. However, a detailed characterization of the molecular mechanisms in CPPS is required in a more physiologically relevant model. Extant models of

bacterial inflammation cannot be associated with a majority of chronic prostatitis where a pathogen could not be identified (Krieger et al., 1999). Animal models based on immune manipulation that require rat prostate extracts or other antigens to activate an immune response in the mouse prostate may not be physiologically relevant (Altuntas et al., 2013; Haverkamp et al., 2011; Rivero et al., 2002; Rudick et al., 2008). In our model, we have overexpressed Interleukin 1β (IL-1β), a proinflammatory cytokine implicated in CPPS. Cytokines are small, soluble, immune-modulatory proteins that are vital in directing an immune response against foreign antigens. However, overexpression of cytokines can result in an over-activated immune response and it is implicated in various autoimmune disorders (Cope, 1998; Dinarello, 2011; O'Shea et al., 2002). IL-1β, a multi-functional protein, belongs to the IL-1 family of cytokines (Barksby et al., 2007). It affects almost every cell type and has synergistic roles with other cytokines and signaling molecules (Jura et al., 2008; Vincenti and Brinckerhoff, 2001). Since IL-1β is highly inflammatory, its gene expression, synthesis, and secretion are tightly regulated (Andrei et al., 1999; Dinarello, 2005; Elssner et al., 2004). IL-1β expression can be induced by a range of factors: lipopolysaccharide (LPS), other cytokines (TNF-α,IL-2, IL-3), cell matrix proteins, clotting factors, lipids, inflammatory by-products (c-reactive protein, neuro-active substances (substance P, melatonin)), and stress factors (Dinarello, 1996).

Elevated levels of IL-1β have been observed in rheumatoid arthritis, asthma, HIV infections, Alzheimer's disease, solid tumors, leukemia, transplant rejections, and pancreatitis (Apte et al., 2006; Elaraj et al., 2006; Forlenza et al., 2009; Lewis et al., 2006). Naturally occurring Interleukin 1 Receptor Antagonist (IL-1ra) inhibits the IL-

1β cascade by competitively binding to its receptor, Interleukin-1R (IL-1R). Importantly, treatment with human recombinant IL-1ra has been used effectively in animal models and in clinical settings (Dinarello, 2010; Hoffman et al., 2008; Larsen et al., 2009; Nuki et al., 2002). In a model of acute pancreatitis, dose-dependent administration of IL-1ra significantly reduced tissue damage (Norman et al., 1995a; Norman et al., 1995b). In the case of prostate diseases, Alexander *et al.* reported elevated levels of IL-1β and Tumor Necrosis Factor (TNF-α) in the seminal plasma of a cohort of CP/CPPS patients (Alexander et al., 1998). Another independent study also reported elevated IL-1β (89% of patients) and TNF-α (45% of patients) in expressed prostatic secretions from CP patients (Nadler et al., 2000). Following these studies, several other cytokines including Interleukin-6 (IL-6) and Interleukin-8 (IL-8) were evaluated as predictors for CP/CPPS (Khadra et al., 2006; Orhan et al., 2001). Additionally, levels of Nerve Growth Factor (NGF) were observed to be significantly increased in the seminal plasma of CPPS patients compared to controls (Miller et al., 2002). Among these cytokines and growth factor that have been proposed as markers of CPPS, IL-1β could be the most predictive biomarker because it lies at the top of the inflammatory cascade, resulting in the induction of IL-6, IL-8, and NGF expression (McNeeley et al., 1995; Musso et al., 1990; Shimotake et al., 2004).

Using our *TetO-IL-1β|Hoxb13-rtTA* or **I**L-1β-**M**ediated **P**rostate **I**nflammation (IMPI) model described in Chapter 2, we induced IL-1β expression in the mouse prostate at will. In this study, we tested the role of IL-1β in mediating chronic pelvic pain and voiding dysfunction. The presence of referred hyperalgesia (increased sensitivity to mechanical stimuli) was quantified by measuring mechanical threshold

(determined by hypersensitivity to different von Frey filaments). Von Frey assay is useful to determine referred hyperalgesia, pain from visceral organs that can translate to the skin. Furthermore, we provide evidence to support the use of Kineret, an IL-1β-cascade inhibitor, for therapeutic intervention in IL-1β-driven CP cases. Additionally, we identified TRP channels, TRPA1 and TRPV1, as key nociceptors mediating pelvic hypersensitivity in the IMPI model. This study is profound, in the light of clinical evidence supporting IL-1β blockade and a growing body of research highlighting the role of IL-1β in pain (Baamonde et al., 2007; Binshtok et al., 2008; Pillarisetti, 2011; Ren and Torres, 2009; Schäfers et al., 2001).

Materials and Methods

Animal Housing

Animal care was provided in accordance with NIH's *Guide for the care and use of laboratory animals.* All experimental procedures were approved by the Institutional Animal Care and Use Committee (IACUC). Animals were maintained on a 12h light/12h dark cycle and housed in an animal facility with controlled temperature at 22±2°C, and relative humidity at 55±15%. Water and food were made available to the mice *ad libitum.* Aspen shavings were used as bedding within the cages (7.25"W x 11.5"D x 5"H). Mice were fed a diet purchased from Harlan Laboratories (Ref: 2020).

Transgenic Mouse

The generation and characterization of IMPI mice have been discussed in detail previously (Chapter 2)

Von Frey Assay

The von Frey protocol was adapted from publications that employed von Frey filaments in rodent behavioral testing (Radhakrishnan and Nallu, 2009; Rudick et al., 2008). Filaments were tested in ascending order using five individual fibers with forces of 0.02 g, 0.04 g, 0.16 g, 0.4 g, and 1.0 g (Stoelting) and applied perpendicularly to the pelvic region and hind paw. During testing, mice were individually placed on a wire mesh and covered using tinted cups. Mice were allowed to acclimate for 30 minutes before the test began. Each filament was applied for 1-2s, 10 times, with 5s intervals between each stimulus. Ten spots were marked where each filament was tested to avoid desensitization. The area tested was restricted to the pelvic region; in males, testing was conducted 1 cm above the penal region, while testing was done in a homologous region within the female. This region specificity was designed to test for prostate-specific pain sensitivity in males originating from doxycycline (Dox)-induced prostate inflammation. In addition to the pelvic region, the plantar region of the hind paw was used as a control area to demonstrate that pelvic hypersensitivity emerged due to prostate inflammation and that hypersensitivity was not observed in the hind paw. Rapid abdominal withdrawal, scratching the stimulated area, and jumping movements were recorded as positive reactions to filament pressure.

The response frequency was recorded as the percentage of positive responses to the mechanical stimuli (number of positive responses to stimuli out of the 10 trials). For the hind paw, a positive response was defined as either a sharp withdrawal or licking of the test paw. All mice were tested twice to determine the baseline measurements of pain sensitivity before induction as an experimental control. Post

Dox-treatment, mice were tested after 7, 14, 21, and 28 days. Standardized testing was applied to diminish variability, including fixed time of day and blinding the experimenter. Von Frey testing was repeated more than four independent times by separate individuals blinded to the genotype.

Kineret Administration

Kineret, also known by its generic name, Anakinra, was obtained from the pharmaceutical company, Sobi. Kineret was administered at a concentration of 150 mg/kg by diluting it with Phosphate-Buffered Saline (PBS). Intraperitoneal injectons were adminstered twice daily at 12 hour intervals. Control animals received PBS injections.

Urine Void Assay

Male mice, individually housed after three weeks of age to avoid the development of dominance hierarchy between males and its subsequent effects on urine patterns (Desjardins et al., 1973), were placed in standard cages for four hours with bedding replaced by 3 mm Whatman filter paper. Food was allowed *ad libitum*; however, water access was limited during testing. Urine spots were then photographed under UV light to examine any change in micturition pattern throughout the three week testing period. The program ImageJ was used to analyze micturition pattern in order to determine changes in urine spot area before and after Dox-treatment. Mice were fed Dox that was incorporated into their regular diet (Dox 2 g/kg, 2020) purchased from Harlan Laboratories.

Breeding Strategy to Develop IMPI|TRPA1^{null} and IMPI|TRPV1^{null} Mice

We bred the homozygous bi-genic system (Hoxb13-rtTA+/+|TetO-IL-1ß+/+) or previously described IMPI+/+ system onto both TRPA1 and TRPV1 null strains (Figure 5). IMPI mice on an *FVB* background were crossed with B6.129 TrpV1null mice (Jackson Laboratory Stock # 3770) to generate triple heterozygous IMPI+/-|TRPV1+/- offspring. Multiple breeding pairs of triple heterozygous offspring were intercrossed to generate a large cohort of IMPI+/-|TRPV1+/- animals to finally generate the IMPI+/+|TRPV1^{null} genotype. We set up four IMPI+/+|TRPV1^{null} X IMPI+/+|TRPV1^{null} breeding pairs to get a sufficient cohort of males to perform von Frey experiments. An identical strategy was employed to generate IMPI+/+|TRPA1^{null} mice.

Statistical Analysis

Graphing and statistical analyses (paired, two-tailed student's t-test) were performed using Prism software (GraphPad Software, Inc.).

Results

IL-1β-Mediated Inflammation Induces Pelvic Hypersensitivity

To determine whether IL-1β-mediated inflammation results in pelvic hypersensitivity, the von Frey assay was employed. Von Frey filaments have been useful in quantifying pelvic hypersensitivity in mice by measuring referred hyperalgesia (Radhakrishnan and Nallu, 2009; Rudick et al., 2011; Rudick et al., 2008; Traub et al., 2008). The von Frey assay is based on the principle that application of normal force to the skin can result in abnormal responses because of underlying visceral pain. In a blinded study, a cohort of doubly heterozygous IMPI$^{+/-}$ mice were tested using a range of forces applied to the abdomen

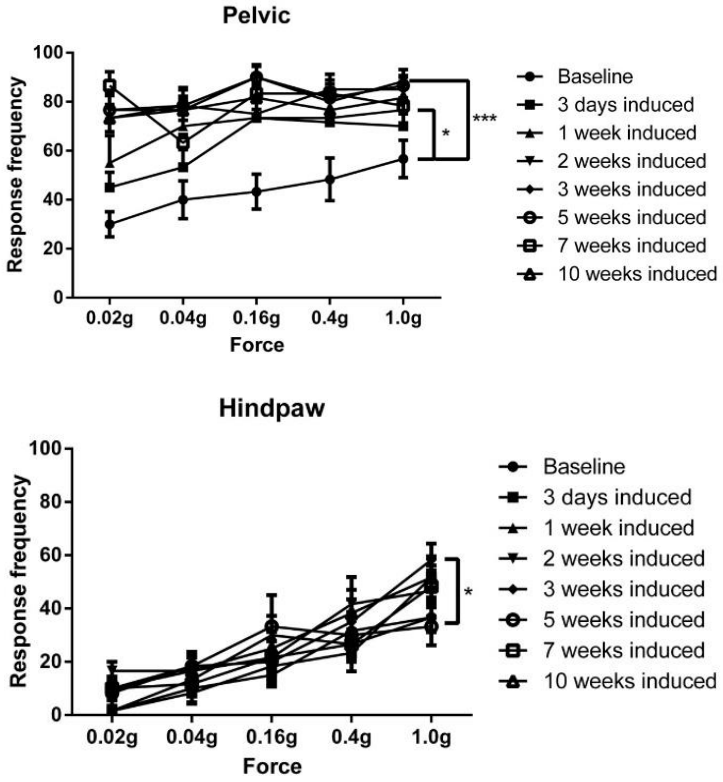

Figure 1: Quantification of referred hyperalgesia in IMPI+/- Dox-treated mice: Mechanical threshold for pelvic area and hind paw was quantified by von Frey filaments (at each force (g) represented on X –axis) at baseline, 3 days, 1 week, 2 weeks, 3 weeks, 5 weeks, 7 weeks and 10 weeks post treatment. Note, for the pelvic area, statistical significance in response frequency was not observed at 3 days (P=0.08341), however pelvic hypersensitivity was observed at 1 week (P=0.01590), 2 weeks (P=0.00206), 3 weeks (P=0.00175), 5 weeks (P=0.00128), 7 weeks (P=0.00426) and 10 weeks (P=0.00072). For the hind paw, majority of the time points exhibited no change in response frequency from baseline, except for at 10 weeks (P=0.039). A paired t-test was used to determine statistical significance. P<0.05 was considered significant. Error bars represent mean±SEM *P<0.05, ***P<0.001

in the vicinity of the prostate. Apart from the lower abdominal region, the hind paw was also tested and served as a control area. Before Dox treatment, referred hyperalgesia was measured to determine baseline levels of sensitivity. The response frequency was calculated and recorded as the percentage of reactions (jumping, licking, scratching) received after prodding 10 times with the same filament. Once the thresholds for mechanical stimuli in the pelvic area and hind paw were established, the cohort was administered Dox (mixed in drinking water) to initiate IL-1ß expression in the prostate gland. After three days of treatment, the von Frey assay was repeated to quantify referred hyperalgesia. At three days post Dox-treatment, the difference in mechanical threshold was not statistically significant as determined by a paired t-test. Statistically significant pelvic hypersensitivity was observed at one week, two weeks, three weeks, five weeks, seven weeks, and 10 weeks post treatment ($p= 0.00072$) (Figure 1). One week post Dox-treatment, the response frequency increased from 42% at baseline to 70%, indicating a 75% increase in threshold with respect to baseline . The hind paw was tested simultaneously as a control region. No referred hyperalgesia was observed in the hind paw except for at three weeks and 10 weeks post treatment ($p=0.0395$) (Figure 1). The increase in hind paw sensitivity could be attributed to an overall increase in general irritability due to increased pelvic pain. As seen in figure 1, the difference from baseline measurement was larger in the pelvic region than the hind paw. Wild-type animals on Dox were tested to control for the effect of Dox on pelvic hypersensitivity. No difference in mechanical threshold was observed in wild-type mice before and after Dox-treatment (data not shown). These results suggest that pelvic

hypersensitivity in response to IL-1β expression was observed as early as one week post Dox-treatment and was sustained up to 10 weeks.

Heightened Hypersensitivity Associated with Inflammation Resolves After Dox Withdrawal

Having established the development of pelvic hypersensitivity in the doubly heterozygous IMPI $^{+/-}$ mice, we examined referred hyperalgesia in our doubly homozygous *Hoxb13-rtTA*$^{+/+}$ |*TetO-IL-1ß*$^{+/+}$ IMPI mice. As described in Chapter 2, histologically, in the IMPI+/+ mice we observed a more robust inflammation in all the prostate lobes. However, in the IMPI+/- mice, inflammation was pre-dominantly located in the ventral lobes with low-to-mild inflammation in the remaining lobes. The IMPI+/- mice exhibited a 75% increase in pelvic hypersensitivity from baseline whereas the IMPI+/+ mice displayed a 300% increase from baseline threshold for pelvic sensitivity (comparisons drawn between figure 1 and figure 2). These data suggest that the degree of inflammation could correlate with pelvic hypersensitivity.

To determine the effect of Dox withdrawal, a cohort of IMPI+/+ mice were tested to establish baseline, and Dox-treated for two weeks. Using the von Frey assay, the pelvic and hind paw thresholds were quantified at one week and two weeks post treatment. As expected, statistically significant pelvic hypersensitivity was observed at one week and two weeks post treatment ($p < 0.05$). Mice were then reverted to regular drinking water. After Dox withdrawal, pelvic

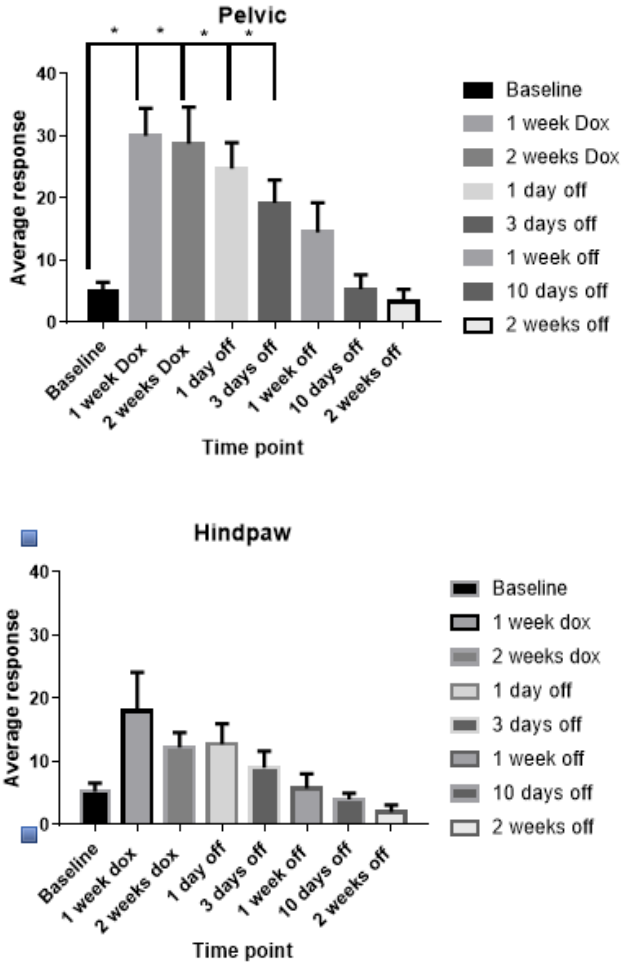

Figure 2: Quantification of referred hyperalgesia in IMPI+/+ mice after Dox withdrawal: Average response for pelvic area and hind paw were quantified by adding the total response from all four filament forces and calculating mean. For the pelvic area, statistical significance was observed at 1 week Dox, 2 weeks Dox, 1 day off and 3 days off compared to baseline. However, statistical significance was not observed at subsequent time points. Note, average pelvic response returns to baseline levels at 10 days off Dox. For hind paw, no significant differences were observed compared to baseline. A paired t-test was used to determine statistical significance. $P<0.05$ was considered significant. Error bars represent mean±SEM *$P<0.05$

hypersensitivity was sustained at 'one day off' and 'three days off' ($p=0.0267$). However, after one week of Dox withdrawal, the difference between baseline and 'one week off' were not statistically significant. Similar observations were made at '10 days off' and 'two weeks off'. No difference in hind paw thresholds was observed before

and after Dox. These data suggest that pelvic hypersensitivity observed in the IMPI mice was mediated by IL-1β-driven prostate inflammation that subsided after one week from Dox withdrawal, with downregulation of IL-1β expression.

Kineret Abolishes Referred hyperalgesia Mediated by IL-1β-Induced Inflammation

To determine the efficacy of Kineret, an IL-1β-cascade inhibitor, a baseline von Frey testing was performed on a cohort of IMPI$^{+/+}$mice (n=12). This study was performed to determine whether Kineret treatment could prevent referred hyperalgesia associated with IL1ß-induced inflammation. The cohort was treated with Dox at 2 mg/ml in drinking water prior to assignment into two treatment groups. One group (Kineret cohort) received two Kineret injections daily at 12 hour intervals at 150 mg/kg body weight. For the 'Kineret cohort', Kineret was co-administered with Dox for three weeks. The second group (Dox-only cohort), received Dox treatment for the same duration. Referred hyperalgesia was quantified using the von Frey assay in both groups. The control group displayed a 300% increase in pelvic hypersensitivity (p=1.43E-05) (Figure 3) while the drug group exhibited no significant change compared to the baseline (p=0.84) (Figure 3). The hind paw data from the control group showed no

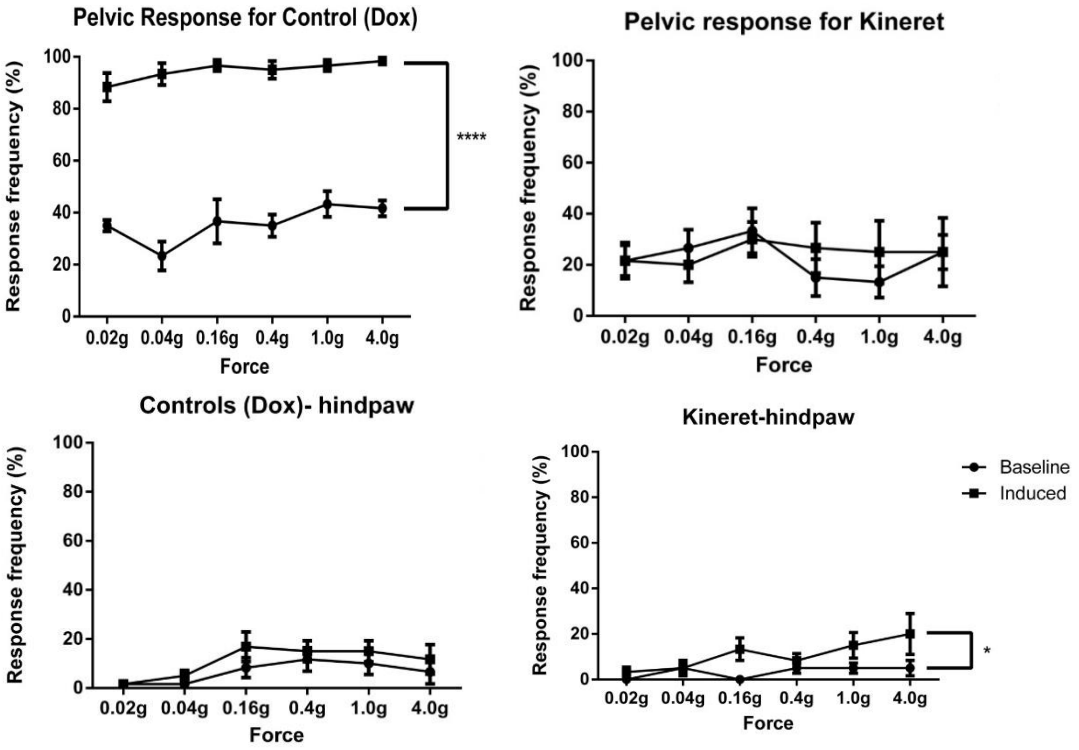

Figure 3: Quantification of referred hyperalgesia to determine the efficacy of Kineret: Response frequency for Dox group and Kineret group were quantified and graphed at each filament. For the Dox group, statistical significance was observed at 3 weeks post Dox treatment, for the pelvic region. For the Kineret+Dox-treated group, no significant difference were observed compared to baseline. Note, significant increase in pelvic hypersensitivity in the Dox group, however, it was not observed in the Kineret group. For hind paw, no statistically significant difference was observed in Dox group, however , the Kineret group was significant (P=0.030) A paired t-test was used to determine statistical significance. P<0.05 was considered significant. Error bars represent mean±SEM ****P<0.0001

difference from baseline, indicating that the effect was localized to the pelvic region (Figure 3). However, for the drug group, a small increase in hind paw sensitivity was observed (p= 0.030). As discussed earlier this could be attributed to an increase in overall irritability induced by pelvic pain. This study further validated our previous experiments and supports our hypothesis that IL-1β-induced pelvic hypersensitivity

can be prevented by therapeutic intervention with Kineret. Therefore, IL-1β-blockade could be beneficial to control pain in CP/CPPS patients where IL-1β is implicated.

Voiding Dysfunction Observed in Mice with Prostate Inflammation

Micturition complications for example dribbling, painful urination, nocturia, and incomplete bladder emptying, are the major urinary symptoms experienced by CP/CPPS patients. We designed a study to test whether similar symptoms develop in the IMPI mouse model. To determine change in voiding, we employed a urine void assay that allowed the quantification of urine spots before and after inflammation.

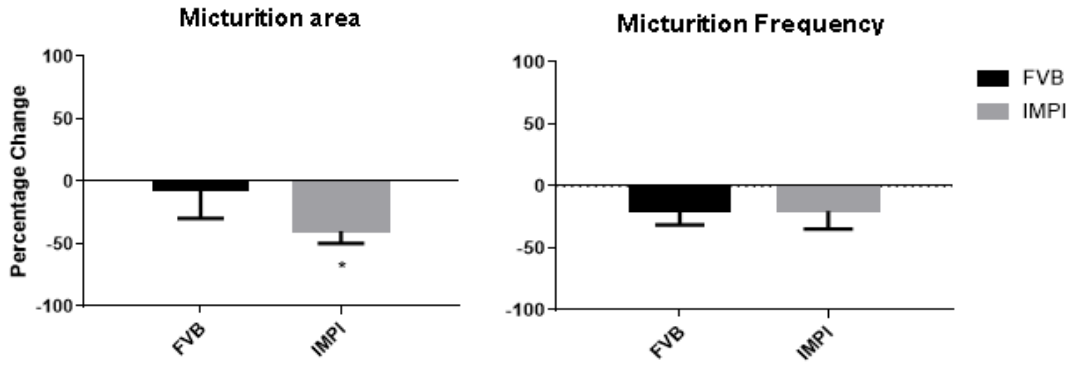

Figure 4: Graphical representation of micturition patterns collected from Dox-treated IMPI and FVB mice- The micturition area graph represents percent change from baseline in micturition frequency (number of urine spots on the filter paper collected over a period of four hours). The FVB/WT group (n=6) and IMPI cohort (n=5) was observed to have a 20% decrease in the number of spots after Dox administration (statistically insignificant). The micturition frequency graph represents the percent change in micturition area or the total area voided on the filter paper (calculated in pixels using image j). The FVB cohort had a 6% decrease in total void area compared to baseline measurements. However, the IMPI cohort had a 40% decrease in total void area compared to baseline measurements ($P<0.05$). This could indicate urine retention and loss of bladder control * indicates statistical significance measured by a paired t-test. $P<0.05$ was considered significant. Error bars represent mean±SEM

Dox is well known to reduce water consumption in mice due to its bitter taste (Hojman et al., 2007). To circumvent this problem, Dox was incorporated into regular

mouse diet to improve accuracy and consistency in studying the urodynamics of the mouse bladder affected by chronic inflammation.

Bedding was removed, and replaced with 3mm Whatmann filter paper to determine micturition pattern for individually housed mice. A cohort of IMPI and FVB/N mice (n=11) were tested for a period of four hours before and after Dox treatment. For baseline measurements, micturition patterns were determined on three consecutive days at the same time of the day. For Dox treatment, we replaced the regular mouse diet with Dox-incorporated food (2g/kg) that was administered for three weeks. Three weeks post-Dox treatment, micturition patterns were determined on three consecutive days. Since urine fluoresces under UV light, the urine patterns collected from all the animals were imaged under UV light. The collected images were then analyzed by ImageJ. Change in micturition frequency was analyzed by averaging the number of urine spots in the baseline and Dox-treated patterns followed by determining statistical significance. As shown in figure 4, there was a 20% decrease in micturition frequency post Dox treatment in the FVB and transgenic cohort with respect to their baseline measurements. However, this difference was not statistically significant. Using ImageJ, the total void area before and after Dox treatment was quantified. The FVB cohort exhibited a 6% decrease in total void area from baseline, however this change was not statistically significant. The IMPI cohort exhibited a statistically significant 40% percent decrease in micturition area, from the pre-Dox measurement. This indicates a change in urine void volume in the mice with prostate inflammation. These data suggest that IL-1β-mediated inflammation induces a voiding dysfunction, which could indicate potential urinary retention.

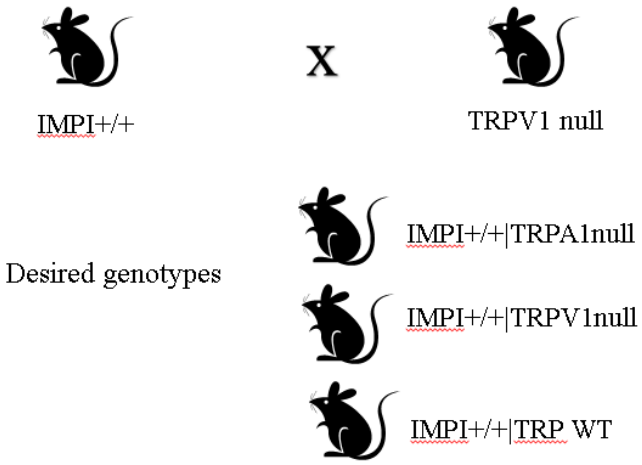

Figure 5: Breeding strategy: Genotypes of strains inter-crossed to generate the desired genotypes for von Frey experiments shown as described in materials and methods. Intervening generations of triple heterozygotes not shown for simplicity.

Our next aim was to define the molecular basis of pain and voiding symptoms in CP/CPPS to guide the development of effective therapies to alleviate morbidity associated with this disease. Transient Receptor Potential (TRP) channels have been associated with other forms of inflammatory pain but have not been investigated for pelvic pain (Stucky et al., 2009). The overall objective was to determine the contributions of two TRP channels in mediating pain in the IMPI mouse model. Our central hypothesis was that activation of TRPA1 and TRPV1 channels in response to a prostatic inflammatory milieu mediates pain and voiding symptoms.

The breeding strategy to develop IMPI|TRPA1^{null} and IMPI|TRPV1^{null} mice is described in the materials and methods section (Figure 5). Given that all of our observations on the performance of the Dox-inducible inflammation were made on a pure FVB background, it was critical to demonstrate that crossing the system onto the mixed B6.129 background did not affect the onset of inflammation. To determine whether the onset of inflammation is in a similar fashion to FVB background, we performed pathological analyses of prostate glands from Dox-treated IMPI|TRPA1^{null},

IMPI|TRPV1^{null} and IMPI|TRP^{WT} mice. The data shown in figure 8 demonstrate that the system continues to perform well in the mixed genetic background. Robust inflammation was observed even in the absence of functional TRP channels.

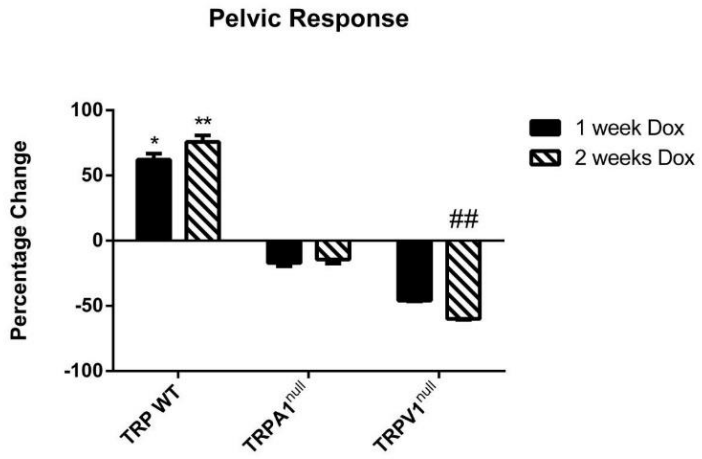

Figure 6: TRPA1 and TRPV1 ion channels mediate prostate inflammatory pain. von Frey filaments were used to test baseline levels of hyperalgesia in pelvic area for cohorts of Trp WT (n=10), TrpA1^{null} (n=10) and TrpV1^{null} (n=7) (Black bars). All cohorts were tested for baseline response to mechanical stimuli using von Frey filaments after one week Dox-treatment (diagonal stripped bars) and after 2 weeks of Dox-treatment (vertical stripped bars). Results for all filaments were pooled, and represented as percent change with respect to baseline. A paired student t-test was performed and significant differences were observed for Trp WT baseline vs one week post-treatment (marked single asterisk) and two weeks post-treatment (marked double asterisks). Note no increase in hypersensitivity observed in the knockout groups. A one-way ANOVA analysis determined no significant differences between the baselines across all cohorts. Error bars represent mean±SEM. *indicates $p<0.05$ with respect to Trp WT baseline.** indicates $p<0.01$ with respect to Trp WT baseline. ## indicates $p<0.01$ with respect to Trpv1 KO baseline.

Having demonstrated that robust inflammation was present on the mixed genetic background, referred hyperalgesia was quantified on cohorts of Dox-treated IMPI|TRPA1^{null}, IMPI|TRPV1^{null} and IMPI|TRP^{WT} (n=30) to determine whether TRP channel nullity would affect the level of referred hyperalgesia experienced in the IMPI model. Baseline pelvic and hind paw referred hyperalgesia measurements were performed on all the cohorts. Although the average baseline responsiveness within the TRPA1 and TRPV1 knockout cohorts appeared to be reduced compared to the cohort with WT TRP channels, statistical analyses demonstrated that the differences were not significant.

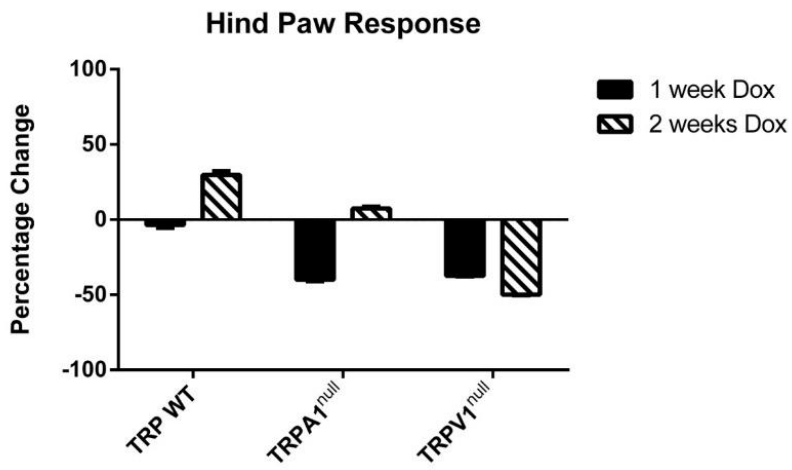

Figure 7: Prostate inflammatory pain restricted to pelvic area. von Frey filaments were used to test baseline levels of hyperalgesia in the hind paws for cohorts of Trp WT (n=10), TrpA1^{null} (n=10) and TrpV1^{null} (n=7) (Black bars). All cohorts were tested for baseline response to mechanical stimuli using von Frey filaments after one week Dox-treatment (diagonal stripped bars) and after 2 weeks of Dox-treatment (vertical stripped bars). Note, no increase in hypersensitivity observed in any cohort. A one-way ANOVA analysis determined no significant differences between the baselines across all cohorts. Error bars represent mean±SEM.

After baseline measurement, all three cohorts were then treated with Dox for one week. A second von Frey assay was then performed, and the animals were Dox-treated for a second week. A third von Frey assay was performed at the end of the second week of Dox exposure. There was a greater than 50% decrease in pain threshold, indicating increased hypersensitivity observed in the IMPI|TRP^{WT} animals after one week of Dox treatment. After two weeks, a 75% change in pain threshold was observed. Strikingly, in the IMPI|TRPA1^{null} and IMPI|TRPV1^{null} cohorts, there was no statistically significant change with respect to their baseline. The data shown in figure 7 demonstrate that nullity for either TRPA1 or TRPV1 essentially eliminates the pelvic hypersensitivity that accompanies prostatic inflammation, as quantified by the von Frey assay. The loss of referred hyperalgesia in the TRPA1 and TRPV1 mice demonstrate that both these channels are required to mediate pelvic hypersensitivity. These data strongly suggest that the inflammatory referred hyperalgesia measured by von Frey is associated with prostatic inflammation and is

mediated at least in part by TRP channels. It further suggests that both TRPA1 and TRPV1 channels must be present to mediate nociception, given that loss of function of either channel led to the elimination of pelvic pain that accompanies cytokine-mediated prostate inflammation.

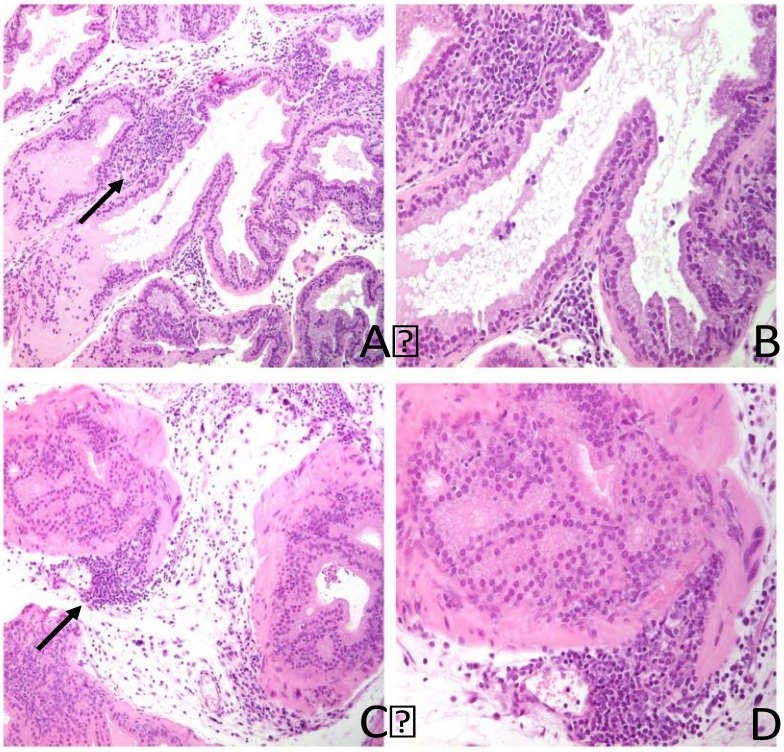

Figure 8: Histological examination of *Hoxb13-rtTA*$^{+/+}$|*TetO-IL-1ß*$^{+/+}$|*Trpa1*^{null} Dox-treated for 2 months. (A,B) H&E stained ventral prostates at 200X and 400X magnification. Note pockets of inflammatory cells (black arrows). (C,D) H&E stained sections of anterior prostate at 200X and 400X magnification. Inflammation was observed in all lobes of the mouse prostate in TrpA^{null} mice.

Discussion

In this study, we showed that IL-1β-induced inflammation mediates pelvic hypersensitivity in Dox-treated IMPI males, but not in untreated IMPI males. The referred hyperalgesia in IMPI mice was not significant at three days post Dox treatment; however, in subsequent time points from one week to ten weeks, the referred hyperalgesia was significantly different from baseline measurements. These data suggest that inflammation-induced pelvic hypersensitivity requires more than three days post IL-1β expression to develop. Furthermore, we demonstrated that Dox-treatment followed by Dox withdrawal can induce referred hyperalgesia, which then

gradually returns to baseline measurements with Dox withdrawal. Treatment with Kineret prevented the development of referred hyperalgesia in IMPI mice but not in the untreated group. Taken together, these data strongly suggest that IL-1β-mediated inflammation can induce pelvic hypersensitivity in the male IMPI mice. The voiding dysfunction and the pelvic hypersensitivity observed in the IMPI mice closely recapitulate the symptoms of CP/CPPS. This is the first inducible genetic model of prostatic inflammation and is a significant contribution towards studying the mechanisms of IL-1β-mediated prostate inflammatory disorders.

Nociceptors are specialized ion channels located on primary afferent nerve fibers that detect pain stimuli (Binshtok et al., 2008). In this study, we have established that IL-1β-mediated inflammation establishes chronic pelvic pain. Because the IMPI model closely recapitulates the features of CPPS, we endeavored to discern the nociceptors mediating pain. TRP ion channels, including TRPA1 and TRPV1, have emerged as important contributors to pain and inflammation (Brain, 2011; Stucky et al., 2009). TRPV1 is a heat-activated channel that responds to a variety of stimuli including capsaicin (Tsuji and Aono, 2012). The TRPA1 channel is activated by ingredients of mustard oil and garlic (Lapointe and Altier, 2011). Decades of research on TRPV1 and TRPA1 have resulted in the development of TRP antagonists that are currently being clinically tested (Kaneko and Szallasi, 2014; Nilius and Szallasi, 2014; Okuhara et al., 2007). Testing the efficacy of a small molecule inhibitor for TRPV1, ABT 102, is currently on-going. The success of this study would further validate our hypothesis that TRP channels are crucial nociceptors mediating pelvic pain, and that

therapeutic intervention with TRP antagonists could be a clinical success for CP/CPPS patients.

. To summarize, we have developed a pre-clinical model physiologically relevant to CP/CPPS disease. We have demonstrated the role of IL-1β in potentially mediating chronic pelvic pain, and characterized the pelvic hypersensitivity in the model. The model can now serve as a platform to test similar TRPV1 and TRPA1 inhibitors. From our genetic studies, we believe that blocking either one of the channels should be sufficient to produce a therapeutic effect. Further studies can aid to discern the molecular pathways, key immune infiltrates, and cytokines/chemokines regulating pelvic pain.

References

Alexander, R. B., S. Ponniah, J. Hasday, and J. R. Hebel, 1998, Elevated levels of proinflammatory cytokines in the semen of patients with chronic prostatitis/chronic pelvic pain syndrome: Urology, v. 52, p. 744-9.

Altuntas, C. Z., F. Daneshgari, E. Veizi, K. Izgi, F. Bicer, A. Ozer, K. O. Grimberg, B. Bakhautdin, C. Sakalar, C. Tasdemir, and V. K. Tuohy, 2013, A novel murine model of chronic prostatitis/chronic pelvic pain syndrome (CP/CPPS) induced by immunization with a spermine binding protein (p25) peptide: Am J Physiol Regul Integr Comp Physiol, v. 304, p. R415-22.

Andrei, C., C. Dazzi, L. Lotti, M. R. Torrisi, G. Chimini, and A. Rubartelli, 1999, The secretory route of the leaderless protein interleukin 1beta involves exocytosis of endolysosome-related vesicles: Mol Biol Cell, v. 10, p. 1463-75.

Apte, R. N., Y. Krelin, X. Song, S. Dotan, E. Recih, M. Elkabets, Y. Carmi, T. Dvorkin, R. M. White, L. Gayvoronsky, S. Segal, and E. Voronov, 2006, Effects of micro-environment- and malignant cell-derived interleukin-1 in carcinogenesis, tumour invasiveness and tumour-host interactions: Eur J Cancer, v. 42, p. 751-9.

Baamonde, A., V. Curto-Reyes, L. Juárez, A. Meana, A. Hidalgo, and L. Menéndez, 2007, Antihyperalgesic effects induced by the IL-1 receptor antagonist anakinra and increased IL-1beta levels in inflamed and osteosarcoma-bearing mice: Life Sci, v. 81, p. 673-82.

Barksby, H. E., S. R. Lea, P. M. Preshaw, and J. J. Taylor, 2007, The expanding family of interleukin-1 cytokines and their role in destructive inflammatory disorders: Clin Exp Immunol, v. 149, p. 217-25.

Binshtok, A. M., H. Wang, K. Zimmermann, F. Amaya, D. Vardeh, L. Shi, G. J. Brenner, R. R. Ji, B. P. Bean, C. J. Woolf, and T. A. Samad, 2008, Nociceptors are interleukin-1beta sensors: J Neurosci, v. 28, p. 14062-73.

Brain, S. D., 2011, TRPV1 and TRPA1 channels in inflammatory pain: elucidating mechanisms: Ann N Y Acad Sci, v. 1245, p. 36-7.

Collins, M. M., R. S. Stafford, M. P. O'Leary, and M. J. Barry, 1998, How common is prostatitis? A national survey of physician visits: J Urol, v. 159, p. 1224-8.

Cope, A. P., 1998, Regulation of autoimmunity by proinflammatory cytokines: Curr Opin Immunol, v. 10, p. 669-76.

Desjardins, C., J. A. Maruniak, and F. H. Bronson, 1973, Social rank in house mice: differentiation revealed by ultraviolet visualization of urinary marking patterns: Science, v. 182, p. 939-41.

Dinarello, C. A., 1996, Biologic basis for interleukin-1 in disease: Blood, v. 87, p. 2095-147.

Dinarello, C. A., 2005, Blocking IL-1 in systemic inflammation: J Exp Med, v. 201, p. 1355-9.

Dinarello, C. A., 2010, Why not treat human cancer with interleukin-1 blockade?: Cancer Metastasis Rev, v. 29, p. 317-29.

Dinarello, C. A., 2011, Interleukin-1 in the pathogenesis and treatment of inflammatory diseases: Blood, v. 117, p. 3720-32.

Elaraj, D. M., D. M. Weinreich, S. Varghese, M. Puhlmann, S. M. Hewitt, N. M. Carroll, E. D. Feldman, E. M. Turner, and H. R. Alexander, 2006, The role of interleukin 1 in growth and metastasis of human cancer xenografts: Clin Cancer Res, v. 12, p. 1088-96.

Elkahwaji, J. E., W. Zhong, W. J. Hopkins, and W. Bushman, 2007, Chronic bacterial infection and inflammation incite reactive hyperplasia in a mouse model of chronic prostatitis: Prostate, v. 67, p. 14-21.

Elssner, A., M. Duncan, M. Gavrilin, and M. D. Wewers, 2004, A novel P2X7 receptor activator, the human cathelicidin-derived peptide LL37, induces IL-1 beta processing and release: J Immunol, v. 172, p. 4987-94.

Forlenza, O. V., B. S. Diniz, L. L. Talib, V. A. Mendonça, E. B. Ojopi, W. F. Gattaz, and A. L. Teixeira, 2009, Increased serum IL-1beta level in Alzheimer's disease and mild cognitive impairment: Dement Geriatr Cogn Disord, v. 28, p. 507-12.

Haverkamp, J. M., B. Charbonneau, S. A. Crist, D. K. Meyerholz, M. B. Cohen, P. W. Snyder, R. U. Svensson, M. D. Henry, H. H. Wang, and T. L. Ratliff, 2011, An inducible model of abacterial prostatitis induces antigen specific inflammatory and proliferative changes in the murine prostate: Prostate, v. 71, p. 1139-50.

Hoffman, H. M., M. L. Throne, N. J. Amar, M. Sebai, A. J. Kivitz, A. Kavanaugh, S. P. Weinstein, P. Belomestnov, G. D. Yancopoulos, N. Stahl, and S. J. Mellis, 2008, Efficacy and safety of rilonacept (interleukin-1 Trap) in patients with cryopyrin-associated periodic syndromes: results from two sequential placebo-controlled studies: Arthritis Rheum, v. 58, p. 2443-52.

Hojman, P., J. Eriksen, and J. Gehl, 2007, Tet-On induction with doxycycline after gene transfer in mice: sweetening of drinking water is not a good idea: Anim Biotechnol, v. 18, p. 183-8.

Jura, J., P. Wegrzyn, M. Korostyński, K. Guzik, M. Oczko-Wojciechowska, M. Jarzab, M. Kowalska, M. Piechota, R. Przewłocki, and A. Koj, 2008, Identification of interleukin-1 and interleukin-6-responsive genes in human monocyte-derived macrophages using microarrays: Biochim Biophys Acta, v. 1779, p. 383-9.

Kaneko, Y., and A. Szallasi, 2014, Transient receptor potential (TRP) channels: a clinical perspective: Br J Pharmacol, v. 171, p. 2474-507.

Keith, I. M., J. Jin, D. Neal, B. D. Teunissen, and T. D. Moon, 2001, Cell relationship in a Wistar rat model of spontaneous prostatitis: J Urol, v. 166, p. 323-8.

Khadra, A., P. Fletcher, G. Luzzi, R. Shattock, and P. Hay, 2006, Interleukin-8 levels in seminal plasma in chronic prostatitis/chronic pelvic pain syndrome and nonspecific urethritis: BJU Int, v. 97, p. 1043-6.

Krieger, J. N., L. Nyberg, and J. C. Nickel, 1999, NIH consensus definition and classification of prostatitis: JAMA, v. 282, p. 236-7.

Lapointe, T. K., and C. Altier, 2011, The role of TRPA1 in visceral inflammation and pain: Channels (Austin), v. 5, p. 525-9.

Larsen, C. M., M. Faulenbach, A. Vaag, J. A. Ehses, M. Y. Donath, and T. Mandrup-Poulsen, 2009, Sustained effects of interleukin-1 receptor antagonist treatment in type 2 diabetes: Diabetes Care, v. 32, p. 1663-8.

Lewis, A. M., S. Varghese, H. Xu, and H. R. Alexander, 2006, Interleukin-1 and cancer progression: the emerging role of interleukin-1 receptor antagonist as a novel therapeutic agent in cancer treatment: J Transl Med, v. 4, p. 48.

McNeeley, P. A., P. A. Baecker, N. L. Jones, C. J. Emmett, R. M. Eglen, E. H. Wong, and R. M. Johnson, 1995, Interleukin-1 beta induces nerve growth factor release and gene expression in human glioblastoma cells: Proc West Pharmacol Soc, v. 38, p. 63-6.

Miller, L. J., K. A. Fischer, S. J. Goralnick, M. Litt, J. A. Burleson, P. Albertsen, and D. L. Kreutzer, 2002, Nerve growth factor and chronic prostatitis/chronic pelvic pain syndrome: Urology, v. 59, p. 603-8.

Musso, T., I. Espinoza-Delgado, K. Pulkki, G. L. Gusella, D. L. Longo, and L. Varesio, 1990, Transforming growth factor beta downregulates interleukin-1 (IL-1)-induced IL-6 production by human monocytes: Blood, v. 76, p. 2466-9.

Nadler, R. B., A. E. Koch, E. A. Calhoun, P. L. Campbell, D. L. Pruden, C. L. Bennett, P. R. Yarnold, and A. J. Schaeffer, 2000, IL-1beta and TNF-alpha in prostatic secretions are indicators in the evaluation of men with chronic prostatitis: J Urol, v. 164, p. 214-8.

Naslund, M. J., J. D. Strandberg, and D. S. Coffey, 1988, The role of androgens and estrogens in the pathogenesis of experimental nonbacterial prostatitis: J Urol, v. 140, p. 1049-53.

Nickel, J. C., 1998, Effective office management of chronic prostatitis: Urol Clin North Am, v. 25, p. 677-84.

Nilius, B., and A. Szallasi, 2014, Transient receptor potential channels as drug targets: from the science of basic research to the art of medicine: Pharmacol Rev, v. 66, p. 676-814.

Norman, J., M. Franz, J. Messina, A. Riker, P. J. Fabri, A. S. Rosemurgy, and W. R. Gower, 1995a, Interleukin-1 receptor antagonist decreases severity of experimental acute pancreatitis: Surgery, v. 117, p. 648-55.

Norman, J. G., M. G. Franz, G. S. Fink, J. Messina, P. J. Fabri, W. R. Gower, and L. C. Carey, 1995b, Decreased mortality of severe acute pancreatitis after proximal cytokine blockade: Ann Surg, v. 221, p. 625-31; discussion 631-4.

Nuki, G., B. Bresnihan, M. B. Bear, D. McCabe, and E. G. O. C. Investigators, 2002, Long-term safety and maintenance of clinical improvement following treatment with anakinra (recombinant human interleukin-1 receptor antagonist) in patients with rheumatoid arthritis: extension phase of a randomized, double-blind, placebo-controlled trial: Arthritis Rheum, v. 46, p. 2838-46.

O'Shea, J. J., A. Ma, and P. Lipsky, 2002, Cytokines and autoimmunity: Nat Rev Immunol, v. 2, p. 37-45.

Okuhara, D. Y., A. Y. Hsia, and M. Xie, 2007, Transient receptor potential channels as drug targets: Expert Opin Ther Targets, v. 11, p. 391-401.

Orhan, I., R. Onur, N. Ilhan, and A. Ardiçoglu, 2001, Seminal plasma cytokine levels in the diagnosis of chronic pelvic pain syndrome: Int J Urol, v. 8, p. 495-9.

Pillarisetti, S., 2011, Targeting interleukin-1β for pain: CNS Neurol Disord Drug Targets, v. 10, p. 571-5.

Radhakrishnan, R., and R. S. Nallu, 2009, Development and characterisation of a novel animal model of prostate inflammation-induced chronic pelvic pain: Inflammopharmacology, v. 17, p. 23-8.

Rees, J., M. Abrahams, A. Doble, A. Cooper, and P. E. R. G. (PERG), 2015, Diagnosis and treatment of chronic bacterial prostatitis and chronic prostatitis/chronic pelvic pain syndrome: a consensus guideline: BJU Int, v. 116, p. 509-25.

Ren, K., and R. Torres, 2009, Role of interleukin-1beta during pain and inflammation: Brain Res Rev, v. 60, p. 57-64.

Rivero, V., C. Carnaud, and C. M. Riera, 2002, Prostatein or steroid binding protein (PSBP) induces experimental autoimmune prostatitis (EAP) in NOD mice: Clin Immunol, v. 105, p. 176-84.

Rudick, C. N., R. E. Berry, J. R. Johnson, B. Johnston, D. J. Klumpp, A. J. Schaeffer, and P. Thumbikat, 2011, Uropathogenic Escherichia coli induces chronic pelvic pain: Infect Immun, v. 79, p. 628-35.

Rudick, C. N., A. J. Schaeffer, and P. Thumbikat, 2008, Experimental autoimmune prostatitis induces chronic pelvic pain: Am J Physiol Regul Integr Comp Physiol, v. 294, p. R1268-75.

Schäfers, M., J. Brinkhoff, S. Neukirchen, M. Marziniak, and C. Sommer, 2001, Combined epineurial therapy with neutralizing antibodies to tumor necrosis factor-alpha and interleukin-1 receptor has an additive effect in reducing neuropathic pain in mice: Neurosci Lett, v. 310, p. 113-6.

Shimotake, T. K., F. M. Izhar, K. Rumilla, J. Li, A. Tan, K. Page, A. R. Brasier, M. D. Schreiber, and M. B. Hershenson, 2004, Interleukin (IL)-1 beta in tracheal

aspirates from premature infants induces airway epithelial cell IL-8 expression via an NF-kappa B dependent pathway: Pediatr Res, v. 56, p. 907-13.

Stucky, C. L., A. E. Dubin, N. A. Jeske, S. A. Malin, D. D. McKemy, and G. M. Story, 2009, Roles of transient receptor potential channels in pain: Brain Res Rev, v. 60, p. 2-23.

Traub, R. J., B. Tang, Y. Ji, S. Pandya, H. Yfantis, and Y. Sun, 2008, A rat model of chronic postinflammatory visceral pain induced by deoxycholic acid: Gastroenterology, v. 135, p. 2075-83.

Tsuji, F., and H. Aono, 2012, Role of transient receptor potential vanilloid 1 in inflammation and autoimmune diseases: Pharmaceuticals (Basel), v. 5, p. 837-52.

Vincenti, M. P., and C. E. Brinckerhoff, 2001, Early response genes induced in chondrocytes stimulated with the inflammatory cytokine interleukin-1beta: Arthritis Res, v. 3, p. 381-8.

Vykhovanets, E. V., M. I. Resnick, G. T. MacLennan, and S. Gupta, 2007, Experimental rodent models of prostatitis: limitations and potential: Prostate Cancer Prostatic Dis, v. 10, p. 15-29.

Zhang, R., S. Sutcliffe, E. Giovannucci, W. C. Willett, E. A. Platz, B. A. Rosner, J. D. Dimitrakoff, and K. Wu, 2015, Lifestyle and Risk of Chronic Prostatitis/Chronic Pelvic Pain Syndrome in a Cohort of United States Male Health Professionals: J Urol, v. 194, p. 1295-300.

Chapter 4: Interleukin-1β-Mediated Inflammation Develops Pathological Features Consistent with Human PIA and PIN

Disclaimer: This chapter is a manuscript in preparation that has been modified to adhere to dissertation format

Abbreviations

CK5	Cytokeratin 5
H&E	Hematoxylin & Eosin
IMPI	IL-1β-Mediated Prostate Inflammation
iNOS	Inducible Nitric Oxide Synthase
IL-1ra	IL-1 Receptor Antagonist
IPA	Ingenuity Pathway Analysis
LCM	Laser Capture Microdissection
LGPIN	Low Grade Prostate Intraepithelial Neoplasia
mPIN	Mouse Prostate Intraepithelial Neoplasia
NSAIDs	Non Steroid Anti-Inflammatory Drugs
PCA	Principal Component Analysis
PIA	Proliferative Inflammatory Atrophy
PIN	Prostate Intraepithelial Neoplasia
PPDE	Posterior Probability of Differential Expression
ROS	Reactive Oxygen Species
TPM	Transcript Per Million

Abstract

Epidemiological data point to a link between chronic inflammation and prostate carcinogenesis. However, direct evidence regarding the role of human proinflammatory lesions in prostate cancer initiation and progression is lacking. Extant mouse models of chronic inflammation have several limitations, and do not reflect the true etiology of human prostate inflammation. By employing Tet-On inducible technology to drive the expression of a proinflammatory cytokine, Interleukin 1β, we have developed a novel prostate inflammation model. This transgenic mouse model closely recapitulates the pathological features of human Proliferative Inflammatory Atrophy (PIA) and Prostate Intraepithelial Neoplasia (PIN) as observed in human prostatic lesions. Inflamed mouse prostates exhibited overexpression of Myc, a proto-oncogene strongly implicated in a vast majority of cancers, including aggressive prostate cancer. After nine weeks of IL-1β-induced inflammation, the mouse prostate epithelium appeared atrophic and exhibited features that resembled human PIA. At six months, the prostate gland exhibited extensive remodeling and hyperplasia. After one year of chronic inflammation, the prostate epithelium was multi-layered and presented with nuclear pleiomorphism, a higher mitotic index, and enlarged nucleoli. These histopathological features are consistent with human PIN. Combining Laser Capture Microdissection (LCM) and next-generation RNA sequencing, we examined genome-wide gene expression changes mediated by chronic inflammation. The results of this study support the hypothesis that chronic inflammation can injure the prostate epithelium and provide an environment conducive to formation of benign and pre-malignant lesions. This genetic model can be bred to extant models of prostate cancer

in the context of oncogene overexpression or loss of tumor suppressors to provide valuable insights into the link between inflammation and cancer. Clinical validation of the gene expression data set will aid in the development of inflammatory biomarkers and novel therapeutics.

Introduction

A report published in the cancer journal for clinicians has estimated 180,890 new cases of prostate cancer and 26,120 prostate cancer-related deaths in 2016 (Siegel et al., 2016). The etiology of prostate cancer is unclear; however, genetic and environmental factors do appear to play a vital role in prostate carcinogenesis. Several studies have attempted to decipher the role of environmental agents such as chronic inflammation. Chronic infection, or inflammation of the stomach, liver, and the large intestine can significantly increase the risk of cancer. In fact, approximately 20% of all adult human cancers are driven by chronic inflammation (De Marzo et al., 2007). The role of chronic inflammation in prostate cancer is unknown; however, epidemiological and histopathological data indicate that chronic inflammation plays a causal role (Gurel et al., 2014; Putzi and De Marzo, 2000). Pathologists have observed merging of Proliferative Inflammatory Atrophy (PIA) with Prostate Intraepithelial Neoplasia (PIN) and prostate adenocarcinoma in several prostate cancer cases (Wang et al., 2009). PIA is a histopathological description for an inflamed prostate gland exhibiting atrophy and epithelial cells displaying a higher mitotic index compared to non-inflamed glands. PIN is a well-known direct precursor of prostate cancer that has distinct histological features like enlarged nucleoli and nuclei. Characteristic gene expression changes also help to identify PIN lesions in prostate biopsies. The hypothesis that PIA is a precursor to PIN

and prostate carcinoma is further supported by key genetic changes in PIA lesions that are hallmarks of PIN and prostate cancer. These genetic changes include downregulation of NKX3.1, p27, and GSTP1 promoter methylation that are rarely observed in normal prostate epithelium but are characteristic features of PIN and adenocarcinoma (Bethel et al., 2006; De Marzo et al., 1999; De Marzo et al., 2007; Nakayama et al., 2003; Sfanos and De Marzo, 2012). Furthermore, a meta-analysis on the use of Non Steroid Anti-Inflammatory Drugs (NSAIDs) in reducing prostate cancer risk reported that using NSAIDs can decrease prostate cancer risk, however the effect is small (Wang et al., 2014). Prostate inflammation is also a frequent histological finding, as supported by numerous reports (Gerstenbluth et al., 2002; Nickel et al., 1999; Schatteman et al., 2000). Studies linking prostatitis and prostate cancer development have been confounding due to detection bias; however, a recent study published in 2014 by De Marzo *et al.* supports the notion that inflammation in benign biopsy cases correlates with an increased risk for Prostate Cancer (PC) development (Gurel et al., 2014).

Studying molecular transitions between PIA, PIN, and adenocarcinoma is almost impossible to do in humans. Animal models of prostate inflammation can serve as a great tool to decipher the genetic alterations mediated by chronic inflammation. Extant animal models of prostate inflammation fall into five different categories: spontaneous prostatitis models, hormone-injected inflammation models, immune modulated inflammation models, infection-based, and irritant-based models (Boehm et al., 2012; Keith et al., 2001; Naslund et al., 1988; Rivero et al., 2002; Vykhovanets et al., 2007). As the names of each category suggest, each of these models have unique

features, however they also have several shortcomings. These shortcomings include elaborate protocols to initiate prostate inflammation, short-lived inflammation, and most importantly, they do not recapitulate the true etiology of human prostate inflammation. For instance, models that use rat prostate extracts to induce inflammation in mice have no relevance to human etiology. Furthermore, bacterial infection models can be irrelevant; to date, no infectious agents have been defined as a causal agent for prostate cancer (Hrbacek et al., 2013). The IMPI (IL-1β-Mediated Prostate Inflammation) model is unique, innovative, and physiologically relevant to human cases. The features characteristic of the IMPI model and its induction kinetics have been described previously (Chapter 2). IL-1β, a pro-inflammatory cytokine, is overexpressed in expressed prostatic secretions and seminal plasma of chronic prostatitis patients (Alexander et al., 1998; Nadler et al., 2000). Polymorphisms in IL-1β are associated with increased risk for the development of aggressive prostate cancer (Zabaleta et al., 2009). More importantly, IL-1β is expressed by prostate epithelial cells in a subset of human prostate cases, as described in Chapter 2.

In this study, we show that IL-1β-induced inflammation established lesions with features similar to human PIA and PIN. IL-1β is an important cytokine that is implicated in prostate diseases, upregulates Myc expression, and activates NF-κB signaling. Taken together, we provide evidence to support the hypothesis that PIA is a precursor lesion to PIN. We have developed an inducible mouse model that can be bred to extant models of prostate cancer to investigate chronic inflammation in the context of genetic abnormalities (oncogenes, tumor suppressors, genome rearrangements, and SNPs). Additionally, we examined genome-wide gene expression changes mediated by

IL-1β-induced chronic inflammation. The results from the RNAseq study have allowed us to characterize the pathways altered in chronic inflammatory conditions.

Materials and methods

Hematoxylin & Eosin (H&E)

The different lobes of the mouse prostate, as well as the bladder, urethra, distal, and proximal colon were fixed in 10% formalin for 48 hours and then switched to 1X PBS. Tissues were then processed for standard paraffin embedded sectioning and stained with hematoxylin and eosin.

Doxycycline regime

Dox treatments for IMPI mice started at around 4-6 weeks of age. Doxycycline was administered at a concentration of 2mg/mL and mixed in regular drinking water. Treatment continued until a pre-determined time point. A minimum of three IMPI animals and untreated control animals were euthanized at each time point for histological examination. These time points included one week, four weeks, nine weeks, twenty four weeks and fifty two weeks post Dox administration. Doxycycline was obtained from Dr.Phuoc Tran at Johns Hopkins Univeristy.

IHC

Immunohistochemical experiments were performed as previously described (Hubbard et al., 2016). They are briefly summarized below. All tissue sections were deparaffinized at 60°C for 10 minutes followed by tissue rehydration with xylene and alcohol gradient. For Nkx3.1 antigen retrieval step, slides were steamed with citrate

buffer for 25 minutes and endogeneous peroxidase activity was quenched by incubating with peroxidase blocking solution for five minutes. Nkx3.1 primary antibody from UMBC (Chen et al., 2005) was diluted 1:6000, added to the tissue samples and left overnight at four degrees. Poly HRP anti-rabbit IgG secondary antibody was added to the sample for 30 mins at room temperature. Signal was detected upon addition of the chromogen, DAB. Slides were rinsed with TBST, counter-stained with Hematoxylin, dehydrated, and mounted. For CK5 staining, antigen retrieval was performed by steaming slides in HTTR for 50 minutes. Primary antibody was added to the tissue samples at 1:15,000 dilution for 45 minutes at room temperature. Subsequent steps were similar to Nkx3.1 staining protocol. For Myc IHC, slides were steamed in EDTA for 50 minutes. The primary antibody was diluted 1:600 and left overnight at four degrees. Subsequent steps were similar to Nkx3.1 staining protocol. For Ki67 staining, antigen retrieval was performed by steaming with HTTR for 50 minutes. Ki67 antibody was diluted 1:3000 for 45 minutes at room temperature. Subsequent steps were similar to Nkx3.1 staining protocol.

Laser Capture Microdissecton (LCM) and RNA Isolation

Twelve IMPI$^{+/+}$ mice were enrolled in our genome-wide expression study. Half of the animals were Dox-treated (nine weeks and one year treatment) while the other half served as untreated age-matched controls. Ventral prostates from all 12 mice were isolated, embedded in OCT, and frozen using liquid nitrogen. Seven-micron sections of the tissue were made on specialized PEN membrane slides (purchased from Leica). After sectioning, the slides were immediately fixed in 70% cold ethanol for three minutes, and subsequently washed in RNase-free water. The slides were then stained

with Hematoxylin, and dried for LCM. LCM was performed with a 10X objective and the tissue was collected in a small microfuge tube.

For RNA isolation, the all-prep DNA & RNA isolation kit from Qiagen was used. The RNA extraction protocol was performed as per Qiagen guidelines. The microdissected prostate tissues collected in microfuge tubes were used for RNA extraction. Thirty microliters of the lysis buffer was added to the microfuge tube containing tissue sample and spun down to remove tissue material from the microfuge tube. This process was repeated thrice to ensure all material was collected. Finally, RNA was eluted in 30ul of RNase free water. Extracted RNA was used for cDNA synthesis (Fermentas Maxima cDNA synthesis). Quantitative PCR was performed using the Biorad CFX96 machine to measure RNA concentration. To prepare a standard curve, 10ng of mouse prostate RNA was serially diluted in two-fold increments. GAPDH primers were used in the PCR reaction. GAPDH forward primer sequence- GAAGGTGAAGGTCGGAGT, reverse primer- GAAGAT-GGTGATGGGATTTC. The PCR condition used was as follows, step one, 95°C for 1 minute and 30 seconds. Step two, 95°C for 10 seconds. Step three, 57°C for 20 seconds and step four, 72°C for ten seconds. Step two, three and four were repeated for 40 cycles. Data collection and real-time analysis was enabled including melt-curve data collection. Half the sample was used for RNA quantification and the other half (15ul) was prepped for RNA sequencing.

RNAseq

For next-generation RNA sequencing, total RNA was analyzed by Agilent Bioanalyzer to measure the size distribution. Each RNA sample was subjected to a high-sensitivity, strand-agnostic workflow for RNAseq library preparation, using the Ovation RNAseq System v.2.0 kit (NuGen) according to manufacturer's protocols. This workflow was previously validated for total RNA input amounts as low as 500 pg to have high correlation ($R2 > 0.85$) with high input workflows in terms of gene-level expression measures. Barcoded libraries were quantified using the kappa PCR kit and pooled in equimolar ratios for subsequent cluster generation and sequencing of paired end 100x100 bp reads on the Illumina HiSeq platform. Gene expression measures for each sample, and differential expression calls between sample groups were derived using RSEM (Li and Dewey, 2011) and EBseq (Leng et al., 2013) analysis respectively.

Data Analysis

Illumina's CASAVA 1.8.4 was used to convert BCL files to FASTQ files. Default parameters were used. rSEM-1.2.9 software package was used for alignments, as well as to generate gene and isoform expression levels. The 'rsem-calculate-expression' module was used with the following options; calci-ci, output-genome-bam, paired end, forward-prob 0.5. The data was aligned to mm10 mouse reference genome using RefSeq annotation. A table of estimated gene expression and isoform expression was created using EBseq. Rsem-1.2.19's EBseq was used for differential expression analysis on the gene level. 'rsem-run-ebseq',R script provided by RSEM was used to

run the EBseq package. A final annotated table was created with differentially expressed genes.

A Principal Component Analysis (PCA) was performed using the 'Genomics Suite Software' from Partek (http://www.partek.com/pgs). To perform PCA, a table was generated by compiling TPM (Transcript Per Million) values (generated by RSEM as described above) for each sample. Using this table, a PCA plot was created in Partek software with default settings. To perform hierarchical clustering, a table with TPM values at one-year was used as input. Default settings in Partek were utilized to perform this analysis. For pathway analysis, the differentially expressed gene set for one year was uploaded onto IPA (Ingenuity Pathway Analysis) software (http://www.ingenuity.com/). A core analysis was performed with default settings, with the exception of using a cut-off for PPDE (Posterior Probability of Differential Expression) > 0.99. For upstream regulator prediction, the results from the core analysis were used to explore the upstream predictor function. A list of potential upstream regulators was determined, and a p-value was calculated by IPA using the Fisher's exact test. An activation Z-score was also calculated as described (http://pages.ingenuity.com/rs/ingenuity/images/0812%20upstream_regulator_analysis_whitepaper.pdf). The upstream prediction analysis was based on the expected interactions between upstream regulators and their downstream targets, taking into account the direction of change based on the literature in the Ingenuity Knowledge Base (http://www.ingenuity.com/science/knowledge-base). An activation Z-score greater than 2.0 was considered significant, with a positive score representing activation and a negative score representing downregulation. The activation z-score is

calculated as described here http://pages.ingenuity.com/rs/ingenuity/images/0812%20upstream_regulator_analysis_whitepaper.pdf

Results

Histopathological Examination of Long-Term IL-1ß-Mediated Inflammation on Mouse Prostate Epithelium

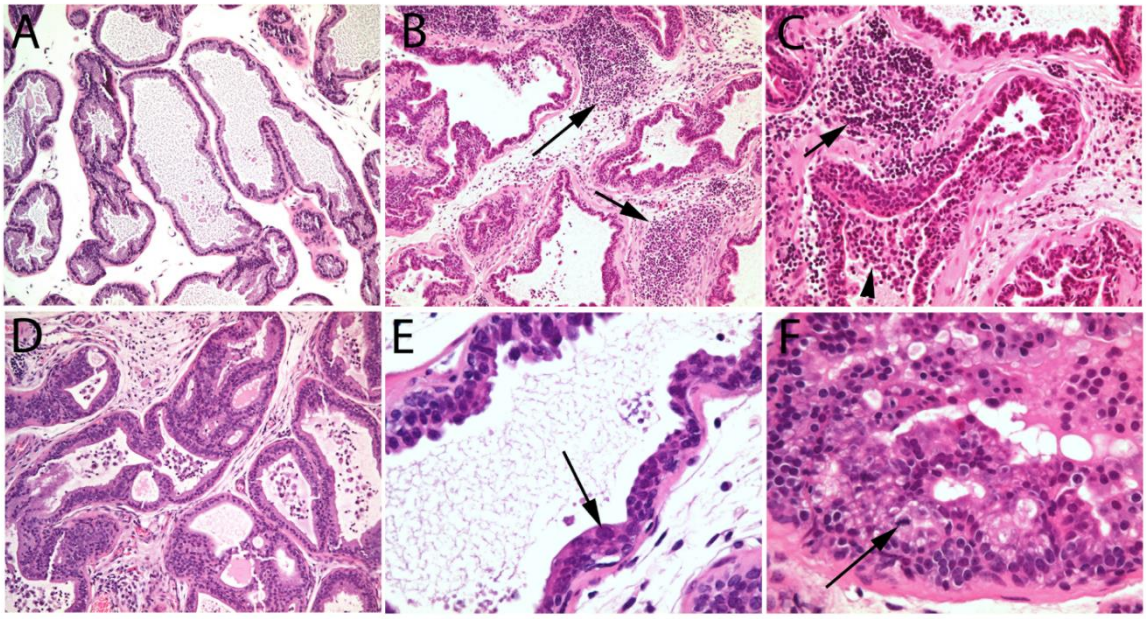

Figure 1: Histopathological examination of nine week and twelve week Dox-treated IMPI- A, Normal ventral prostate from untreated mouse (original magnification, x 100). **B,** Ventral prostate from mouse induced for 12 weeks. Note atrophic appearance to epithelial cells resembling human PIA. Arrows indicate infiltrates of mononuclear inflammatory (mostly consisting of lymphocytes) cells in dense collections within the prostatic stroma (original magnification, x 100). **C**, Higher power view of mouse similarly treated as in B. Arrow shows collections of mononuclear inflammatory (mostly consisting of lymphocytes) cells in the stroma. Arrowhead shows mononuclear inflammatory cells accumulating in the glandular lumen (original magnification, X 200). **D,** Lateral prostate from mouse induced for 9 weeks showing remodeled epithelium with cribriform structures and mononuclear inflammatory cells in the glandular lumens and stroma. **E,** High power view (original magnification X 400) of ventral prostate of mouse induced for 9 weeks showing atrophy with atrophic luminal epithelial cells showing nuclear atypia consisting of enlarged nuclei and nucleolar prominence (arrow). **F,** High power view of remodeled area from induced mouse showing proliferating epithelial cells as seen by mitotic figure (arrow) (original magnification X 400).

To determine the long-term consequences of IL-1β-induced inflammation on the mouse prostate epithelium, a cohort (n= 30) of Dox-inducible mice were enrolled for the study. Mice were euthanized at pre-determined intervals. For convenience, *Hoxb13-rtTA*$^{+/+}$ |*TetO-IL-1ß*$^{+/+}$ will be referred to as IMPI$^{+/+}$ or IMPI (IL-1β-Mediated Prostate Inflammation). Untreated age-matched IMPI mice served as controls. It was

important to chronologically characterize the effects of IL-1β-mediated inflammation on the mouse prostate. To determine the pathological consequence, IMPI mice were Dox-

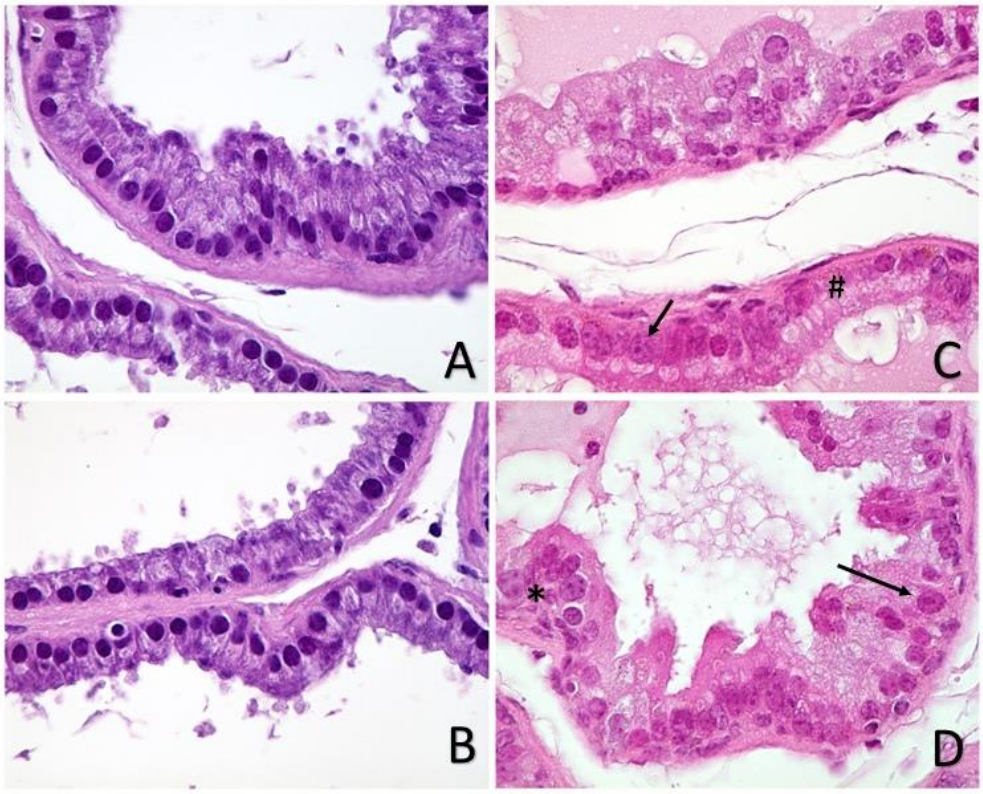

Figure 2: Histological examination of one-year Dox-treated IMPI reveal PIN-like phenotype: A,B, Represent H&E stained ventral prostate sections from untreated IMPI mouse and **C,D,** represent similar sections from age-matched Dox-treated IMPI. Arrows indicate nucleoli enlargement, * represents chromatin clumping, # indicates nuclear pleomorphism. Note, in untreated mouse prostate (A,B), single layer of columnar epithelial cells are observed, however, in inflamed prostate (C,D) epithelial cells have lost organization and appear undulated. Magnification 600X with oil immersion

treated and euthanized at pre-determined intervals. To monitor the histological changes, Dox treatment after 1 week, 4 weeks, 9 weeks, 24 weeks and 52 weeks were examined. The short term effects of IL-1β-induced inflammation including 1 week and 4 weeks has been characterized in chapter 2. The remaining time points including 9 week, 24 weeks and 52 weeks has been discussed in this chapter.

After nine weeks of chronic inflammation, histopathological examination of the prostate sections revealed significant changes in prostate gland morphology in

comparison to age-matched untreated IMPI mice (Figure 1A). The ventral prostates of nine week Dox-treated IMPI mice exhibited focal atrophy, nuclear atypia consisting of enlarged nuclei and nucleolar prominence (Figure 1E). The lateral prostate at nine weeks had a remodeled epithelium with cribiform structures (Figure 1D). Pockets of inflammatory infiltrates mainly lymphocytes (Figure 1B,C) and an increase in mitotic figures was also observed (Figure 1F). In the anterior prostate, atrophy was not observed, however, there was extensive remodeling and hyperplasia. Among the cases examined at nine and twelve weeks, 3/4 had focal atrophy and PIA-like features (Table 1). Examining age-matched, untreated IMPI prostates revealed striking similarities to wild-type mouse prostates (Figure 1A). Overall, the inflamed ventral prostate had sites of focal atrophy with striking similarity to human PIA. PIA, a lesion often observed in human prostate biopsies, is defined by the presence of inflamed focal atrophic glands containing luminal epithelial cells with a high proliferative index. As described by De Marzo *et al.* morphological transitions between PIA and PIN are predicted in human prostate cancer cases (Putzi and De Marzo, 2000). PIA was found adjacent to carcinoma lesions and merging with high-grade PIN (Wang et al., 2009).

At 24 weeks, the prostate glands had features not completely consistent with mPIN (Mouse PIN) but had few PIN like features (Figure 3). The prostate glands appeared to be in a transition phase between chronic state and PIN phenotype. The

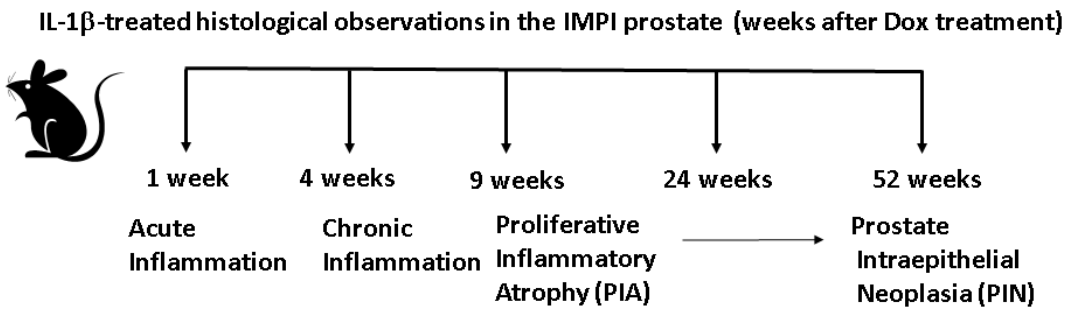

Figure 3: Illustration depicting histological features observed in Dox-treated IMPI mice at various time points

Dox-treated ventral prostate presented with focal atrophy, mid to moderate inflammation, mixed cell population in the stroma, chromatin clumping in the epithelium, and appearance of plasma cells in the stroma.

After one year of continuous Dox treatment, histological features consistent with PIN appeared (Figure 2). In the ventral prostate, these features included a multi-layered epithelium, enlarged nuclei, prominent enlarged nucleoli, nuclear pleiomorphism, and hyperchromasia (Figure 2C,D).

Signs of atrophy was seldom observed in all cases. Some cases had epithelial cells with pervasive chromatin clearing, a feature most commonly observed in human PIN and adenocarcinoma. Mild inflammation was observed in the stroma with pockets of mixed chronic infiltrate. In 12 cases examined (Table 1), the lateral prostate exhibited Low Grade PIN (LGPIN)-like features in eight cases. These features include nuclear changes and remodeling, and presented with mild to moderate inflammation. The anterior prostate displayed architectural changes in gland morphology along with increased tufting with an infolding-like appearance. Additionally, mitotic figures, enlarged nucleoli, and focal remodeling were observed. In 12 cases examined, the ventral prostate exhibited LGPIN/ PIN in 10 cases, and the anterior prostate exhibited

LGPIN/PIN in 12/14 cases examined (Table 1). The PIN-like lesions also displayed upregulation of Myc and the proliferation marker, Ki67 (discussed below).

Duration of Dox treatment	**Ventral lobe**	**Anterior lobe**	**Dorsal/Lateral lobe**	**Untreated age-matched IMPI (all lobes (control mice)**	
9-12 weeks	3/4 PIA	3/4 remodeling	2/4 remodeling	3/3 benign	
24 weeks	1/2 PIN-like	1/2 focal PIN	1/2 PIN-like	2/2 benign	
52 weeks	10/12 LGPIN or PIN		12/14 LGPIN or PIN	8/12 LGPIN or PIN	3/3 benign

Table 1: Table summarizing histopathological phenotype as a consequence of chronic inflammation in all mouse prostate lobes. The first number represents the number of mice that exhibit a given phenotype such as PIA or PIN, and the second number represents the total number of mice observed within each group. Control animals examines are presented in the last column LGPIN- low grade PIN

Examination of the age-matched, untreated control animals revealed no chromatin clumping, nuclear atypia, or layered epithelial cells. Moreover, the control prostate exhibited columnar epithelial cells with normal appearance of stroma. However, we seldom observed sites of age-related inflammation and enlarged nucleoli. It is important to note that these sites were rare and dramatically different from Dox-treated prostates. Similar observations were made in wild-type (FVB) Dox-treated animals to control for potential effects of Dox on the prostate epithelium. No adverse effects of Dox were observed. The Hoxb13 regulatory elements used to drive expression of rtTA in the model described here, are also active in the mouse distal colon. Therefore, the phenotypic consequences of chronic inflammation in the distal colon were examined. No changes in the colon were observed after 52 weeks of IL-1β expression (data not shown).

See figure 3, a chronological representation on the histological effects of chronic inflammation on Dox-treated IMPI mice.

Examining Molecular Markers of Human PIA/PIN in the IMPI Model Using Immunohistochemistry

As we observed histopathological features in the IMPI model consistent with human PIN and PIA, it became important to determine whether molecular markers of human PIA/PIN are represented in the mouse lesions. For example, an important marker of human PIA is a higher mitotic index compared to benign glands .

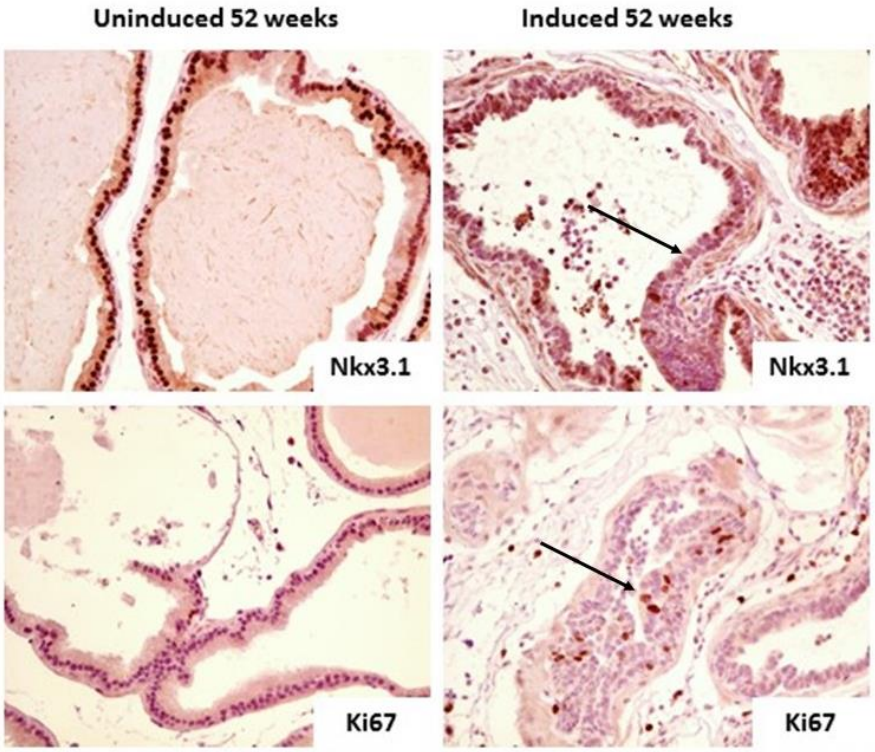

Figure 4: Immunohistochemical staining for NKX3.1 and KI67, comparing expression in untreated vs. one-year Dox-treated IMPI mice. Note, robust nuclear NKX3.1 (brown color) expression in uninduced (untreated) prostate, whereas in treated prostate, NKX3.1 expression is more diffused and heterogeneous. Arrows indicate a region where almost no NKX3.1 staining is observed. Ki67 positive cells observed in induced prostate epithelium (arrow) but not in uninduced mouse prostate (absence of brown staining). Images captured at 100X

Immunohistochemical staining for the proliferation marker, Ki67, was performed on Dox-treated IMPI mice (at all time points). Comparing Ki67 staining between treated and untreated IMPI mice at 52 weeks revealed rapidly cycling cells in the inflamed

epithelium and stroma compared to controls (Figure 4). As expected, pockets of chronic inflammatory cells were also positive for Ki67. This study was followed by IHC staining for Myc and NKX3.1, since both are implicated in human prostate cancer. In

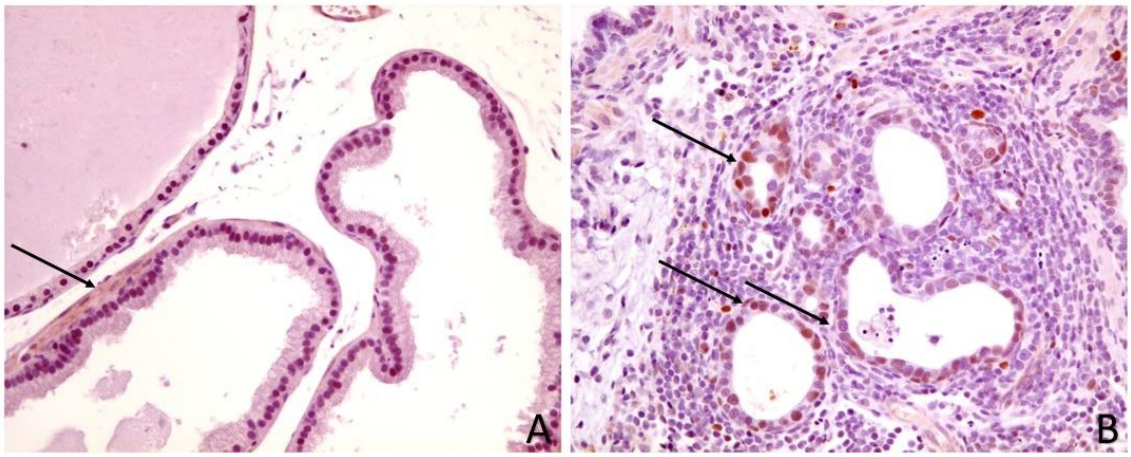

Figure 5: Immunohistochemical staining for Myc, comparing expression in untreated vs. one-year Dox-treated IMPI mice. A, Control tissue had almost no positive staining in epithelial cells. Arrow indicates positive stain in the stroma. **B,** One year inflamed ventral prostate presented with Myc positive cells (arrows, red/brown color). Note, the presence of inflammatory infiltrates. Images captured at 200X

the 52 week inflamed ventral prostates, NKX3.1 expression, which is typically nuclear , was more diffused into the cytoplasm, with diminished expression in the nucleus (Figure 4). However, in the control animals, robust expression was observed in the nuclei, yet almost no expression in the cytoplasm. Strikingly, Myc expression was upregulated in inflamed glands at nine weeks, six months, and in one-year Dox-treated mice (Figure 5).

As expected, Myc was also upregulated in the immune infiltrates. Glands that were more inflamed had a higher percentage of cells with Myc overexpression (Figure 5). The untreated prostate epithelium (control animals) had almost no Myc expression in the luminal cells with the exception of a few stromal cells that stained positive (Figure 5). The results from the IHC revealed increased proliferation, Myc overexpression, and decreased NKX3.1 expression in nine week and one year inflamed mouse prostate epithelia. Taken together, the IHC data show that these molecular features of chronically inflamed mouse prostates follow trends that are also observed in human prostate cases. Combining the histopathological and immunohistochemical analyses, there is strong evidence to support the notion that the lesions observed in the IMPI mice have features that resemble human inflammatory and pre-neoplastic lesions. Therefore, the data presented here are profound and support the hypothesis that human PIA is a precursor to PIN.

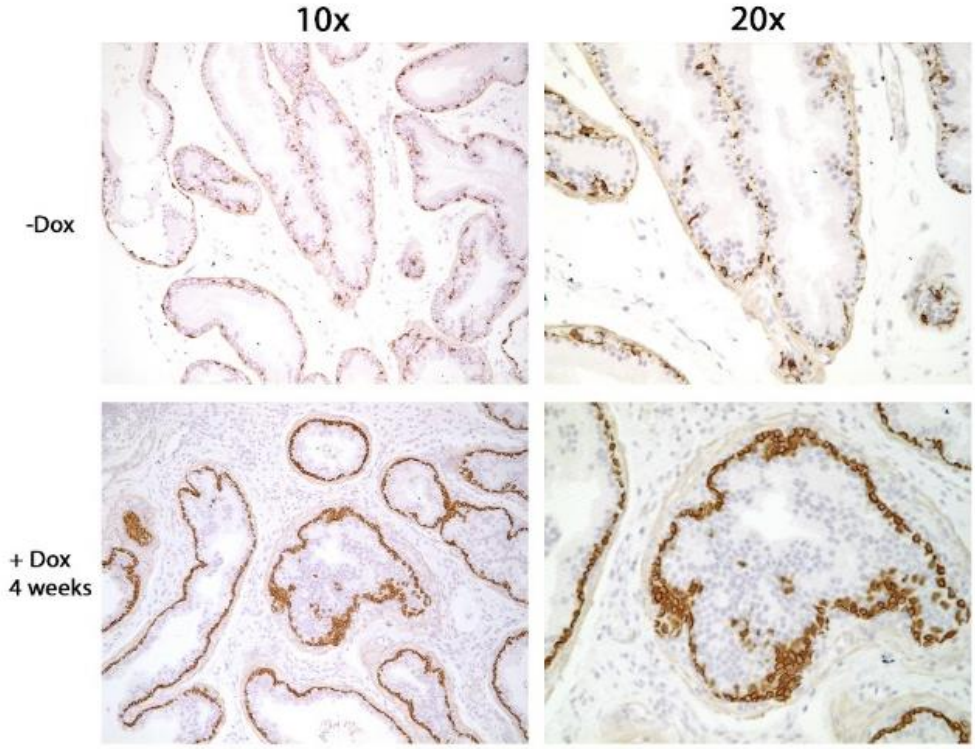

Figure 6: Immunohistochemical staining for Cytokeratin 5 (basal cell marker), comparing expression in untreated vs. Dox-treated IMPI mice. Note, in control tissue (**-Dox**), few cells stained CK5 positive. At **+Dox 4 weeks** and **+Dox 9 weeks** there was an increase in CK5 positive cells (denoted by brown stain).

Inflammation has been reported to alter the cell differentiation program (Kwon et al., 2014). To determine if there was a change in the basal cell population (Cytokeratin 5 (CK5)-positive cells), IHC was performed on four week, and nine week, Dox-treated ventral prostate tissue. A comparison of the staining revealed a significant increase in the cells that stained positive for CK5 (Figure 6). Intermediate cell populations wherein cells stain for both luminal and basal cell markers have been reported in human PIA lesions (van Leenders et al., 2003). Further studies are warranted to determine the presence of an intermediate cell population in the IMPI model.

Determining genome-wide gene expression changes influenced by IL-1β-mediated inflammation

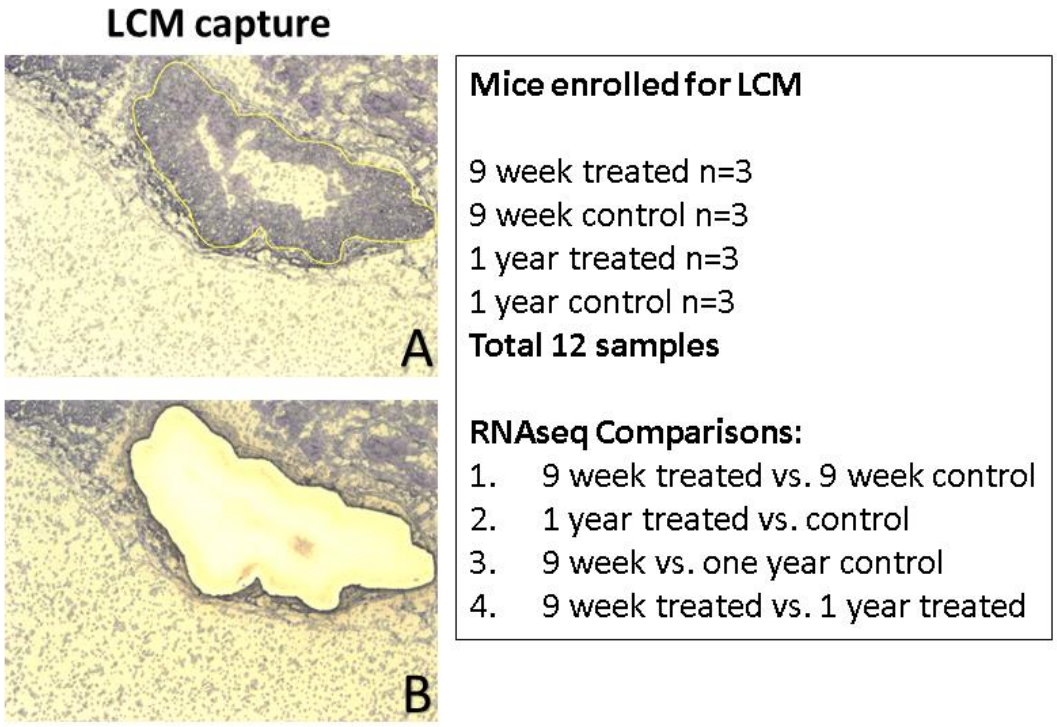

Figure 7: Images captured during laser capture microdissection: A, Prostate epithelial cells were selected for LCM **B,** Post-LCM capture image. Images captured at 100X. RNAseq comparisons and mice enrolled in the study are listed.

To determine the global consequences of chronic inflammation on the transcriptome of prostate epithelial cells, a cohort of 12 IMPI males were identified. Six animals were Dox-treated to induce inflammation, and six were left untreated to serve as controls. After nine weeks, three animals in each group were euthanized and the ventral prostates were prepared for frozen tissue sectioning. After one year of chronic inflammation, the remaining mice in each group were euthanized and the prostate glands were removed.

LCM is a laser-assisted microdissection technique that allows isolation of a specific tissue/cells from a heterogeneous tissue section. Using LCM, gene expression changes specific to prostate epithelial cells were identified. Images captured before and after LCM is shown in figure 7. Next, RNA was extracted from LCM-captured tissue, quantified, quality checked, and prepared for low-input next-generation sequencing. Sequencing was performed on the Illumina Hi-seq platform. Sequencing analysis was completed as described in the methods section. The output generated from this analysis included Transcripts Per Million (TPM) values for each sample and a table with

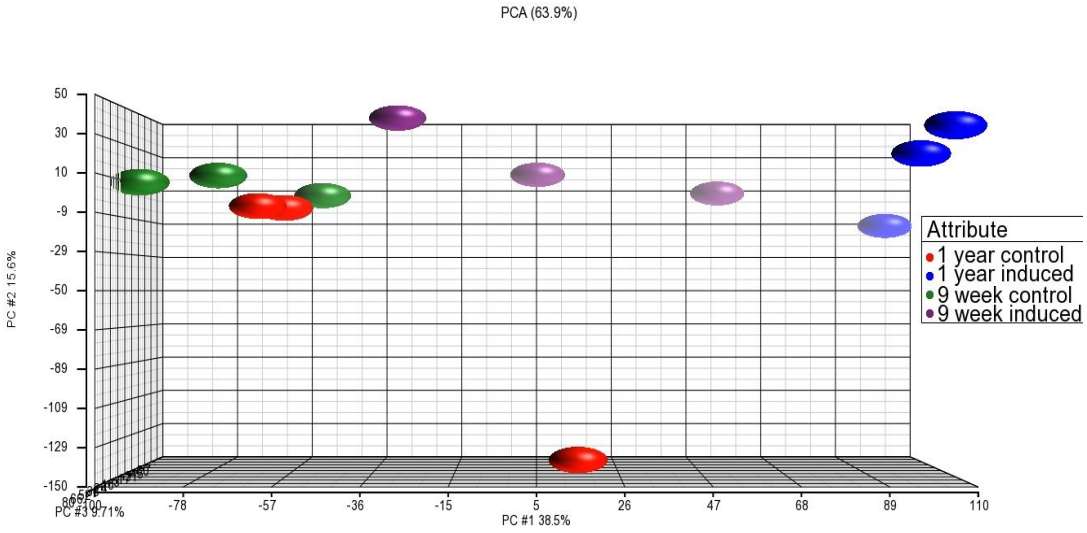

Figure 8: Principal Component Analysis performed on 1 year and 9 week cohort's RNA expression values: A PCA analysis is a mathematical derivation that converts the expression values into a new coordinate system. The highest variance is represented as principal component 1, depicted on X-axis. The other two components are depicted on Y and Z-axis. The following PCA analysis was prepared using Partek software. Each animal is represented as a sphere and color-coded depending on the treatment type. The one year control animals are represented in red spheres while the treated animals are presented in blue. Similarly, the 9 week control and treated cohort are represented in green and purple respectively. As seen in the figure, samples within a group clustered together with the exception of one outlier (red sphere). Note, global gene expression patterns in 1 year induced group (blue spheres) is distant from other cohorts.

differentially expressed genes for the four comparisons: nine weeks control vs. treated,

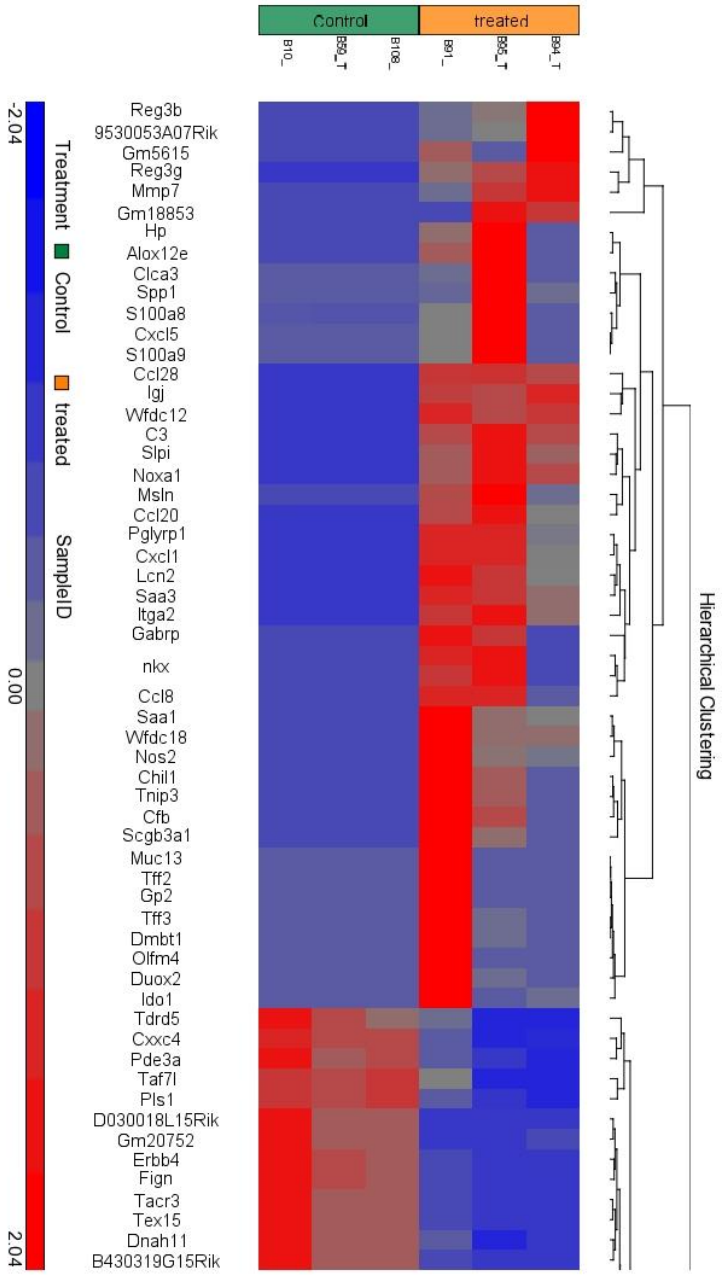

one year control vs. treated, nine week control vs. nine week treated, and nine week treated vs. one year treated (Figure 7).

A Principal Component Analysis (PCA) of the genome-wide gene expression data from all 12 samples was performed to allow the visualization of variance among each of the 12 samples and detect patterns between them. PCA is a statistical

Figure 9: Graphical representation of top 50 differentially expressed genes in the one year inflamed gene expression data set- Transcripts per million (TPM) values for three control (top green panel) and three treated mice (orange panel) are presented in a heat map. The gene annotations are shown on the left y-axis. The right y-axis displays hierarchical clustering. Using the Partek software, similar objects were grouped into clusters based on given observations. The expression values were normalized as follows. The software forces each sample to have a normal distribution (mean=0 and SD=1). The mean expression value for each gene across all 6 samples (treated + control) were calculated. The z score or color scale shown on Y-axis is calculated by subtracting expression value of each gene from the grand mean and divided by the SD. Values greater than zero are upregulated genes (red) ,below zero are downregulated genes (blue) while values unchanged are shown in grey. Note, consistency among biological replicates.

analytical tool that converts a set of observations into variables termed 'principal components' using orthogonal transformation. The PCA plot was determined by using the PCA algorithm tool available in the Genomic suite of the Partek software. The principal component analysis using the gene-level expression data revealed distinct clustering within all four groups, with the exception of one 1 year control sample (red sphere, Figure 8). The one year induced/ treated cluster has distinct variability compared to both control clusters (red and green spheres) (Figure 8). Therefore, from this unsupervised comparison analysis of the four groups, we can conclude that there is consistency among the samples in each cluster and the data can be analyzed for differential gene expression changes.

Identifying differentially expressed genes in the inflamed cohort

From the PCA plot analyses, global changes in gene expression were observed between the one-year treated and control cluster. Using the TPM values from each sample, an unsupervised hierarchical clustering was performed using the Partek software. Similar to the PCA analyses, unsupervised clustering does not take into account experimental variables such as treatment, phenotype etc. Default settings were used for the clustering analysis. Figure 9 is a graphical representation of the top 50 genes differentially expressed in the one-year cohort. By default, the expression of each gene was standardized to a mean of zero and a standard deviation of one. Genes unchanged were colored grey, upregulated were colored red and downregulated were colored blue. Gene annotations were denoted on the left y-axis. As seen in figure 9, the gene expression values correlated well within the control and treated group. Low variability within the biological replicates was important to identify differentially expressed genes with

statistical significance. Genes involved in chemokine signaling and oxidative stress were observed in this list. These genes included CXCL5, CXCL1, CCL8, NOS2 and NOXa1.

Next, a supervised analysis was performed, wherein the three control samples and three treated one year samples were grouped together to determine the differentially expressed genes within these two major groups. Differentially expressed genes were identified with the help of rsem-1.2.19's EBseq software package as described in methods section. Using the table generated by EBSeq, we narrowed the gene list using statistical significance and identified genes that have a PPDE (Posterior Probability of Differential Expression) > 0.99. For the nine-week cohort, we identified 1669 genes that were differentially expressed in the inflamed cohort in comparison to the untreated controls. We observed a greater number of differentially expressed genes in the one-year cohort, totaling 3962 genes. Of the 3962 genes, 972 genes overlapped with the nine week differentially expressed gene set, indicating this overlapping gene-set to be involved in cytokine signaling, chemokine signaling, or genes related to oxidative stress. Overexpressed genes that are worth noting in the one year expression dataset include, members of the apoptosis family (BCL2), chemokines (CCL2, CXCL2), and genes involved in the generation of reactive oxygen species (NOXA1). Downregulated genes included epithelial mucins (MUC13), and the SPINK family of genes.

Pathways enriched in the RNAseq expression data set

Ingenuity Pathway Analysis (IPA) software was used to determine pathways enriched in the dataset. The differentially expressed genes at the one-year time point were

generated as described in materials and methods section. IPA analysis revealed several pathways that were enriched in the dataset including NF-κB signaling, p53 signaling, iNOS signaling, and TGF-β signaling. The full list is described in figure 10. The bars in the graph represent the –log (p-value). Therefore, the higher the bar, the more significant the result. A threshold greater than 1.3 was nominated as significant, and is identified by the orange dotted line in figure 10. The color of the bars represents the activation Z-score, referenced in materials and methods section. The orange bars

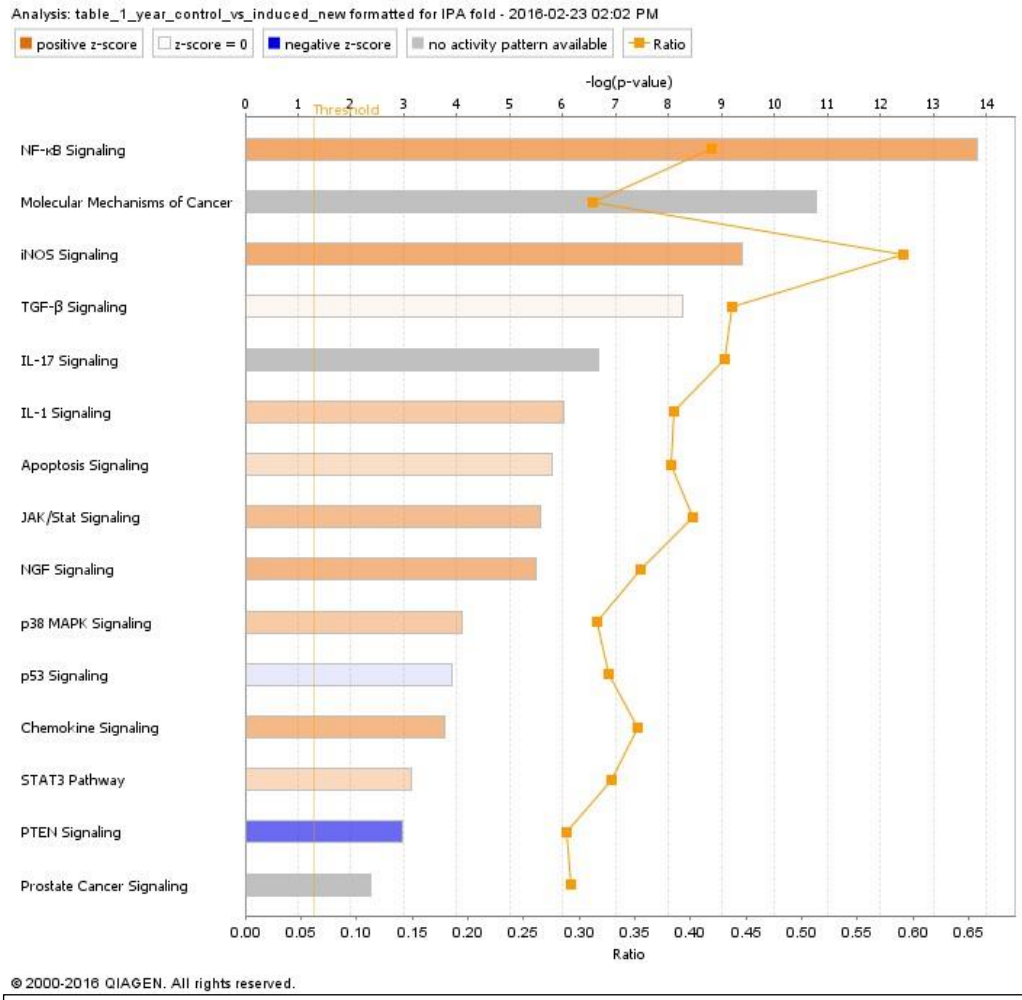

Figure 10: Pathway enrichment in the one-year gene expression data set: Statistical significance was determined using Fisher exact t test and p-value was obtained. Statistical analyses was performed in IPA software. The colored bars represent –log (p-value). Therefore, higher the bar, the more significant the result. A threshold greater than 1.3 was nominated as significant and is identified by the orange dotted line. The color of the bars represents the activation Z-score. The orange bars represent pathway activation, the blue bars represent pathway downregulation. The grey bars indicate that no trend was determined. The bottom Y-axis represent the ratio, calculated as the number of genes in the dataset over the number of genes in the pathway (data retrieved from the Ingenuity Knowledge Base)

represent pathway activation while the blue bars represent pathway downregulation. The grey bars indicate that no trend was determined. The bottom Y-axis (Figure 10) represents the ratio, calculated as the number of genes in the dataset over the number of genes in the pathway (data retrieved from the Ingenuity Knowledge Base). Pathways that were expected to be enriched served as positive controls for this analysis. For

example, the IL-1 pathway and chemokine signaling pathway activation were expected in this study. Since IL-1β is known to induce the expression of NF-κB via IL-1 signaling, upregulation of this pathway served as another positive control for this analysis. Interestingly, iNOS (Inducible Nitric Oxide Synthase) signaling was upregulated in our dataset. iNOS has been shown to be elevated in chronic inflammatory conditions like rheumatoid arthritis, multiple sclerosis, and even neoplastic conditions of the prostate, lung, breast, and colon (http://carcin.oxfordjournals.org/content/early/2012/08/17/carcin.bgs241.full). Other activated pathways that are worth noting include apoptosis signaling, JAK/STAT, and p38 MAPK signaling pathways. Among the pathways that were downregulated, the most interesting finding was the effect on PTEN signaling. As indicated in figure 10, PTEN signaling was downregulated with a Z-score of -2.611 . PTEN is a known tumor suppressor gene for prostate cancer and is associated with advanced cases (Koksal et al., 2004). This is interesting, since a recently published study demonstrated that Myc overexpression and PTEN loss is sufficient to create genome instability (Hubbard et al., 2016). However, we did not observe loss of PTEN expression in IMPI samples, which could explain the lack of an invasive cancer phenotype in our model. The enrichment of pathways closely linked with neoplasia provide further evidence to support the PIN-like histopathological features observed after one year of chronic inflammation in the IMPI model.

Upstream regulator prediction

Similar to pathway analysis, the core analysis tool in IPA was used to predict upstream regulators of differentially expressed genes. The predicted upstream regulators helped explain the changes in gene expression in the one-year data set. The IPA software was used to make predictions based on expected trend for downstream target genes as per published literature. A z-score was calculated as explained in materials and methods. |Z-score|>2 was considered significant with a positive Z-score indicating activation (red bars) and a negative Z-score indicating downregulation (blue bars) of the upstream regulator. Statistical significance was determined using Fisher exact test in IPA software. In the activated gene list, IL-1β was among the most activated upstream

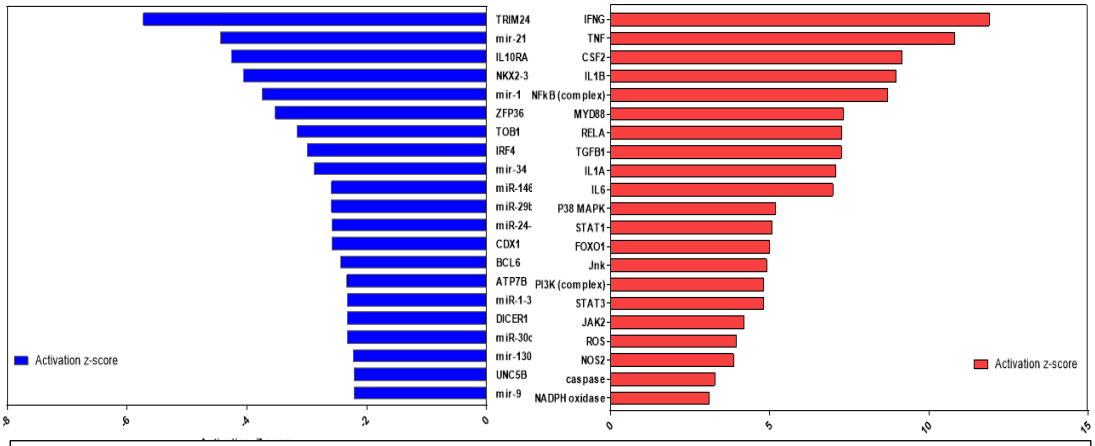

Figure 11: Upstream regulator prediction for gene expression studies from one-year treated mice: The upstream regulator analysis performed in IPA software helped identify potential upstream transcriptional regulators that was useful in explaining the expected gene expression changes in the one year treated dataset. This is based on the expected effects between upstream regulators and their downstream targets. For a specific upstream regulator, if the fold change of downstream target genes is as expected as per published literature, then bases on a statistical test (Fisher exact test) a prediction is made (activated or repressed). Based on a weighted approach, a z-score is calculated by IPA as described in methods. Blue bars represent a list of downregulated genes that are potential upstream regulators. The length of the bar indicates the activation z-score. A z-score greater than 2.0 indicates gene activation and a negative score indicates downregulation.

regulators that appeared with a high activation score, a highly significant p-value, and served as a good positive control for this analysis. Other notable upstream regulators

included TNF-α, IFN-γ, STAT1, STAT3, and Reactive Oxygen Species (ROS) among others listed in figure 11. The downregulated list included several microRNAs, zinc finger protein 36, NKX2.3, and IL-10RA among others (Figure 11)

Discussion

In this study, we show that IL-1β-mediated inflammation induces histological features that are consistent with human PIA and PIN. The immunohistochemical analyses for Myc, Nkx3.1, and Ki67 exhibited a similar trend to that observed in human inflammatory and pre-neoplastic cases. Moreover, we also examined genome-wide gene expression changes influenced by IL-1β-mediated inflammation at nine week and one-year time points, which correlated with PIA-like and PIN-like histological features respectively. The pathway analyses and upstream regulator prediction suggested processes including inflammation, apoptosis, upregulation of reactive oxygen species, and downregulation of PTEN signaling to be enriched in the dataset. This study is profound as it suggests that IL-1β-mediated inflammation may play a role in prostate diseases. Most importantly, the histological and IHC data suggest the emergence of PIA and PIN lesions in the context of chronic inflammation. Although we do not observe the incidence of invasive cancer in the IMPI model, we show compelling evidence to support that PIA is a precursor to PIN. For the first time, an inducible genetic model is available to dissect the potential link between chronic inflammation and prostate adenocarcinoma. Breeding the IMPI model to extant models of prostate cancer, for example, a genetic alteration commonly observed in prostate cancer would

be informative. These studies would help to discern whether chronic inflammation may synergize with activated oncogenes/ tumor suppressors.

Interleukin-1β is an important mediator of inflammation as it protects the host against infections and aids in tissue repair. However, IL-1β has several links to cancer. IL-1 overexpression has been reported in several cancers including human lung, breast, colon, head, and neck, as well as melanomas (Apte et al., 2006; Dinarello, 1996; Elaraj et al., 2006; Lewis et al., 2006). Additionally, IL-1-producing tumors have poor prognosis (Lewis et al., 2006). IL-1β polymorphisms are strongly associated with increased risk of gastric cancer (Machado et al., 2001), and associated with aggressive prostate cancer (Zabaleta et al., 2009). Naturally occurring IL-1 Receptor Antagonist (IL-1ra) can block the IL-1 receptor and inhibit IL-1-mediated signaling. Moreover, the blockade of IL-1 signaling in smoldering or indolent myeloma patients by administrating recombinant IL-1ra prolongs progression-free survival (Lust et al., 2009). Evidence to support the role of IL-1β in cancer is inevitable. More importantly, there are FDA-approved therapies available that have been successful in blocking the IL-1-cascade and have demonstrated clinical success (Dinarello, 2010; Hoffman et al., 2008; Larsen et al., 2009; Nuki et al., 2002). Here, we present evidence to suggest the role of IL-1β-mediated inflammation in prostate inflammatory disease and propose IL-1β blockade as a clinically effective therapy to treat IL-1β–driven prostate malignancies.

One of the most striking findings from this study was the expression of an oncogene, Myc, in the inflamed mouse prostates. Our IHC studies revealed overexpression of Myc in the prostate luminal cells, a characteristic that is suggested

to be one of the early signatures of human prostate cancer (Gurel et al., 2008). The study by Gurel *et al.* examined normal, atrophic, PIN, and prostate adenocarcinoma cases for Myc upregulation. The results from this study supports the hypothesis that Myc protein upregulation observed in human PIN lesions is a critical oncogenic event, occurring early in prostate carcinogenesis. Moreover, overexpression of Myc in mouse models resulted in PIN formation and invasive cancer (Iwata et al., 2010). Here we report that expression of IL-1β alone in the mouse luminal epithelial cells results in Myc upregulation. The exact mechanism of Myc upregulation is unclear; however, Myc upregulation as a result of IL-1β-mediated inflammation suggests a link between chronic inflammation and cancer.

In summary, we have developed a valuable, physiologically relevant, animal model that closely recapitulates the features observed in human prostate diseases. This study is profound as we provide histological, molecular, and immunohistochemical evidence that support the hypothesis that chronic inflammation can alter the prostate microenvironment and initiate pre-neoplastic changes. Furthermore, as discussed above, IL-1β-blockade is well tolerated and clinically effective in patients as demonstrated by success in IL-1β-mediated diseases. Lastly, clinical validation of the gene expression data will be a valuable resource to develop inflammatory biomarkers for IL-1β-mediated prostate disorders.

References

Alexander, R. B., S. Ponniah, J. Hasday, and J. R. Hebel, 1998, Elevated levels of proinflammatory cytokines in the semen of patients with chronic prostatitis/chronic pelvic pain syndrome: Urology, v. 52, p. 744-9.

Apte, R. N., Y. Krelin, X. Song, S. Dotan, E. Recih, M. Elkabets, Y. Carmi, T. Dvorkin, R. M. White, L. Gayvoronsky, S. Segal, and E. Voronov, 2006, Effects of micro-environment- and malignant cell-derived interleukin-1 in carcinogenesis, tumour invasiveness and tumour-host interactions: Eur J Cancer, v. 42, p. 751-9.

Bethel, C. R., D. Faith, X. Li, B. Guan, J. L. Hicks, F. Lan, R. B. Jenkins, C. J. Bieberich, and A. M. De Marzo, 2006, Decreased NKX3.1 protein expression in focal prostatic atrophy, prostatic intraepithelial neoplasia, and adenocarcinoma: association with gleason score and chromosome 8p deletion: Cancer Res, v. 66, p. 10683-90.

Boehm, B. J., S. A. Colopy, T. J. Jerde, C. J. Loftus, and W. Bushman, 2012, Acute bacterial inflammation of the mouse prostate: Prostate, v. 72, p. 307-17.

Chen, H., L. N. Mutton, G. S. Prins, and C. J. Bieberich, 2005, Distinct regulatory elements mediate the dynamic expression pattern of Nkx3.1: Dev Dyn, v. 234, p. 961-73.

De Marzo, A. M., V. L. Marchi, J. I. Epstein, and W. G. Nelson, 1999, Proliferative inflammatory atrophy of the prostate: implications for prostatic carcinogenesis: Am J Pathol, v. 155, p. 1985-92.

De Marzo, A. M., E. A. Platz, S. Sutcliffe, J. Xu, H. Grönberg, C. G. Drake, Y. Nakai, W. B. Isaacs, and W. G. Nelson, 2007, Inflammation in prostate carcinogenesis: Nat Rev Cancer, v. 7, p. 256-69.

Dinarello, C. A., 1996, Biologic basis for interleukin-1 in disease: Blood, v. 87, p. 2095-147.

Dinarello, C. A., 2010, Why not treat human cancer with interleukin-1 blockade?: Cancer Metastasis Rev, v. 29, p. 317-29.

Elaraj, D. M., D. M. Weinreich, S. Varghese, M. Puhlmann, S. M. Hewitt, N. M. Carroll, E. D. Feldman, E. M. Turner, and H. R. Alexander, 2006, The role of interleukin 1 in growth and metastasis of human cancer xenografts: Clin Cancer Res, v. 12, p. 1088-96.

Gerstenbluth, R. E., A. D. Seftel, G. T. MacLennan, R. N. Rao, E. W. Corty, K. Ferguson, and M. I. Resnick, 2002, Distribution of chronic prostatitis in radical prostatectomy specimens with up-regulation of bcl-2 in areas of inflammation: J Urol, v. 167, p. 2267-70.

Guedes, L., C. Morais, F. Almutairi, M. C. Haffner, Q. Zheng, J. T. Isaacs, E. S. Antonarakis, C. Lu, H. Tsai, J. Luo, A. M. De Marzo, and T. L. Lotan, 2016, Analytic Validation of RNA In Situ Hybridization (RISH) for AR and AR-V7 Expression in Human Prostate Cancer: Clin Cancer Res.

Gurel, B., T. Iwata, C. M. Koh, R. B. Jenkins, F. Lan, C. Van Dang, J. L. Hicks, J. Morgan, T. C. Cornish, S. Sutcliffe, W. B. Isaacs, J. Luo, and A. M. De Marzo, 2008, Nuclear MYC protein overexpression is an early alteration in human prostate carcinogenesis: Mod Pathol, v. 21, p. 1156-67.

Gurel, B., M. S. Lucia, I. M. Thompson, P. J. Goodman, C. M. Tangen, A. R. Kristal, H. L. Parnes, A. Hoque, S. M. Lippman, S. Sutcliffe, S. B. Peskoe, C. G. Drake, W. G. Nelson, A. M. De Marzo, and E. A. Platz, 2014, Chronic inflammation in benign prostate tissue is associated with high-grade prostate cancer in the placebo arm of the prostate cancer prevention trial: Cancer Epidemiol Biomarkers Prev, v. 23, p. 847-56.

Hoffman, H. M., M. L. Throne, N. J. Amar, M. Sebai, A. J. Kivitz, A. Kavanaugh, S. P. Weinstein, P. Belomestnov, G. D. Yancopoulos, N. Stahl, and S. J. Mellis, 2008, Efficacy and safety of rilonacept (interleukin-1 Trap) in patients with cryopyrin-associated periodic syndromes: results from two sequential placebo-controlled studies: Arthritis Rheum, v. 58, p. 2443-52.

Hrbacek, J., M. Urban, E. Hamsikova, R. Tachezy, and J. Heracek, 2013, Thirty years of research on infection and prostate cancer: no conclusive evidence for a link. A systematic review: Urol Oncol, v. 31, p. 951-65.

Hubbard, G. K., L. N. Mutton, M. Khalili, R. P. McMullin, J. L. Hicks, D. Bianchi-Frias, L. A. Horn, I. Kulac, M. S. Moubarek, P. S. Nelson, S. Yegnasubramanian, A. M. De Marzo, and C. J. Bieberich, 2016, Combined MYC Activation and Pten Loss Are Sufficient to Create Genomic Instability and Lethal Metastatic Prostate Cancer: Cancer Res, v. 76, p. 283-92.

Iwata, T., D. Schultz, J. Hicks, G. K. Hubbard, L. N. Mutton, T. L. Lotan, C. Bethel, M. T. Lotz, S. Yegnasubramanian, W. G. Nelson, C. V. Dang, M. Xu, U. Anele, C. M. Koh, C. J. Bieberich, and A. M. De Marzo, 2010, MYC overexpression

induces prostatic intraepithelial neoplasia and loss of Nkx3.1 in mouse luminal epithelial cells: PLoS One, v. 5, p. e9427.

Keith, I. M., J. Jin, D. Neal, B. D. Teunissen, and T. D. Moon, 2001, Cell relationship in a Wistar rat model of spontaneous prostatitis: J Urol, v. 166, p. 323-8.

Koksal, I. T., E. Dirice, D. Yasar, A. D. Sanlioglu, A. Ciftcioglu, K. H. Gulkesen, N. O. Ozes, M. Baykara, G. Luleci, and S. Sanlioglu, 2004, The assessment of PTEN tumor suppressor gene in combination with Gleason scoring and serum PSA to evaluate progression of prostate carcinoma: Urol Oncol, v. 22, p. 307-12.

Kwon, O. J., L. Zhang, M. M. Ittmann, and L. Xin, 2014, Prostatic inflammation enhances basal-to-luminal differentiation and accelerates initiation of prostate cancer with a basal cell origin: Proc Natl Acad Sci U S A, v. 111, p. E592-600.

Larsen, C. M., M. Faulenbach, A. Vaag, J. A. Ehses, M. Y. Donath, and T. Mandrup-Poulsen, 2009, Sustained effects of interleukin-1 receptor antagonist treatment in type 2 diabetes: Diabetes Care, v. 32, p. 1663-8.

Leng, N., J. A. Dawson, J. A. Thomson, V. Ruotti, A. I. Rissman, B. M. Smits, J. D. Haag, M. N. Gould, R. M. Stewart, and C. Kendziorski, 2013, EBSeq: an empirical Bayes hierarchical model for inference in RNA-seq experiments: Bioinformatics, v. 29, p. 1035-43.

Lewis, A. M., S. Varghese, H. Xu, and H. R. Alexander, 2006, Interleukin-1 and cancer progression: the emerging role of interleukin-1 receptor antagonist as a novel therapeutic agent in cancer treatment: J Transl Med, v. 4, p. 48.

Li, B., and C. N. Dewey, 2011, RSEM: accurate transcript quantification from RNA-Seq data with or without a reference genome: BMC Bioinformatics, v. 12, p. 323.

Lust, J. A., M. Q. Lacy, S. R. Zeldenrust, A. Dispenzieri, M. A. Gertz, T. E. Witzig, S. Kumar, S. R. Hayman, S. J. Russell, F. K. Buadi, S. M. Geyer, M. E. Campbell, R. A. Kyle, S. V. Rajkumar, P. R. Greipp, M. P. Kline, Y. Xiong, L. L. Moon-Tasson, and K. A. Donovan, 2009, Induction of a chronic disease state in patients with smoldering or indolent multiple myeloma by targeting interleukin 1{beta}-induced interleukin 6 production and the myeloma proliferative component: Mayo Clin Proc, v. 84, p. 114-22.

Machado, J. C., P. Pharoah, S. Sousa, R. Carvalho, C. Oliveira, C. Figueiredo, A. Amorim, R. Seruca, C. Caldas, F. Carneiro, and M. Sobrinho-Simões, 2001, Interleukin 1B and interleukin 1RN polymorphisms are associated with increased risk of gastric carcinoma: Gastroenterology, v. 121, p. 823-9.

Nadler, R. B., A. E. Koch, E. A. Calhoun, P. L. Campbell, D. L. Pruden, C. L. Bennett, P. R. Yarnold, and A. J. Schaeffer, 2000, IL-1beta and TNF-alpha in prostatic secretions are indicators in the evaluation of men with chronic prostatitis: J Urol, v. 164, p. 214-8.

Nakayama, M., C. J. Bennett, J. L. Hicks, J. I. Epstein, E. A. Platz, W. G. Nelson, and A. M. De Marzo, 2003, Hypermethylation of the human glutathione S-transferase-pi gene (GSTP1) CpG island is present in a subset of proliferative inflammatory atrophy lesions but not in normal or hyperplastic epithelium of

the prostate: a detailed study using laser-capture microdissection: Am J Pathol, v. 163, p. 923-33.

Naslund, M. J., J. D. Strandberg, and D. S. Coffey, 1988, The role of androgens and estrogens in the pathogenesis of experimental nonbacterial prostatitis: J Urol, v. 140, p. 1049-53.

Nickel, J. C., J. Downey, I. Young, and S. Boag, 1999, Asymptomatic inflammation and/or infection in benign prostatic hyperplasia: BJU Int, v. 84, p. 976-81.

Nuki, G., B. Bresnihan, M. B. Bear, D. McCabe, and E. G. O. C. Investigators, 2002, Long-term safety and maintenance of clinical improvement following treatment with anakinra (recombinant human interleukin-1 receptor antagonist) in patients with rheumatoid arthritis: extension phase of a randomized, double-blind, placebo-controlled trial: Arthritis Rheum, v. 46, p. 2838-46.

Putzi, M. J., and A. M. De Marzo, 2000, Morphologic transitions between proliferative inflammatory atrophy and high-grade prostatic intraepithelial neoplasia: Urology, v. 56, p. 828-32.

Rivero, V., C. Carnaud, and C. M. Riera, 2002, Prostatein or steroid binding protein (PSBP) induces experimental autoimmune prostatitis (EAP) in NOD mice: Clin Immunol, v. 105, p. 176-84.

Schatteman, P. H., L. Hoekx, J. J. Wyndaele, W. Jeuris, and E. Van Marck, 2000, Inflammation in prostate biopsies of men without prostatic malignancy or clinical prostatitis: correlation with total serum PSA and PSA density: Eur Urol, v. 37, p. 404-12.

Sfanos, K. S., and A. M. De Marzo, 2012, Prostate cancer and inflammation: the evidence: Histopathology, v. 60, p. 199-215.

Siegel, R. L., K. D. Miller, and A. Jemal, 2016, Cancer statistics, 2016: CA Cancer J Clin, v. 66, p. 7-30.

van Leenders, G. J., W. R. Gage, J. L. Hicks, B. van Balken, T. W. Aalders, J. A. Schalken, and A. M. De Marzo, 2003, Intermediate cells in human prostate epithelium are enriched in proliferative inflammatory atrophy: Am J Pathol, v. 162, p. 1529-37.

Vykhovanets, E. V., M. I. Resnick, G. T. MacLennan, and S. Gupta, 2007, Experimental rodent models of prostatitis: limitations and potential: Prostate Cancer Prostatic Dis, v. 10, p. 15-29.

Wang, W., A. Bergh, and J. E. Damber, 2009, Morphological transition of proliferative inflammatory atrophy to high-grade intraepithelial neoplasia and cancer in human prostate: Prostate, v. 69, p. 1378-86.

Wang, X., Y. W. Lin, J. Wu, Y. Zhu, X. L. Xu, X. Xu, Z. Liang, Z. H. Hu, S. Q. Li, X. Y. Zheng, and L. P. Xie, 2014, Meta-analysis of nonsteroidal anti-inflammatory drug intake and prostate cancer risk: World J Surg Oncol, v. 12, p. 304.

Zabaleta, J., L. J. Su, H. Y. Lin, R. A. Sierra, M. C. Hall, A. O. Sartor, P. E. Clark, J. J. Hu, and A. C. Ochoa, 2009, Cytokine genetic polymorphisms and prostate cancer aggressiveness: Carcinogenesis, v. 30, p. 1358-62.

Chapter 5: Conclusions and Future Directions

Abbreviations

BAC	Bacterial Artificial Chromosome
BPH	Benign Prostatic Hyperplasia
CK15	Cytokeratin 5
CP	Chronic Prostatitis
CRISPR	Clustered Regularly Interspaced Short Palindromic Repeats
Dox	Doxycycline
FOXA	Forkhead Class A
H&E	Hematoxylin & Eosin
IMPI	IL-1β-Mediated Prostate Inflammation
IPA	Ingenuity Pathway Analysis
iNOS	Inducible Nitric Oxide Synthase
LCM	Laser Capture Microdissection
MDSCs	Myeloid Derived Suppressor Cells
PIA	Proliferative Inflammatory Atrophy
PIN	Prostatic Intraepithelial Neoplasia
PPDE	Posterior Probability of Differential Expression
PSA	Prostate Specific Antigen
PTEN	Phosphatase and Tensin Homolog
rtTA	Reverse Tetracycline Transactivator

Conclusions

We have developed and characterized a new mouse model of prostate inflammation that closely recapitulates the pathological features of human prostate inflammatory and pre-neoplastic lesions. Although, nearly all human prostate cancer cases show histological evidence of inflammation, the question of whether inflammation

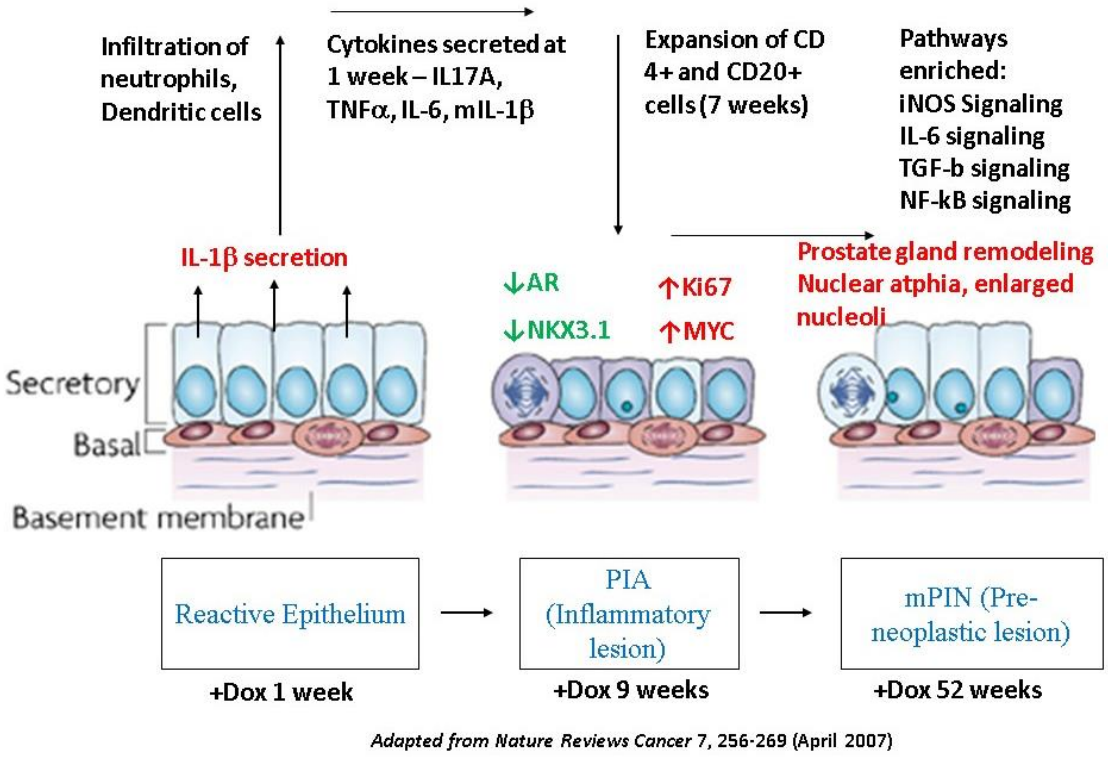

Adapted from Nature Reviews Cancer 7, 256-269 (April 2007)

Figure 1: Molecular changes induced by IL-1β-mediated inflammation: Major histological changes in the inflamed prostate epithelium include reactive epithelia at + Dox 1 week, atrophic glands or PIA at + Dox 9 weeks, and pathological features consistent with PIN at +Dox 52 weeks. Changes in cytokine expression, immune cell populations, molecular markers, and pathways altered are depicted above.

contributes to the initiation/ progression of the prostate cancer, is still unclear. Moreover, inflammation has been implicated in the etiology of benign prostatic hyperplasia (BPH) and chronic prostatitis. Characterization of IL-1β-mediated prostate pathology provides unprecedented opportunities to explore the relationships between inflammation and prostate disease. The IL-1β-Mediated Prostate Inflammation (IMPI)

model is highly innovative, as the inflammation can be induced at will by administering doxycycline (Dox). Moreover, inflammation is mediated by Interleukin-1β, a physiologically relevant cytokine overexpressed in a subset of chronic prostatitis patients, and expressed by human prostate epithelial cells (described in Chapter 2). Some of the key findings from this research project are briefly summarized below:

1. **Characterization of the IMPI Model:** IL-1β expression in the prostate recruited several immune cells including neutrophils, and triggered an acute inflammatory response after one week of treatment. IMPI prostates treated for three weeks displayed the transition of acute inflammation to a more chronic inflammatory environment, with the enrichment of lymphocytes such as CD4+ (T cells), CD20+ (B cells), and CD11b+ GR1+ (potentially Myeloid Derived Suppressor Cells, MDSCs) cells. Additionally, mice with prostate inflammation exhibited stromal thickening and significant increase in prostate size. The characterization of the immune cells, prostate histology, cytokines secreted, and functional kinetics of the model described in Chapter 2, will permit other researchers to exploit the model in their respective research endeavors.
2. **Discerning Pelvic Hypersensitivity and Potential Therapeutic Strategies to Mitigate IL-1β-Mediated Referred Hyperalgesia:** Prostate inflammation-mediated pelvic hypersensitivity observed in Dox-treated IMPI mice was quantified using the von Frey assay. The detailed characterization of the onset of referred hyperalgesia is documented in Chapter 3. Moreover, the pelvic hypersensitivity attenuated in Dox-treated IMPI mice after Dox withdrawal. To provide further evidence that pelvic hypersensitivity was mediated by IL-1β,

we performed a preventative study with an IL-1β-cascade inhibitor. Kineret, a human recombinant IL-1 receptor antagonist, binds to the same receptor as IL-1β and blocks the IL-1β-initiated signal cascade. Co-administration of Kineret and Dox prevented the development of pelvic hypersensitivity observed in Dox-treated IMPI mice. Based on our findings, there is evidence to support that Kineret can attenuate IL-1β-mediated pelvic hypersensitivity in chronic prostatitis (CP) patients.

3. **Examining Voiding Dysfunction Associated with Prostate Inflammation**: Using a quantitative approach such as the urine void assay, Dox-treated IMPI mice were observed to have a lower urine void area compared to controls, indicating potential urinary retention. Often urinary complications are observed in men with signs of inflammation in the expressed prostatic secretions or urine voided after a prostate massage. Our model recapitulates similar complications in urine voiding as quantified by our micturition patterns. A deeper analysis on the urodynamics using advanced techniques like cytometry will provide insight into potential mechanisms and therapeutic strategies.
4. **IMPI Model Presents Histopathological Features Resembling Human Prostate Diseases**: After nine weeks of chronic inflammation, PIA (Proliferative Inflammatory Atrophy) lesions were observed in Hematoxylin & Eosin (H&E) stained ventral prostates of Dox-treated IMPI mice. As observed in human prostate cases, epithelial cells in PIA lesions appeared to be rapidly cycling, determined by Ki67 staining, and expressed higher levels of Myc compared to benign glands.

At 26 weeks of Dox treatment, the inflamed IMPI prostates had features transitioning to PIN morphology. At 52 weeks of Dox treatment, we observed histopathological features consistent with human Prostatic Intraepithelial Neoplasia (PIN), for example, nuclear pleomorphism, enlarged nucleoli, extensive remodeling and hyperplasia. This study is profound as it supports the hypothesis that chronic inflammation can lead to tissue injury and provide a transformative environment for pre-malignant changes to develop. This finding also supports epidemiological study where morphological transitions between PIA and PIN was observed.

5. **Identifying Molecular Changes Associated with IL-1β-Mediated Inflammation**: Using Laser Capture Microdissection (LCM), we dissected epithelial cells at nine weeks and 52 weeks to examine genome-wide gene expression changes mediated by inflammation. More than 3000 genes were differentially expressed with a PPDE (Posterior Probability of Differential Expression) of 0.99 or greater in the inflamed 52 week Dox-treated prostates compared to controls. Enriched pathways in the RNAseq data set included Inducible Nitric Oxide Synthase (iNOS) signaling, Transforming Growth Factor (TGF-β signaling, Interleukin-6 (IL-6) signaling and NF-κB signaling. Using the Ingenuity Pathway Analysis (IPA) software, upstream regulators enriched in one-year expression dataset were identified, which included TP53, STAT3, Myc, TNF and mir-21 (complete list in Chapter 4). This study is valuable as we have laid the foundation to determine potential inflammatory biomarkers that could be clinically relevant. More importantly, using this gene

expression data set, the molecular changes associated with PIA and PIN can be tested in the IMPI model by in-situ hybridization.

Our contribution is significant because this study established the role of IL-1β-mediated inflammation in the development of lesions, with features consistent with human PIN, and identified for the first-time, genome-wide gene expression changes in the inflamed prostate epithelia. Thus, important advances in the treatment of prostate inflammatory diseases can be expected with clues to understanding the etiology of these diseases. Additionally, this model serves as a highly valuable preclinical model to test potential therapeutic drugs against inflammation and to develop novel inflammatory biomarkers.

Future Directions

1. ***Next Generation IMPI Model***

   To generate the double transgenic IMPI model, we developed two independent transgenic mouse strains: the TetO-IL-1β strain and the Hoxb13-rtTA strain. Being a genetic model, the IMPI mice can be bred to extant mouse models of prostate cancer or knockout models to dissect the role of specific molecules in prostate inflammatory diseases. Generating a next-generation IMPI model by condensing the double transgenic system to a single transgene will greatly enhance the utility of the model. This will significantly decrease the number of breeding pairs and offspring screened by half, saving both time and money.

   To generate the Hoxb13-rtTA strain, a former graduate student used recombineering techniques to clone Reverse Tetracycline Transactivator (rtTA)

under the transcriptional control of Hoxb13 regulatory elements in the context of a 218kb Bacterial Artificial Chromosome (BAC). To establish the next generation IMPI model on a single allele, the TetO-IL-1β fragment needs to be carefully cloned into the Hoxb13- rtTA BAC without disrupting the regulatory elements that support Hoxb13 transcriptional activity. Another former graduate student in our lab examined the Hoxb13 BAC to isolate prostate-restricted regulatory elements by BAC-based reporter gene deletion analysis (McMullin et al., 2010). He concluded that the elements important for transcriptional activity of Hoxb13 were located +15 to +61kb. His work also reported a 37-bp region downstream of *Hoxb13*, a potential binding site for FOXA (Forkhead Class A) transcription factor, to be important for Hoxb13 expression. Guided by his work, an integration site in the Hoxb13- rtTA BAC can be selected to clone the TetO-IL-1β fragment and condense the IMPI system to a single transgene.

Using the bi-directional Tet-On 3G system that allows co-expression of a transgene and a reporter gene will further extend the utility of the model. The new bi-directional TetO-IL-1β-mCherry-antibiotic resistance cassette can be recombineered into the Hoxb13-rtTA BAC. The next generation IMPI model will be an extremely valuable tool to the scientific community, especially to breed to other extant models of prostate cancer.

2. *Inflammation in the Context of Pten Loss*

As described in Chapter 4, IL-1β-mediated inflammation results in pathological features consistent with human pre-neoplastic prostate lesions, however it does not become invasive. IL-1β induced a local inflammatory microenvironment that is conducive to pre-malignant transformation. A recently published paper (Hubbard et al., 2016) reported that combined Myc activation and Pten loss could result in genomic instability and lethal prostate cancer. As discussed in Chapter 4, IL-1β expression results in Myc activation in the IMPI prostate epithelium. Therefore, we can hypothesize that the combination of inflammation and Pten loss could exacerbate the phenotype observed in mice exhibiting inflammation alone, or mice with Pten loss alone.

To develop the IMPI Pten^{null} mice, we will breed the IMPI+/+ mice to our Pten^{null} mice (Hoxb13-Cre|Pten Fl/Fl). Since tissue-wide loss of Pten is embryonically lethal, a conditional Pten knockout mouse was developed using the Cre-LoxP system. Cre recombinase is a bacterial enzyme that recombines a pair of specific sequences called Lox sequences. Floxed Pten (Pten Fl) can be achieved by incorporating the LoxP sites in the exon 4 of the Pten gene. Since Cre recombinase is driven by Hoxb13, a prostate specific promoter, PTEN loss was achieved specifically in the prostate.

Breeding the IMPI+/+ mice to Hoxb13-Cre+/+|Pten Fl/Fl will generate heterozygous IMPI+/-|Cre+/-|Pten Fl/WT mice. These mice will be bred to IMPI+/+ mice and their offsprings will be inter-bred to finally generate our desired genotype IMPI+/+ Pten ^{null} mice. Transgenes (IL-1β, rtTA, Cre, floxed

Pten and WT Pten) will be screened using PCR. A cohort of mice with desired genotype will be Dox-treated to determine the histological consequence of PTEN loss combined with chronic inflammation. The results from this study will test our hypothesis that MYC activation during chronic inflammation combined with PTEN loss can induce genomic instability.

3. ***Developing novel inflammatory biomarkers and diagnostics***

In Chapter 4, we discussed the genome-wide gene expression changes mediated by IL-1β-induced inflammation. By combining LCM and RNA-sequencing technologies, we identified pathways and key upstream regulators enriched under chronic inflammatory conditions. By discerning the molecular changes mediated by chronic inflammation, we have laid the foundation for the development of novel inflammatory biomarkers and improved diagnostic assays in IL-1β-mediated prostate disease.

We observed differentially expressed chemokines, oncogenes and other mediators in the inflamed epithelia that require validation. Validating these genes in our IMPI system followed by clinical validation, will lead to the development of new diagnostic markers for human PIN and prostate inflammation.

Prostate Specific Antigen (PSA) tests have been extensively used to predict the risk of prostate cancer. However, the PSA test has been severely scrutinized, as PSA is upregulated in several other conditions such as BPH, prostatitis, and even in false positive prostate cancer cases. There is an urgent need to develop new tests that accurately determine the prognosis of prostate

diseases like BPH, chronic prostatitis, and prostate cancer. Validation of different genes in our IMPI system and human patients is required to determine the utility of these assays.

4. IL-1β Overexpression in the Context of Bacterial Infection.

Tu *et al.* reported that IL-1β overexpression in the stomach results in chronic inflammation and dysplasia (Tu et al., 2008). Moreover, IL-1β overexpression in the context of *H.felis* infection accelerates the development of gastric carcinoma. It is well-established that *H.Pyroli* infection is a high risk factor for gastric carcinoma; moreover, the etiology of prostate cancer has been proposed to be similar to gastric cancer (Sfanos et al., 2013). However, the inability to detect bacterial agents in prostate cancer samples have made it difficult to find evidence to support this hypothesis. Moreover, cryptic bacteria have been proposed to play a role in prostate inflammatory cases without a detectable foreign entity. A recently published report in a subset of Asian prostate cancer patients presented molecular evidence for the presence of *H.pyroli*; however, the sample size was small (Al-Marhoon et al., 2015). Examination of IL-1β overexpression in the context of bacterial inflammation will reveal if there is a potential link between bacterial inflammation, IL-1β expression and prostate cancer.

5. Inflammation Alters the Cell Differentiation Program in Prostate Epithelium

The prostate epithelium largely consists of two main cell populations: basal and luminal epithelial cells. Basal and luminal cells can be distinguished by staining

for specific markers. Basal cells express Cytokeratin 5 (CK5), p63, and CK14, whereas luminal cells express CK8 and CK18 but only low levels of p63 (van Leenders et al., 2003). As discussed in Chapter 4, inflammation in the IMPI model results in the increase of CK5 positive cells. Dr. De Marzo reported that cells in the PIA lesions are often rapidly cycling and are enriched for intermediate cells (van Leenders et al., 2003). These intermediate cells are potential precursor cells for prostate cancer (van Leenders et al., 2003). Additionally, Kwon *et al.* described that chronic inflammation enhances basal to luminal cell differentiation by utilizing a lineage tracing mouse model of bacterial prostatitis (Kwon et al., 2014). Clearly, these studies are contradicting and a more detailed understanding on the effect of inflammation on the cell differentiation program is required.

After nine weeks of Dox-treatment, we observed atrophic lesions in the IMPI prostate consistent with features of human PIA. Co-immunostaining with different markers of basal and luminal cells will help identify if there is a presence of intermediate cell population. This study will also help to determine if inflammation alters the cell differentiation program.

References

Al-Marhoon, M. S., A. Ouhtit, A. O. Al-Abri, K. P. Venkiteswaran, Q. Al-Busaidi, J. Mathew, I. Al-Haddabi, O. Shareef, S. Aquil, K. Rahman, I. Al-Hashmi, I. Gupta, and S. S. Ganguly, 2015, Molecular Evidence of Helicobacter Pylori Infection in Prostate Tumors: Curr Urol, v. 8, p. 138-43.

Hubbard, G. K., L. N. Mutton, M. Khalili, R. P. McMullin, J. L. Hicks, D. Bianchi-Frias, L. A. Horn, I. Kulac, M. S. Moubarek, P. S. Nelson, S. Yegnasubramanian, A. M. De Marzo, and C. J. Bieberich, 2016, Combined MYC Activation and Pten Loss Are Sufficient to Create Genomic Instability and Lethal Metastatic Prostate Cancer: Cancer Res, v. 76, p. 283-92.

Kwon, O. J., L. Zhang, M. M. Ittmann, and L. Xin, 2014, Prostatic inflammation enhances basal-to-luminal differentiation and accelerates initiation of prostate cancer with a basal cell origin: Proc Natl Acad Sci U S A, v. 111, p. E592-600.

McMullin, R. P., A. Dobi, L. N. Mutton, A. Orosz, S. Maheshwari, C. S. Shashikant, and C. J. Bieberich, 2010, A FOXA1-binding enhancer regulates Hoxb13 expression in the prostate gland: Proc Natl Acad Sci U S A, v. 107, p. 98-103.

Sfanos, K. S., W. B. Isaacs, and A. M. De Marzo, 2013, Infections and inflammation in prostate cancer: Am J Clin Exp Urol, v. 1, p. 3-11.

Tu, S., G. Bhagat, G. Cui, S. Takaishi, E. A. Kurt-Jones, B. Rickman, K. S. Betz, M. Penz-Oesterreicher, O. Bjorkdahl, J. G. Fox, and T. C. Wang, 2008, Overexpression of interleukin-1beta induces gastric inflammation and cancer

and mobilizes myeloid-derived suppressor cells in mice: Cancer Cell, v. 14, p. 408-19.

van Leenders, G. J., W. R. Gage, J. L. Hicks, B. van Balken, T. W. Aalders, J. A. Schalken, and A. M. De Marzo, 2003, Intermediate cells in human prostate epithelium are enriched in proliferative inflammatory atrophy: Am J Pathol, v. 162, p. 1529-37.